Soil Hydrological Studies for Water Resource Conservation and Management in the Virgin Islands

by

David A. Hensley

A dissertation submitted to the Graduate Faculty of
Auburn University
in partial fulfillment of the
requirements for the Degree of
Doctor of Philosophy

Auburn, Alabama
May 10, 2025

Keywords: Caribbean, small island, mulch, runoff, erosion, soil physics

Approved by

Thorsten Knappenberger, Chair, Associate Professor of Crop, Soil and Environmental Sciences
Eve Brantley, Alumni Professor, Extension Specialist of Crop, Soil and Environmental Sciences
Mariana Dobre, Assistant Professor of Soil and Water Systems, University of Idaho
Joey N. Shaw, Professor Emeritus of Crop, Soil and Environmental Sciences
James R. Lindner, Alumni Professor of Agriscience Education

Abstract

The Virgin Islands face water scarcity due to their small size, topography, and the prevailing climate of the northeastern Caribbean region. At the same time, demands placed on water resources are high, from tourism, population growth, and a stated desire to expand agricultural production. With limited land and freshwater resources, it is imperative that managers have scientific information for decision-making, but soil hydrology in the Virgin Islands has been poorly described. Soil hydrology, the application of soil physics to the fluxes of water through soil, can provide insight into various areas of need: the management of soil water in agriculture, mechanistic understanding of surface runoff and island water budgets, and soil erosion by water. Soil hydrological studies in the Virgin Islands can, therefore, help address the need for water resource conservation and data-driven management at various scales.

This dissertation is composed of three studies of soil hydrological questions. The uniting theme across all three is an attempt, with limited existing datasets, to better describe relevant soil hydrological questions that will ultimately improve water conservation methods in the Virgin Islands. After a literature review of the broad topic of Virgin Islands water resources, we first examine the soil hydrological implications and water balance of agricultural mulch covers in the production of a plantain crop at the plot scale. In the second study, we examine runoff generation mechanisms at the watershed scale and consider the implications of runoff coefficients and connectivity in a Virgin Islands watershed. In the third study, we describe the remaining challenges in parameterizing an erosion prediction model at the watershed scale in the Virgin Islands and Caribbean region.

Acknowledgments

I want to take this opportunity to thank the many exceptional and kind people who contributed to this work through their inspiration, encouragement, or direct assistance with my working life, beginning with my committee, and my advisor, Dr. Thorsten Knappenberger.

A number of people were instrumental in first encouraging me to pursue an interest in plants and soil more than a decade ago, and I wish to acknowledge them for the immense influence they have had on my life and thus on this dissertation: Michael Anderson of the University of Texas, Moctar Coly of Séssène, Senegal, Hilbert Bignal and Donaldson Bernard of Windsor, Jamaica, Cherice Smithers of the New Orleans Fruit Tree Project, Scottie Sklanka of Delgado Community College, Julie Whitbeck of the National Park Service, Richard Sacher of American Aquatic Gardens, and my thesis advisor at the University of Florida, Diane Rowland.

Much of my work was carried out at the Agricultural Experiment Station in the School of Agriculture on the campus of the University of the Virgin Islands (UVI), where I am employed as a staff researcher. I would like to thank my supervisors and administrators for providing the permission, funding, and the space to carry out this research: Kim Waddell, Usman Adamu, Bob Godfrey, Thomas Zimmerman, Stuart Weiss, and Nereida Washington. My many kind and generous colleagues at UVI substantially helped me complete this work; I wish to particularly thank Ephraim Rodriguez, Jose Herrera, Julene Chapman, Fiola Alexander, Olasee “the Bush Man” Davis, and the night security team (who kept me company during late nights in the lab). Direct colleagues within the watershed research team provided major support to the completion of this work as well: Brittany Lancellotti, Race Stryker, N’Bari Alexander, Zavie Wilson, and SaVaughna John-Baptiste. I also thank the faculty and staff of the Center for Marine and Environmental Studies at UVI, who were excellent collaborators throughout this project, as well

as Hilary Lohmann and Sabrina Pickett of the Virgin Islands Department of Planning and Natural Resources, whose real-world professional demand for the results of this work was a constant inspiration to get the job done, and get it done right. This work would also not have been possible without the permission of several agencies and private landowners who allowed this research to proceed on their property, and I thank them for their commitment to this project and to science: the Virgin Islands Department of Agriculture, the U.S. National Park Service, Bush Tribe Eco Adventures, Captain John "Big Beard" Macy, Nate Olive and the Ridge to Reef Farm, and Brian McCullough of Tropics Hydroponics Farm.

More friends that can be named here have been supporters of this endeavor; to name a few: Alex, Erin, Sabrina, Natalie, Bob, Jesse, Christine, Kaitlyn, Louis, Kelly, Kyle, Sarah, Ali, Kayleigh, Alec, Garrett, Matt, Vikas, and David. My parents, Bill and Ruthie, have patiently supported my academic pursuits, and my brother Alan has talked me through many mental logjams. My grandparents have also inspired me: my grandfather William Hensley worked as an engineer on the Apollo program at NASA, inspiring me to pursue science myself, and my nursery-owning grandfather Paul Robinson and his green thumb sparked an interest in the world of plants and soil that came into full flower many years later. My grandmother Betty Robinson also suggested what, under other circumstances, I felt would be a fitting title for this dissertation about soil and water: *How the Dirt Gets Wet and How the Wet Gets Dirty*.

No scholar or scientist would achieve any result without the love of friends and family. I thank them all for their support over many years. The care of so many people gives me the occasion to recall a saying, usually attributed to William James: "We are like islands in the sea; separate on the surface, but connected in the deep." This work is dedicated to the people of the Virgin Islands, past, present, and future, and to these islands in the sea.

Table of Contents

List of Tables

List of Figures

Chapter 1
Literature Review

Introduction

Soil and water conservation and management are critical concerns of any community worldwide, as both natural resources play a central role in a wide array of important economic activities and human life support systems (Cosgrove and Loucks, 2015; Davison et al., 2005; Karlen et al., 2014). Although this is true everywhere, soil and water conservation is even more acutely important in remote or isolated communities, who may depend on local hydrology and land productivity even more than average (Gheuens et al., 2019). On small islands far from larger landmasses, such as the Virgin Islands, water resources are even more starkly limited, with limited area for rainfall catchment and normally fewer physical and economic resources than the mainland (Robins, 2013). Thus, an adequate understanding of the soil hydrology of any island should be of interest to a wide variety of stakeholders tasked with promoting the welfare and development of their constituents (Bremer et al., 2021).

Water security for human and commercial use may depend on a mixture of surface reservoirs, catchments, storage, groundwater reserves, or desalination in island water systems (Falkland, 1999). When agricultural and ecological production are also taken into account, the water of the vadose zone in soil is also of major importance as a driver of plant productivity (Vereecken et al., 2022; White et al., 1999). An understanding of the efficiencies and capacities of each of these components is useful for a variety of fields: land management and zoning, water use and public utilities, wastewater planning and management, agricultural production, biodiversity conservation, tourism, disaster preparation, and more (Cosgrove and Loucks, 2015).

On small islands where rainfall is limited, availability of water resources can become a critical issue for human development and ecosystem health (Falkland, 1999; Robins, 2013). In such places, a prolonged drought can lead to major consequences for water security (Scalley, 2012). But a combination of careful long-term resources management and good understanding of island hydrology can help allay the potential impact of droughts or other natural disasters that may put strain on the water system of an island (e.g. Bremer et al., 2021).

The Virgin Islands is an archipelago of some 100 islands and cays in the northeastern Caribbean region, geographically a part of the Leeward Islands chain in the Lesser Antilles. Geologically and ecologically, however, the Virgin Islands form a part of the Greater Antilles, located on the Puerto Rico platform (except for the more isolated island of St. Croix, located on its own microplate some 60 km to the south of the other islands; Speed, 1989). Politically, the Virgin Islands include three divisions: the British Virgin Islands (BVI), a British Overseas Territory; the United States Virgin Islands (USVI), an unincorporated territory of the United States; and Vieques and Culebra islands, which are politically part of the Commonwealth of Puerto Rico (itself also an unincorporated territory of the United States). The principal islands, in order of land area, are St. Croix (220 km^2), Vieques (135 km^2), St. Thomas (83 km^2), Tortola (56 km^2), St. John (52 km^2), Anegada (38 km^2), Culebra (30 km^2), Virgin Gorda (21 km^2), and Jost van Dyke (8 km^2). The total population of the archipelago is approximately 129,000, the majority of whom are in the USVI (approximately 80,000; U.S. Census Bureau, 2020).

In the Virgin Islands as a whole, but especially the USVI, tourism is the dominant economic sector (Culbertson et al., 2020). The current population represents a large increase over the last half-century, and a significant degree of land development has taken place with the growth of the population and the tourism sector beginning in the 1960s (Francois et al., 1983;

Johnston, 1987), and in the USVI, a significant migration of Americans from the mainland United States purchasing property and constructing homes (Roopnarine, 2020). The population growth has been most impactful on the island of St. Thomas, the most densely populated island with approximately 40,000 inhabitants, with the capital city of the USVI, Charlotte Amalie. Receiving approximately 1000 mm of rainfall annually, the Virgin Islands are vulnerable to the water resource concerns of small islands described above, and conflicts exist over alternative priorities for the management of these resources (DPNR, 2024; Johnston, 1987; Soden, 1990). To safeguard the potential for human development and ecosystem health in the Virgin Islands, relevant authorities, policymakers, and community stakeholders across political boundaries require information on the structure and function of the hydrological system of these islands (Falkland, 1999), but existing data is limited, as we will demonstrate in this literature review (Lancellotti and Hensley, 2024). Indeed, little information on the generally water-limited islands of the northeastern Caribbean is available, so we hope this document is beneficial to the broader region as well, to the extent that the geological, climatological, social, political, or economic situations of the various islands in this region are similar to one another.

This literature review is divided into sections that will help the reader appreciate the various aspects of soil hydrology's importance to the Virgin Islands. We begin with a general overview of water resources in the Virgin Islands to provide context. This leads to the opportunity for studies in soil hydrology to address several of the concerns summarized in the overview section. For each topic, we provide a discussion of literature and background information in each area of study: first at the field scale for soil water management of the vadose zone and agricultural production, then increasing to the watershed scale to discuss runoff

generation processes and ephemeral stream hydrology, and finally soil and sedimentation issues in Virgin Islands hydrology.

Water Resources of the Virgin Islands

Historical background

There is evidence that freshwater was more available in historical times than at present in the Virgin Islands, though it is also clear from the historical record that the Virgin Islands have always experienced periods of water shortages. The climate of the islands is described as a "tropical savanna climate with dry winters" or the Köppen-Geiger "*Aw*" classification, with average annual precipitation of about 1000 mm and a mean annual temperature of 26.4°C (Beck et al., 2018; Menne et al., 2012). With an extended dry season often lasting from December through April, and sometimes till September, evapotranspiration in the warm tropical climate can quickly create drought stresses without consistent rainfall (Larson et al., 2015). The primary rainy season, usually from August through November, corresponds to the Atlantic hurricane season, in which significant proportions (i.e., ~10–20%) of annual rainfall may be received within a short period of only a day or two (Giannini et al., 2001; Menne et al., 2012). Orogenic precipitation does occur, particularly on the windward slopes of taller mountains (the highest peak is Sage Mountain, Tortola, 521 m above sea level, where annual precipitation is often 2000 mm; Martin-Kaye, 1954). In general though, the overall low topography of the Virgin Islands necessarily limits the total quantity of precipitation generated by the islands' landmass (Menne et al., 2012), especially compared to nearby Puerto Rico (Moraes et al., 2023). Additionally, the generally rocky, thin soils of volcanic origin, and steepness of much of the islands' terrain, limits groundwater storage and recharge (Jordan, 1975).

Despite these intrinsic limitations, the historical and archaeological record suggest that surface freshwater was relatively common in the past (Lancellotti and Hensley, 2024). Limited evidence suggests certain stream courses (e.g. Salt River in St. Croix, Turpentine Run in St. Thomas) were used for water transport by indigenous Taíno and Kalinago people in pre-colonial times, and indigenous settlements were usually sited along stream courses (Chanca, 1494; Dookhan, 1994; Righter, 2002). Today these stream courses are now either intermittent or ephemeral and incapable of bearing watercraft. In the 17th and 18th centuries, scattered historical sources from various European ship captains, colonial governors, and missionaries attest to the presence of "rivers" on the island of St. Croix, where several waterways including Salt River were deemed significant streams (Highfield, 2013; Hopkins, 1987; Oldendorp, 1777). Later, when sugarcane cultivation had reached its peak during Danish colonial rule in the 19th and into the early 20th century, many of the streams were remembered as perennial (Eggers, 1879; Knox, 1852; Seaman, 1980). In the Virgin Islands, these streams are usually called "*guts*" (occasionally also spelled "*ghuts*" or "*ghauts*," mainly in neighboring islands such as St. Kitts, Saba, and Montserrat; Wells, 2006). Generally speaking, although it seems clear that drought was also a problem during these early years, the groundwater table particularly in St. Croix must have been higher than its present level to explain this more consistent streamflow (Jordan, 1972). D.G. Jordan, a U.S. Geological Survey (USGS) hydrologist working in the Virgin Islands in the 1970s, noted that many of the guts of St. Croix appeared to be actively drying down during that era, a trend that did not reverse (Jordan, 1972). Hydrological data collection by the USGS began in the USVI on a regular basis starting in the 1970s, but eventually declined and almost completely disappeared beginning in the mid-2000s (Lancellotti and Hensley, 2024), a trend that

was not unique to the USVI across small island developing states (SIDS) during the same era (Falkland, 1999).

Several hypotheses exist as to the cause of the apparent dry down across the Virgin Islands in the last century. A prominent one, given by Jordan (1972; 1975), points primarily to the large-scale abandonment of sugarcane cultivation and the subsequent spread of secondary forests dominated by pioneer species, with the supposed mechanism being deeper rooting depths and higher rates of evapotranspiration interacting with what was once a relatively shallow water table. Other possibilities, however, include long-term fluctuations in precipitation, changes in water extraction (particularly as total population and the tourism industry grew), and the spread of impervious surfaces owing to land use change and property development (Lancellotti and Hensley, 2024). None of these are adequately investigated in scientific literature. Climate data from the Global Historical Climatology Network (Menne et al., 2012) indicates that precipitation does oscillate over many years, but there is no apparent long-term decline in precipitation over the last century.

Surface water

The current status of freshwater resources across the Virgin Islands is only minimally described, though it is clear that water resources overall are limited and possibly threatened in some cases (Lancellotti and Hensley, 2024). Surface water, groundwater, water use/storage, and water quality are all important aspects of the Virgin Islands water resources situation. Here, we treat each of these areas in turn.

Streamflow in the guts of the Virgin Islands is generally rare, with stormflows persisting at most a few days, and baseflow generally low in quantity. After extraordinarily wet periods,

baseflow in some guts may persist for some months at most before drying down, but baseflow does not necessarily occur for more than a few days in any given wet season (Lancellotti and Hensley, 2025). At higher elevations on the volcanic slopes of the islands, groundwater may flow in guts as baseflow, a common pattern for geologically old high-relief volcanic islands (Robins and Lawrence, 2000). For example, a report by Mather (1971) of the British Geological Survey noted that consistent baseflow in Tortola was only observed at elevations greater than 90 m above sea level. As a result, there is no meaningful extraction of freshwater from streamflow for human use. Despite this, gallery forests along the stream courses act as important ecosystems, in many cases these are the only examples of tropical moist forest ecosystems (as opposed to tropical dry forest) in some islands, as the depth to groundwater is less near the streambed and soil water is more abundant near stream courses (Gardner et al., 2008).

In the 20th century, when agriculture (mainly in St. Croix) was dominated by cattle pastures, a significant number (~130 on St. Croix, a few dozen on St. Thomas) of small surface ponds and check dams were constructed to store water for cattle (IRF, 2000; USDA-NRCS, 1973). Many of these ponds were constructed by damming or diverting the course of guts, while others act as surface reservoirs for constructed rainwater surface catchment structures. Today, cattle farming is not a major industry in the Virgin Islands, but the ponds remain functional as surface water impoundments, despite significant siltation (McNair et al., 2006). For example, a large reservoir constructed by damming the course of Creque Gut in northwestern St. Croix at Creque Dam has, according to U.S. Army Corps of Engineers documentation (USACE, 1992), silted in to 59% of its original volume since construction in 1926, based on measurements we took in 2023. Records of the original scope and dimensions of most ponds in the USVI were maintained by the Virgin Islands Department of Agriculture, but these records were destroyed in

Hurricane Hugo in 1989 (former Agriculture Commissioner B. Lawaetz, pers. comm.), making an adequate determination of the total number and storage capacity of these various reservoirs difficult. However, a few ponds remain in use for agricultural purposes, while others have been abandoned and are surrounded by secondary forest today. It is important to note that naturally occurring freshwater ponds are rare to nonexistent in the Virgin Islands (though coastal salt ponds and lagoons are commonplace), such that these anthropogenic ponds are normally the only significant surface freshwater by volume at any given time (McNair et al., 2006).

Groundwater

Nearly all groundwater reserves in the Virgin Islands are found in fractured rock storage in the volcanic rocks of the island chain, described as "volcanic rock aquifers" by the USGS (USGS, 1984). The available groundwater storage and yield in such hydrogeological conditions is variable, but extremely limited overall (e.g. 2.6 L min^{-1}; Jordan and Cosner, 1973). Additionally, "coastal embayment aquifers" may exist in immediate coastal zones where alluvial sedimentation affords the opportunity for groundwater storage in quaternary depositional material (USGS, 1984); these usually provide the best yields (129 L min^{-1} was reported in the Esperanza alluvial valley of Vieques; Renken et al., 2002; up to 150 L min^{-1} was reported by Robinson, 1972 for St. Croix; and a maximum of 300 L min^{-1} was reported by Cederstrom, 1950, also on St. Croix).

However, two notable exceptions to these hydrogeologic types exist in the Virgin Islands. In Anegada (BVI), a young, Pleistocene-age karstic limestone feature exists that permits only limited freshwater storage and a few wells with high chloride content (IRF, 2013; Martin-Kaye, 1954). Anegada is the only island of the Virgin Islands with no hills or mountains, formed as a

coral platform, similar to the island of Barbuda (Martin-Kaye, 1954). Another carbonate groundwater feature, the Kingshill Aquifer of St. Croix, is much more significant as a water source. This aquifer, of Miocene age, is much deeper and represents by far the most significant groundwater reserve in the Virgin Islands (Miller et al., 1999). Robinson (1972) estimated the total storage capacity of the Kingshill Aquifer at 4.92×10^8 m^3. Robinson (1972) also estimated 3,800 m^3 d^{-1} of pumpage from the aquifer at the time, one of the few existing statistics on water extraction, though this was purely an estimate according to Robinson.

Troublingly, no attempt in the Virgin Islands has ever been made to quantify possible submarine discharge of groundwater to the sea, to our knowledge. Yet, this flux is acknowledged to represent one of the most important parameters of a small island's water budget (Robins, 2013; Robins and Lawrence, 2000), and reports from marine scientists and divers around the islands indicate that this freshwater submarine discharge could be occurring in a number of places (E. Bowman, pers. comm.). Similarly, unknown quantities of groundwater are lost to evapotranspiration (Jordan, 1972), which may be more relevant when water tables are high. Baseflow to streams, another form of groundwater loss (Robins, 2013; Robins and Lawrence, 2000), is significantly easier to measure than these other sources of water loss, but little information has yet been published regarding baseflow in Virgin Islands guts (Lancellotti and Hensley, 2025). To wit: Ward and Jordan (1963) reported baseflow of 9.1 L min^{-1} at Guinea Gut in St. John, 39.4 L min^{-1} at Turpentine Run, St. Thomas, and 184 L min^{-1} at River Gut, St. Croix. In the BVI, Martine-Kaye (1954) reported flows of 7.6 L min^{-1} in Long Bush Gut and 13.2 L min^{-1} in Huntums Gut near Road Town, Tortola, but no further gauge information was available. Streamflow records by the USGS in the USVI throughout the 1980s and 1990s focused on peak gauges and inferred runoff, rather than records of baseflow (Lancellotti and Hensley, 2024).

Modern records of baseflow anywhere in the Virgin Islands do not exist, except for our measurements and estimates made in later chapters of this work.

Generally, groundwater recharge is driven by three major factors: slope, soil hydrology, and land use (Abdullateef et al., 2021; Brooks et al., 2015). In much of the Virgin Islands, recharge is generally disfavored due to steep slopes, and low permeability in some areas (Tombs and Barton, 1979). In addition, the proliferation of real estate development and road construction across the Virgin Islands, particularly the USVI, exacerbates runoff generation and disfavors recharge (Ramos-Scharrón et al., 2023). Infiltration capacity is generally higher in soils overlying the Kingshill Aquifer of St. Croix, partly explaining the presence of this significant hydrogeologic feature there (Gill et al., 1997). While most human land development has the effect of increasing imperviousness and runoff at the expense of recharge, other land use changes could assist with groundwater recharge in the Virgin Islands. For example, the construction of check dams, retention ponds, settling basins, swales, and so on can help impound and infiltrate stormwater that would otherwise discharge to the sea (Torres-Gonzalez, 1989; Ward and Jordan, 1963). In fact, the degree of recharge offered by the existing network of surface ponds may be significant, as suggested by Jordan (1975). Unfortunately, there is no reliable indication of how significant this effect might be in the Virgin Islands. Alternatively, sensitive “recharge zones” of the islands could be identified by managers with different land development policies in these areas, as has been pursued in other islands (Bremer et al., 2021). Stream courses themselves, which act as losing streams at most times of the year, may also promote groundwater recharge in a similar way (Al-Amri et al., 2023). A losing stream is a stream, or a reach within a stream network, where the groundwater level is well below the streambed elevation, meaning that the hyporheic zone is unsaturated and promotes infiltration as opposed to runoff (Jasechko et al.,

2021). It remains unknown what fraction of water infiltrated in guts and ponds of the Virgin Islands is directed to groundwater recharge as opposed to evapotranspiration. It has been hypothesized that the zone of interaction between volcanic rock hydrogeology and the Kingshill aquifer or coastal embayment aquifers (i.e., foothills) may be an important recharge area, as runoff from the less permeable upland areas contacts the more permeable alluvial or carbonate soils of the lowland zone before reaching the sea (Gill et al., 1997; Tombs and Barton 1979).

Water use

Water use and water utilities have a number of dimensions in the Virgin Islands. For human use, freshwater is sourced from three principal sources: rooftop catchment and cistern storage, groundwater extraction, and desalination treatment (Buscemi, 2003), in common with many small tropical islands (Falkland, 1999). Household water use often uses a combination of all of these water sources – for example, a home connected to the public utility in the USVI (Virgin Islands Water and Power Authority; WAPA) may use the desalinated water from the utility but may also have a rainwater cistern from rooftop catchment for use in emergencies or during power outages. The same household may also have a well on the property whose water is used for other purposes (e.g., landscape irrigation). Because of the complexity of individual water use, as well as poor recordkeeping in general throughout agencies and organizations in the Virgin Islands, it is usually not known how much water is being extracted from the various pools of water storage available, nor is it known how much total water is available on an island-wide basis (Lancellotti and Hensley, 2024). Certainly, the volume of water stored in Virgin Islands groundwater has only ever been estimated from very old reports and preliminary datasets (e.g., Jordan, 1975; Mather, 1971). Similarly, there is no comprehensive assessment of the total

quantity of available cistern water storage, though cursory estimates are sometimes made for operational or research purposes (Buscemi, 2003). Though public water utilities may record quantities of water desalinated, this data is not publicly available. Water trucking companies operate fleets of water trucks that transport backup water supplies to households and businesses and generally use treated groundwater (Borgdorff, 2020). Though these are used extensively by residents, especially during dry season when cisterns routinely run dry, no publicly available data exists as to the overall extraction accounted for by these practices. Agricultural operations are usually either rainfed or make use of micro-irrigation. However, as with all other sectors of water use in the Virgin Islands, no comprehensive estimate of total water use currently exists (Lancellotti and Hensley, 2024).

Water quality

Water quality of freshwater resources is often poor in the Virgin Islands. In particular, problematic sedimentation and erosion appears to have been a problem throughout the agricultural period and into the present (Brooks et al., 2007; Quin, 1907), though siltation may have slowed since the widescale abandonment of sugarcane (Lancellotti and Hensley, 2024). Sedimentation and bank erosion negatively affect stream water quality, and likely have deleterious effects on fragile and poorly studied freshwater aquatic ecosystems along similar lines observed elsewhere (Simpson et al., 2014). Sedimentation is particularly damaging to coral reef ecosystems, which are found throughout the Virgin Islands (Rogers and Ramos-Scharrón, 2022). These ecosystems are under significant stress due to a variety of human impacts including climate change and the spread of pathogens (Brandt et al., 2021; Smith et al., 2013), but among the most important local contributors to coral reef decline is sedimentation from land (Oliver et

al., 2018). Since the coral ecosystem is a significant contributor to the overall tourism economy of the Virgin Islands, and much of the local fishery is centered on reef species, this can be considered both a negative economic as well as ecological impact (Canoy et al., 1983). Numerous reports and studies by marine scientists in the Virgin Islands have reported on the presence of sediments observed in the nearshore environment (e.g., Gray et al., 2017; Nemeth and Nowlis, 2001; Oliver et al., 2011). It is also unknown to what extent widespread trash dumping into waterways may affect the water quality of stream water and runoff entering the marine zone. One study on the island of St. Croix found elevated levels of heavy metals and VOCs in streambed material throughout the island, but the authors were unable to establish a direct cause of this contamination among possibilities such as automotive traffic, septic leakage, trash dumping, improper hazardous chemical dumping, or an oil refinery (Lancellotti et al., 2023).

Work by Ramos-Scharrón over several studies (Ramos-Scharrón et al., 2023; Ramos-Scharrón and LaFevor, 2018; Ramos-Scharrón and MacDonald, 2005, etc.) has demonstrated that, particularly on the island of St. John, unpaved road networks function as major contributors of sediment despite a relatively small footprint of total land area. These road networks, proliferating in order to provide access to subdivided homesites for real estate developments, have the effect of producing Hortonian overland runoff (rainfall intensity overwhelming infiltration capacity) because of the impervious nature of both paved and unpaved roads (Ramos-Scharrón and LaFevor, 2016). However, the unpaved roads in particular are sources of sediment themselves, as they are frequently not adequately engineered to prevent stormwater from being channeled down the length of the road segment. The subsequent deep scouring of the exposed road surface routes significant quantities of sediment to the stormwater and stream network, and

toward the marine environment (Ramos-Scharrón and LaFevor, 2018). The unpaved road, meanwhile, is badly degraded, but may simply be regraded with new sediment material, which allows the process to repeat (Ramos-Scharrón and MacDonald, 2005). Generally speaking, similar processes associated with impervious surfaces and steep terrain can reasonably be expected to operate across the Virgin Islands, with the exception of Anegada.

Besides suspended sediments, surface waters of the Virgin Islands may be impaired by nutrients or pathogenic bacteria. A large proportion of homes and businesses in the Virgin Islands use septic wastewater systems, but a 2011 report determined that the conventional septic system, widely used in the Virgin Islands, is inappropriate to the soil type (Cadmus Group, 2011). As a result, and also because of poorly maintained wastewater systems in general, quantities of effluent and wastewater may seep into surface waters and nearshore waters in particular areas (DPNR, 2004; Mather, 1971). Nutrient fluxes in streams may also be dictated to some extent by the seasonality of nutrient buildup, particularly of nitrogen, during the dry season, and a "flush" of soil surface nutrients in the initial pulses of runoff that come with the onset of rainy season (Lancellotti and Hensley, 2025). Many of the dominant species of the widespread secondary forest cover of the Virgin Islands (e.g. *Leucaena leucocephala*) are leguminous (Daley, 2010), adding further to the likelihood that a seasonal accumulation of surficial nitrogen is "flushed" by overland or shallow subsurface runoff flows into the stream network.

Groundwater quality may suffer from leaching of nutrients or pathogens from wastewater as mentioned above, but also suffers throughout the Virgin Islands from high dissolved solids and chloride content (Cederstrom, 1950; Martin-Kaye, 1954; Miller et al., 1999). Saline intrusion from seawater, as well as connate water from overextraction of individual wells, can

significantly impair groundwater resources (Li et al., 2020). The degree of saltwater intrusion into wells is generally determined by the potentiometric gradient between the freshwater lens and the surrounding seawater—if the gradient reverses near the coast, seawater will intrude into groundwater supplies and result in saline wells, which is occasionally reported in the Virgin Islands (Robinson, 1972). A few potentiometric maps were produced for the USVI by the USGS in 1987 (Torres-Gonzales and Rodriguez-del-Rio, 1990), and chloride concentrations were mapped by Gill and Hubbard (1986), but no up-to-date information is available (an effort is currently ongoing in the USVI to update these data for the Kingshill Aquifer). Baseflow in guts is of similar quality to groundwater (Ward and Jordan, 1963).

Inter-island comparisons

In an overarching sense, one of the most important knowledge gaps is that research and monitoring studies have mostly focused on the USVI, rather than the BVI or Vieques and Culebra. Important exceptions are the works on hydrology of the BVI by Martin-Kaye (1954), Jordan (1966), and Mather, 1971. Although the findings of the reports and studies done in the USVI are transferrable to a certain extent, the intrinsic differences between these islands and those of the USVI are potentially important (Mather, 1971). For example, Vieques, although large, has a relatively small population with very limited groundwater withdrawal (Torres-Gonzales, 1989). This is partly because of the longstanding presence of the U.S. Navy on the island (1943–2003), where large areas of land (76% of land area) were used as munitions testing ranges (Torres-Gonzales, 1989). The net result of this has been that large areas of land remain undeveloped, and interestingly, well water salinity has been reported to be lower than other islands (Torres-Gonzales, 1989). Culebra, with a low topography and thus low rainfall, relies

mainly on rooftop catchment and water transport from mainland Puerto Rico for its water supply (Jordan and Gilbert, 1976). A few wells exist in alluvial valleys of Culebra as in other islands, and Jordan and Gilbert (1976) report 18 surface ponds for livestock in dammed stream courses, similar to those of St. Croix. The smaller islands across the Virgin Islands (e.g. Virgin Gorda, Jost van Dyke, Water Island, Beef Island) normally have much more restricted water supplies apart from rainwater catchment, and the small, mostly uninhabited cays (e.g. Inner and Outer Brass, Hans Lollik, Thatch, Great Tobago, the Dog Islands, etc.) typically have no reliable freshwater resources at all, though most reports only mention them in passing (Damman and Nellis, 1992; Martin-Kaye, 1954).

In general, the climate and geology of all the islands are broadly similar, but the population densities, elevation, land area, and land use regimes are not always comparable from one island to the next. St. Croix, geologically distinct from the rest of the archipelago, merits special consideration to some degree, with its unique hydrogeological scenario of mixed carbonate and volcanic material (Nagle and Hubbard, 1989) making findings from St. Croix only partially transferrable to the rest of the islands. That being said, the mountainous volcanic zones and alluvia of coastal embayments are broadly similar across all the islands besides Anegada (Torres-Gonzales, 1989), and hydrological findings related to these zones are likely broadly applicable to the surrounding region (Jordan, 1966).

Areas for Study

With water in limited supply across the Virgin Islands, many critical decisions regarding the future development of the archipelago hinge on how land and water resources are managed. Yet, as the previous section makes clear, data-driven decisions are difficult in the current

environment where little up to date, synthesized information exists beyond basic descriptions. Soil hydrology, concerned with the interactions of water and soils at various spatial scales, is well positioned to provide targeted information to help address some of the most pertinent data gaps. Three areas for study are described below which lead to the soil hydrological studies presented in this document.

Agricultural soil water management

Agriculture in the Virgin Islands was historically the most important economic sector (Dookhan, 1994). With the onset of industrialization and global tourism economies, the Virgin Islands as a whole began a process of agricultural abandonment as the islands reoriented their economies around finance (especially the BVI), heavy industry (St. Croix), and tourism (all of the Virgin Islands; Johnston, 1987). The net result of this was the withdrawal of major public sector support for agriculture: in St. Croix for example with the collapse of the Virgin Islands Corporation (VICORP) cooperative homesteading system of sugarcane agriculture that was prevalent in the first half of the 20th century (Boyer, 2010; Jordan, 1972). The next phase of agriculture in the islands was centered on cattle and other livestock production (which led to the construction of many of the ponds discussed above; Jordan, 1975), but droughts, general disinvestment, and changing economic realities have seen this sector continually shrink (Gould et al., 2015). Agriculture today in the Virgin Islands is focused on smallholder fruit and vegetable production or market gardening, and is a small portion of the total economy (for instance: $3.3 million of agricultural sales were reported in the USVI in 2018; the gross domestic product of the USVI is $4.7 billion). Some 10% of USVI land area is in active production, but more than half of this is pastureland in St. Croix (USDA-NASS, 2018). It is recognized that

approximately 97% of food is imported to the USVI (and likely a similar figure in the rest of the Virgin Islands, as the situation in general is common throughout the Caribbean region; Agricultural Plan Task Force, 2021; Beckford and Campbell, 2013). This situation has prompted calls for improved food sovereignty through boosting local production, culminating in the USVI Agricultural Plan of 2021. This document, adopted by the USVI legislature, calls for expanding food production to 35% of the total by 2040, a severalfold increase that would necessitate 2% growth every year (Agricultural Plan Task Force, 2021).

For such ambitious goals to have improved chances of being met, the physical and environmental barriers to production must be urgently addressed, in addition to the various administrative, economic, and social obstacles (DPNR, 2024). In the scope of our study, soil water management in agriculture is a critical area of need to boost production with limited water resources. In the USVI in 2018, of 556 ha of cropland harvested, only 236 ha was irrigated (USDA-NASS, 2018), which is representative more of the lack of capacity (irrigation equipment, and water distribution, and water supply) than of lack of water demand. This claim is backed by the repeated complaints of the farmers themselves about lack of adequate water supplies (Agricultural Plan Task Force, 2021). This is especially serious when demands on the Virgin Islands water supply from other sectors are taken into consideration, such as tourism and heavy industry (Francois et al., 1983). The risk of overpumping due to agricultural irrigation, though minimal today, is a common problem in small islands where agriculture is more dominant (Amadio, 2014; White et al., 1999) and should be taken seriously by any effort in the Virgin Islands to expand production. Farmers today and historically have mainly made use of wells and rainwater catchment cisterns for irrigation (Jordan, 1975; USDA-NASS, 2018). Any effort to expand actual recharge, catchment or storage is welcome (e.g. building or restoring more small

pond reservoirs; Ahmad, 2015), but the intrinsic supply constraints outlined in the previous section make any feasible on-farm water conservation measures highly preferred to boost production.

Certain of the most valued and culturally relevant food crops in Caribbean communities also have a high water demand, intensifying the needs outlined above (Scott, 2020). For example, plantain (*Musa* spp.) is a major staple, high in demand across Latin America and the Caribbean (Dita et al., 2013), but requires significant soil water to achieve optimal harvests (Carr, 2009; Turner et al., 2007). Assuming the water supply available to any given farmer is fixed (or at least costly to expand), alternative strategies that use water more efficiently become the primary means of conserving water for a Virgin Islands farmer. One of the most common of these are the micro-irrigation systems that nearly all farmers have adopted to some degree over recent years (Ferrarezi et al., 2020). Another well-known strategy for conserving soil water, though, is mulching (Tuure et al., 2021). Mulching practices, compared to micro-irrigation, are less common in the islands. We suggest two possible factors that influence this. First, the repeated need for mulch material as an input implies capital or labor cost which is already in shortage for Virgin Islands farmers (Agricultural Plan Task Force, 2021). Second, farmers, like all adopters of techniques, require some social proof of the likely success and worth of the innovation (Lindner et al. 2016). Micro-irrigation, as an example, is now considered standard practice, and other forms of irrigation (other than hand watering) have become almost nonexistent, but this only followed years of experiments and demonstrations by the University of the Virgin Islands Agricultural Experiment Station in the 1980s and 90s (Ferrarezi et al., 2020), and research and extension efforts in that domain continue to present.

The theoretical benefits of mulching for soil and water conservation purposes range widely, and are too numerous to completely enumerate. A few possibilities relevant to the case of production in the Virgin Islands: the ability of mulch under certain conditions to promote groundwater recharge (Banihabib et al., 2018), improve soil physical properties (Cook et al., 2006; Fér et al., 2022; McIntyre et al., 2000), resist soil erosion (Ma et al., 2022; Maass et al., 2018), and improve crop growth and soil water retention (Tuure et al., 2021). To provide a practical experiment for the cultivation of plantain under mulch covers, several areas of inquiry should be addressed. First, any sources of easily available or renewable material for mulch should be sourced, to alleviate the input constraint mentioned above. A good candidate for this is *Callisia repens,* a groundcover species found in the wilds in St. Croix, which can independently spread under a canopy (Marconi and Armengot, 2020) and is used as a living mulch in agroforestry systems elsewhere (Puertas et al., 2008). Second, the effect of any mulch on two crucial elements of the soil water balance should be investigated: interception and evapotranspiration. Interception is already known to be a significant factor in banana and plantain crop canopies (Jiménez and Lhomme, 1994; Pak, 2013; Zhang et al., 2021), and mulch covers themselves obviously intercept throughfall to varying degrees (Cook et al., 2006). Evapotranspiration (ET) was shown to be reduced under plastic mulch in a banana crop (Santosh and Tiwari, 2019), but ET is often a difficult variable to measure directly. Still, it can be modeled through the use of soil water and weather monitoring, reasonable documentation of the plantain crop, and soil hydraulic modeling (Graham et al., 2018), such as the HYDRUS-1D soil hydraulic model (Šimůnek et al., 2005). Using this approach, it may be possible to describe the water budget of a plantain crop with and without various mulch covers, which we will investigate further in Chapter 2.

Ephemeral stream hydrology

Runoff generation in Virgin Islands watersheds is important for soil and water conservation. Runoff contributes directly to stormflows in the guts of the Virgin Islands and can cause flooding (Gardner et al., 2008), carry pollutants (Lancellotti et al., 2023; Lancellotti and Hensley, 2025), and lose freshwater from the island's water budget as discharge to the sea—all of which are common issues in the Lesser Antilles (Pratomo et al., 2016; Robins and Lawrence, 2000; Stapel, 2023). The portion of total runoff from a watershed compared to total rainfall over the area, called the runoff coefficient, is an extremely useful statistic for managers to track, but cannot be accurately predicted without an understanding of the ephemeral stream hydrology of Virgin Islands guts. This is especially true given the variability of weather conditions in this region (Burgess et al., 2015). Understanding the soil hydrological mechanisms of runoff generation in a watershed can permit more intelligent land management decisions that have desired effects on runoff and the conservation of soil and water, since changes in these aspects of a watershed are very likely to have an effect on the water regime (Muñoz-Villers and McDonnell, 2013).

Not much beyond generalization is currently known about runoff generation in Virgin Islands ephemeral streams, other than the effect of roadways on runoff initiation, which has been described by Ramos-Scharrón and LaFevor (2018), primarily in St. John. Estimates and reports by past experts (Jordan, 1975; Robinson, 1972) and comparisons with nearby islands must suffice before more detailed data is collected. In Sint Eustatius (Netherlands), a small island 192 km east of St. Croix, a study of runoff generation found that surface water flows persist only in the presence of shallow impermeable rock layers (of the Quill volcano), and that infiltration was

driven by soil preferential flow pathways (Stapel, 2023). In Grenada, soil porosities ranging from 0.4–0.58, and soil hydraulic conductivities (K_{sat}) from 10–69.6 mm h^{-1} were reported by Pratomo et al. (2016), highly dependent on land use types, which they identify as a driver of flash-flooding. Both Sint Eustatius and Grenada are volcanic islands, closer to the active forearc of the Caribbean chain, and thus likely to have steeper slopes and less weathered mineralogy (Speed, 1989), but these observations are nevertheless helpful contextualization of runoff generation in the Virgin Islands. The only estimates of runoff coefficients for Virgin Islands watersheds are found in the 1970s reports of Jordan and his colleagues, which range from 0.01 to 0.09 of total precipitation, and are by their own admission roughly estimated rather than measured directly (a preliminary study of the whole Virgin Islands is found in: Ward and Jordan, 1963; of Tortola: Jordan, 1966; of St. Croix: Jordan, 1972; Jordan, 1975; of St. Thomas: Jordan and Cosner, 1973; of Culebra: Jordan and Gilbert, 1976).

Runoff generation processes have been documented worldwide. Of particular interest is the identification in many catchments of a "runoff threshold" or "initiation" of flow, where researchers identify some set of hydrometeorological variables that must precede the observation of runoff or streamflow (e.g., Penna et al., 2011; Serrano-Notivoli et al., 2022; Wang et al., 2022). Though it is useful here to compare to regions that may have similarities with the Virgin Islands, caution is also warranted. In particular, it may seem appropriate to compare the hydrology of the Virgin Islands to semi-arid regions, since both have high-intensity storms, relatively low total rainfall, high evaporation rates, and ephemeral streams (Herndandez et al., 2000), but Farrick and Branfireun (2014a), who focus on tropical dry forests (the dominant ecosystem type in the Virgin Islands), argue against such comparisons to arid regions. If we restrict our comparisons to tropical dry forests or places nearby to the Virgin Islands, there is still

an indication that runoff thresholds may be an important factor to understand. (in dry forests of Mexico: Farrick and Branfireun, 2014b; and in Puerto Rico: Larsen et al., 1990). If runoff thresholds can be identified in Virgin Islands watersheds, this provides better prediction of flow on the one hand, and on the other, approaches a mechanistic understanding of runoff, especially if thresholds between various catchments can be compared and related to soil hydrological variables. Comparisons of these thresholds in time may also be valuable, because of the large interannual variability of climates in this region (Maass et al., 2018).

Besides identifying a runoff threshold, finding the specific type of runoff that is more active in a watershed at a given time is also useful. Types of runoff flows are normally divided into three categories: surface flow generated by rainfall intensities greater than infiltration capacity (infiltration-excess or "Hortonian" flow); surface flow generated by rainfall on soils with pore spaces already saturated, or saturation-excess flow, and finally, subsurface stormflow (Wang et al., 2020). This last flow type, subsurface, challenges the use of the word "runoff," a point made by Beven (2021), but most hydrologists continue to group subsurface stormflow (called stormflow to distinguish it from baseflow) as a kind of runoff for practical purposes (e.g. Mirus and Loague, 2013). Still, distinguishing the type can be extremely important. Soil hydrophobicity, for example, may be an important factor in tropical dry forest watersheds during the dry season (being linked to Hortonian flow), while saturation-excess flows become important in wet season (Farrick and Branfireun, 2014b). In other cases, subsurface flows dominate and actually push "pre-event" water from the soil water into the hydrograph. Beven (2021) argues this occurs much more commonly than classical hydrology usually allows, and Farrick and Branfireun (2015) report this effect in a tropical dry forest in Mexico. The seminal hydrological paper by Hewlett and Hibbert (1967) that introduced the concept of "variable source areas,"

among other things, also supports the idea of pre-event water being an important, often neglected component of hydrographs – especially in catchments that bear similarities to the Virgin Islands (i.e. small, forested catchments).

In practice, actual observed runoff and streamflow will not be attributable to only one type of flow, but is better visualized as a spectrum between the three types (see: Dunne, 1978; Mirus and Loague, 2013). A few soil hydrological parameters and hydrogeological parameters are repeatedly confirmed in research to be the main governing factors for the type of flow. The saturated hydraulic conductivity, K_{sat}, is commonly cited (Mirus and Loague, 2013), and this variable also has an influence on the "wetting-front velocity," which is described as influencing runoff generation through subsurface pathways (Singh et al., 2021). Meanwhile, soils with very high stone contents (common throughout the islands) may have higher than expected K_{sat} because of the macropores formed in between irregular stone shapes that resist compaction (Naseri et al., 2019). Also important is the soil water retention curve, i.e., the parameters of the van Genuchten (1980) equation, which link watershed-scale dynamics to soil hydrological properties (Mirus and Loague, 2013). Finally, the level of groundwater can be extremely important in ephemeral systems, promoting streambed infiltration when low, and saturation excess flow when high (Gutiérrez-Jurado et al., 2019).

This distinction between losing and gaining streams is crucial in ephemeral stream systems (Jasechko et al., 2021). Ephemeral streams by definition are losing streams most of the time, but in periods of soil saturation, or with a perched water table, baseflow, lateral flow, and saturated streambed conditions may persist for weeks or months, with important implications for hydrologic connectivity. A common hydrologic feature of guts all over the Virgin Islands appear to be rocky slopes of upland areas that see runoff generation and sustained streamflow relatively

easily. Then, these guts interface with the alluvial coastal zone, where an alluvial (i.e. Quaternary) unsaturated zone absorbs all streamflow (Mather, 1971) — disrupting ridge-to-reef connectivity (Gill et al., 1997). Therefore, understanding runoff generation in various conditions in Virgin Islands watersheds can also help predict when important pulses of pollutants or freshwater are released to the marine zone (Lancellotti and Hensley, 2025). Equally, understanding the dynamics of the unsaturated hyporheic zone may improve estimates of groundwater recharge (e.g. Al-Amri et al., 2023), just as reliable estimates of baseflow give insight into groundwater loss to the surface. These research needs and promising benefits of results motivated our study of runoff generation in Salt River, presented in Chapter 3.

Watershed-scale erosion and sedimentation

A primary water quality concern in the Virgin Islands is sedimentation, which has three negative impacts: loss of productive soil, siltation of reservoirs, and degradation of surface water and marine water quality, as discussed above. Though suspended sediments are recognized by local governments as problematic (e.g., DPNR of the USVI considers sediment nonpoint source pollution; S. Pickett, pers. comm.), no wide-scale monitoring (such as in Hawaii; Izuka et al., 2010) or even estimation exists of the rates of erosion or sedimentation within the Virgin Islands (Lancellotti and Hensley, 2024). Here, we contrast erosion studies that measure or estimate rates of soil loss from land, to marine sediment studies that focus on sediment settling rates in a marine environment (examples in the Virgin Islands of the latter: Canoy et al., 1983; Gray et al., 2008; Gray et al., 2017; Larson et al., 2015; Nemeth and Nowlis, 2001; Oliver et al., 2011; Oliver et al., 2018). Correlations presumably exist between this and terrigenous erosion, but

direct linkage between the two kinds of measures is difficult without a better model or mechanistic understanding of erosion processes on land (Rogers and Ramos-Scharrón, 2022).

Erosion studies can be carried out at the benchtop, plot, field, watershed, or whole-island scale, but few such studies have been attempted within the immediate region; though we enumerate a few notable exceptions here. In one study (Stryker, 2023), runoff flumes were constructed to test the ability of vegetative buffer strips to accept run-on and slow sedimentation, which found that a weedy fallow ground cover outperformed a young vetiver planting in this respect. In an example of a field-scale study, Madramootoo et al. (1999) showed that terraced banana cultivation in St. Lucia, as opposed to strip-cropped, contour drained, or conventional hillside cultivation, produced less runoff and soil loss than the alternatives. Though the volcanic slopes of St. Lucia are generally steeper than Virgin Islands hillslopes, the significant difference made by the cropping system indicates the likely importance of land management practices on soil loss anywhere in the Caribbean basin. This point is underscored by the watershed-scale study of Cox et al. (2006), also in St. Lucia, where it was found that agricultural lands lost some 20 times the soil of a similar, forested catchment. In all these studies, it is not explicitly stated what the mechanisms of runoff generation are. In Stapel's (2023) study in Sint Eustatius, he reported widespread deposition of sediment fans on roadways and near culverts resulting from high flow events and gully erosion on the slopes of the volcano, which he attributed to a restricting bedrock layer causing saturation excess flow. At the island- or basin-scale, Bégin and colleagues (2014) used GIS-modelling to estimate island-wide marine sedimentation in St. Lucia due to land use changes over 15 years, and in Puerto Rico, Gellis et al. (2006) discuss the rapid sedimentation of reservoirs in the Lago Loíza basin of Puerto Rico, also due to land use changes. Rad et al. (2013) estimate erosion rates in the Lesser Antilles over geologic timescales. Finally,

as discussed above, the most extensive literature on erosion in the region comes from Ramos-Scharrón and colleagues over several decades, pertaining to erosion from roads and trails (this corpus of work is summarized in Ramos-Scharrón et al., 2023). Though these studies are few overall, are located only in certain island systems, and vary by scale, a consistent theme emerges of an intrinsic vulnerability to erosion due to the prevailing climate, topography, and soils, while highlighting the key role of human land use and management that can badly exacerbate these vulnerabilities to erosion.

There are a number of challenges and complexities in studying catchment-scale erosion, some of which relate directly to the runoff-generation processes mentioned in the last section (Collins et al., 2001). Direct field measurements of hillslope erosion often require relatively extensive investments into field structures that are adequately representative and hardy, able to withstand harsh conditions (Peart and Walling, 1988). This has the practical effect of making such studies in challenging terrain comparatively uncommon (as opposed to similar studies carried out on farmland or municipal land on gentle terrain). Another difficulty is correctly identifying source areas of erosion that are representative of the area, which requires a knowledge of runoff generation processes that are themselves a challenge to study (Hsieh et al., 2009; and q.v. previous section).

Besides hillslope erosion, watershed-scale erosion can be complicated by the existence of sediment sinks in the catchment, a process strongly influenced by hydrological connectivity (Boardman et al., 2019). The best example in the Virgin Islands is likely the network of artificial ponds, often built in stream courses (IRF, 2000). Natural salt ponds, frequently found at the mouth of Virgin Islands watersheds, also act as an important sediment sink (Rennis et al., 2006). Land management practices, particularly those geared toward soil and water conservation, also

have important sinking effects (Koshiba et al., 2013; Maass et al., 2018). Such sinks may at times exhibit a flushing behavior that is necessary to understand before simple rates of hillslope erosion can be connected to sediment delivery to the marine zone. Though it is usually possible through stream gauges and suspended sediment sampling to quantify sediment flux over time, at the watershed scale it is difficult to know more about the sources of the sediment observed at the catchment outlet without either a distributed network of representative hillslope samplers or a sediment source tracking technique (sediment source tracking techniques are reviewed in Guan et al., 2017).

Process-based hydrological and erosion models are an attractive option in this context. Such models can simulate the hydrological behavior of a hillslope or watershed, from inputs such as slope, soil, and weather from geospatial datasets (Juliá et al., 2021), remote sensing (Melville et al., 2022), or observation networks on the ground to predict the flux of water and sediment throughout a catchment. A large number of hydrological models exist and are used for various purposes (Migliaccio and Srivastava, 2007), but specific additional parameters and subroutines for erosion models can incorporate soil physical characteristics as well as, crucially, land use, management, and even sediment sinks, to accurately model sediment yields once calibrated. A promising option for these capabilities is the Water Erosion Prediction Project (WEPP) model (Laflen et al., 1997), which can simulate water flux and sediment yields at both the hillslope and catchment scale and includes a wide variety of parameters for land use, management, and channel impoundments (Flanagan and Livingston, 1995; Lew et al., 2022).

Adopted successfully for both agricultural and forested catchments (Dobre et al., 2022b), the model has been used elsewhere to guide management and land use decisions aimed at reducing erosion (Dobre et al., 2022a; Srivastava et al., 2020). Though not yet applied in the

Caribbean, WEPP could prove useful to address the challenges of erosion in the region. To guide land and water use practices in the Virgin Islands with scientific decision making (called for explicitly by the USVI's Comprehensive Land and Water Use Plan, for example; DPNR, 2024), models of this kind should be applied and calibrated for regional use. For example, though total maximum daily loads (TMDL) would be useful, as a metric used successfully elsewhere in the world to guide management (Miller et al., 2023), they have not seen actual use in the Virgin Islands because of a lack of information. As a ridge-to-reef process (Rogers and Ramos-Scharrón, 2022), soil loss and sedimentation must be understood on a holistic level for meaningful progress to be made in management soil and water resources of the Virgin Islands.

Soil Hydrological Studies for the Virgin Islands

A clear theme in this literature review has been a general lack of information and detailed datasets related to these issues in the Virgin Islands. A relatively complete account of the various research needs and knowledge gaps was compiled recently by Lancellotti and Hensley (2024), which we have drawn from extensively in this chapter. A uniting theme, however, is that the methods and discipline of soil hydrology can be helpful in resolving many of the underlying water resource challenges facing the Virgin Islands.

The methods and datasets of soil hydrology can often overlap across scales. Thus, similar techniques and data types can be applied to the three areas of study outlined above. In the following chapters, we describe three soil hydrological studies carried out in the Virgin Islands with the aim of providing information that can improve the management of land and water resources in the islands. Though all three studies are based on the island of St. Croix, it is hoped that many of the findings will be useful across the archipelago and wider region. The first study,

a field-scale investigation of mulch covers and modeled soil hydrological effects under a plantain crop, is geared toward the agricultural water resource concerns of the islands. The second, a watershed-scale study of runoff generation processes in an important watershed, is intended to provide better understanding of the ephemeral stream hydrology of Virgin Islands guts. The third, which applies the WEPP model for the first time to the Virgin Islands, provides a foundation for future calibration efforts and gives an indication of the likely practical uses of this model for land and water managers in the region.

Chapter 2
Soil Water Regimes in Tropical Plantain Production under Organic and Living Mulches

Abstract

Plantain is a major food crop in the Caribbean that requires significant water input despite persistent regional droughts. When water is limited due to persistent drought, smallholder farmers frequently make use of on-farm inputs such as mulch to improve production. We investigated the effects of a hay mulch and a living mulch groundcover (callisia; *Callisia repens*) compared to a bare soil control on the crop growth, yield, and soil water responses of a plantain (*Musa* spp.) crop. The intended study duration was three years, but only the first harvest was ultimately included due to the detection of *Fusarium* fungus in the field and subsequent early crop termination. We did not detect crop growth or yield differences according to mulch covers with one year of data. Similarly, no mean soil water content difference or measured soil physical differences emerged according to mulch treatments, but callisia living mulch did demonstrate a significantly longer lag time from rainfall to soil water response. Regression of discrete rain storms by total rainfall on magnitude of soil water response indicated the callisia ground cover may have had a higher interception storage, possibly explaining the observed lag times. We also used external optimization of van Genuchten soil hydraulic parameters in HYDRUS-1D to confirm that mulch treatments did not significantly influence estimated soil hydraulic parameters, leaving interception as the most important hydrologic difference between callisia and the other treatments in water balance simulations. The extended establishment time of the living mulch, combined with the possible increase in lost precipitation to interception, necessitates caution in using living mulch species compared to organic mulch.

Introduction

In the Caribbean and Latin America, plantain (*Musa* spp.) is a culturally important staple food crop (Dita et al., 2013), and banana and plantain, more generally, are major crops across the tropics (Scott, 2020). In the Caribbean archipelago, extended droughts and limited water availability are commonplace (Giannini et al., 2001; Moraes et al., 2022), even as plantain has a relatively high water demand compared to other crops (Carr, 2009; Turner et al., 2007).

Farmers in resource-limited conditions, such as smallholders on small Caribbean islands, may often turn to on-farm inputs or management practices to address a lack of resources, such as irrigation water or labor (Beckford and Campbell, 2013; Scott, 2020). Mulching under a plantain crop is an attractive and commonly used practice to both reduce total weed pressure and manual weeding time, as well as to retain soil water, reduce irrigation demand, and improve total yield and crop growth (McIntyre et al., 2000; Tuure et al., 2021).

Living mulches offer the opportunity for a self-renewing mulch that requires less attention and input, even than conventional on-farm mulches such as hay straw (Andrews et al., 2020). Mulches also offer soil conservation benefits, potentially slowing or preventing runoff or increasing deep drainage and groundwater recharge (Banihabib et al., 2018; Ngetich et al., 2014). Caribbean islands suffer from problems associated with direct runoff from land to sea, with detrimental impacts on marine life and loss of soil and freshwater resources from the land surface (Rogers and Ramos-Scharrón, 2022).

On the island of St. Croix (U.S. Virgin Islands), farmers face low-resource conditions in all major respects: land, labor, agrochemicals, irrigation supplies, and water availability (Agricultural Plan Task Force, 2021). Combined with the island's erratic rainfall patterns (Gill et al., 2004), mulching for an improved water balance could potentially impact the feasibility of future plantain production on the island. The adoption and diffusion of agricultural innovations

(Lindner et al., 2016) such as optimal mulching strategies may help mitigate issues related to crop production in drought conditions.

Callisia repens (Jacq.) L. is a locally available plant (Fig. 2-1) in the wilds of St. Croix. Typically found as an understory plant in forests, it has a low, creeping growth habit and can propagate easily by vegetative fragments being distributed on the surface of wet, bare soil (Puertas et al., 2008). It has been used occasionally as a living mulch on the island by farmers in plantain production, and its use has been documented in agroforestry systems elsewhere (Marconi and Armengot, 2020), but no known study on its soil hydrological effects exists. This study was conducted with the goal of investigating the soil hydrological effects of mulching strategies, including living mulch, in plantain production on the island of St. Croix.

Objectives

1. Quantify yield effects and changes in plant growth and phenology from hay and living mulch practices in plantain production
2. Determine the effect of mulch cover on soil water content response to rain events in terms of infiltration and soil water retention

Methods

Experimental setup and measurements

Site description

The experiment was conducted on the island of St. Croix, U.S. Virgin Islands, at the campus of the Agricultural Experiment Station (University of the Virgin Islands School of Agriculture) in experimental field plots (17.7204° N, 64.7948° W, 28 m elev.). The climate of St.

Croix is considered a “tropical savanna climate with dry winters” according to the Köppen climate classification. St. Croix has a distinct wet-dry seasonality, with the dry months generally extending from December through July (with a weak wet period sometimes occurring in May or June) and the rainy season extending from August through November (Larson et al., 2015). Climate data from the St. Croix airport 1972–2022 (approximately 2 km south of the experimental site) indicates a long-term average annual precipitation of 962 mm (NOAA, 2023).

Pre-experiment soil characterization

The soil at the experimental site is Sion clay, a calciustoll (Mollisol) of marine origin with a calcium carbonate subsoil typically beginning at 30–41 cm profile depth (USDA-NRCS, 2024). Before planting and plot layout (on 4 February 2021), pre-experiment soil sampling was conducted to characterize the soil at the experimental site. The field was defined using geographic information systems software (QGIS; v.3.34.7), and five sampling points were chosen according to a stratified random sampling design. At these five sites, soil was sampled to a depth of 100 cm using an auger, and a soil profile characterization was carried out according to Munsell color classifications, with depths of various colorimetric horizons recorded. Gravimetric soil water content (θ_g) was recorded for aggregated samples from each horizon in each of the sampling locations. Consistent with USDA soil survey information, the pinkish-white carbonate layer was observed at 29, 36, 37, 29, and 36 cm. Soil water content information and profile coloration with depths from this pre-experiment survey are summarized in Table 2-1.

Experimental design and management

On 23 April 2021, plantain (*Musa acuminata* x *M. balbisiana*, AAB, cv. 'Maricongo') tissue culture propagules were planted into roto-tilled soil (to 30 cm depth) with equal spacing of 1.5 m. Each plant was uniformly irrigated with a drip emitter at the plant base, and water use was tracked throughout the experiment with an in-line flow gauge, irrigation timer, and regular random checks of individual emitters to confirm standard flow rates. Liquid fertilizer (20-20-20 and chelated iron) was applied through drip emitters as necessary (total of 1,008 kg ha^{-1} 20-20-20 and 13 kg ha^{-1} chelated iron applied over eight months). From planting to 9 December 2021, a total of 570 mm of irrigation was applied across the field (mean of 2.5 mm d^{-1}), or 1,323 L $plant^{-1}$. An automatic weather station at the site was used to collect local weather data (ATMOS 41, Meter Group, Pullman, WA, USA). This weather station became operational on 8 October 2021. Weather data before this date was collected from a separate weather station also on the experiment station grounds. A total of 527 mm of precipitation was recorded during the experiment.

The experiment was divided into plots according to a randomized complete block design (RCBD) with four spatial replicate blocks and three treatment levels in a single-factor design with 12 plots. Each plot had dimensions of 7.5 m by 15 m (50 plants per plot), and a total cropping area of 0.14 ha. Buffer plants were planted around all sides of the field, with three buffer rows planted on the eastward side (to serve as a windbreak from prevailing winds). These plants were not considered part of any plot, and no data was collected from them.

The three treatments were: 1) a control (bare soil) treatment, which was regularly hand weeded and maintained weed-free; 2) hay mulch, which was applied with 20 cm thickness and 100% ground coverage (Fig. 2-2); and 3) a living ground cover, *Callisia repens* (a.k.a "turtle vine" or "callisia") propagated to the base of plantain plants and allowed to grow over the soil

surface to create a living mulch. Other weeds competing with this ground cover were controlled through hand weeding. Mulch treatments were applied on 27 May 2021 (the establishment period for callisia followed this). Callisia propagates easily by placing cuttings in contact with a moist soil surface, so cuttings were placed near the drip emitters at the base of plantain plants. Hay mulch was sourced from a local farm; callisia was sourced from native stands in the forest elsewhere on the island.

Measurement of crop growth, agronomic performance, and yield

Crop growth traits were measured (excluding plants at the edges of each plot) approximately monthly throughout the cropping season. Crop growth traits measured were: plant height, measured from the soil surface to the crown of the plant; canopy density using a spherical crown densiometer (Forestry Suppliers, Jackson, MS, USA); and chlorophyll content index (CCI) to assess leaf chlorophyll status, measured at the second mature leaf (CCM-200plus, Opti-Sciences, Hudson, NH, USA). As the cropping season progressed, suckers began to appear around the base of each plant, which were counted at each monthly data collection. When flowering and fruiting were first observed, the proportion of plants flowering or fruiting in each plot was also recorded.

Harvesting began on 8 April 2022 and continued to 13 June 2022. At each harvest date, the fresh weight of plantain bunches from each plot was recorded (excluding edge plants). Plantain pseudostems from harvested plants were cut down, and plant material was allowed to rest on the soil surface. Although ratoon crops (subsequent crops from the same plots after the first harvest) were planned in this experiment beyond the plant crop (the first crop harvest), *Fusarium oxysporum* f. sp. *cubense* was detected in plant tissue in early 2022, and the

experiment was discontinued after the final harvest. The presence of *Fusarium* did not become apparent until after fruit set, and the harvest yield was not apparently affected, though the infection had progressed significantly by the time of crop termination in summer 2022.

Soil particle size distribution measurements

Before planting, soil samples were collected at seven random locations throughout each plot at depths of 20 cm and 50 cm, and were analyzed according to standard particle size determination protocols using sieves and hydrometer (PARIO, Meter Group, Pullman, WA, USA). The 7 samples collected for particle size characterization were aggregated at each depth across plots and taken to the lab for soil texture analysis. To determine particle size distribution, soil samples were air dried and passed through a 2 mm sieve and were then treated with hydrogen peroxide (30% solution) to remove organic material until effervescence was no longer observed in a water bath at 80 °C. Once the oxidation process was complete, samples were treated with a chemical dispersant (sodium hexametaphosphate, 5 g L^{-1}) and placed on a laboratory shaker for 24 h for mechanical dispersal. After removal of organic matter and aggregate dispersal, the samples were diluted to a volume of 1 L and particle deposition rates were measured using a PARIO automated particle size analyzer (Meter Group, Pullman, WA, USA), including wet sieving of the coarse fraction and oven drying of effluent for the fine fraction, to calculate particle size fractions of sand (> 50 µm), silt (2–50 µm), and clay (<2 µm). Particle size fractions are shown in Table 2-2. Mean particle size classes at 20 cm were: 37.4% sand, 11.9% silt, and 50.4% clay, and at 50 cm: 49.4% sand, 13.8% silt, and 36.9% clay.

Soil hydrological measurements

To measure soil water content *in situ*, volumetric soil water content sensors were installed in each plot at 20 cm and 50 cm depths (TEROS 10, Meter Group, Pullman, WA, USA). These were installed in the inter-row position, equidistant (approximately 1 m) from all plants and drip emitters in the center of each plot (see inset, Fig. 2-2). Volumetric water content ($cm^3\,cm^{-3}$) was recorded every 15 min. Sensor installation was completed on 28 July 2021. The two depths were chosen to allow measurement from within the A and C horizons of the soil profile and to allow measurement within and below the typical 45 cm root zone of plantain reported in Puerto Rico (Irizarry et al., 1981).

Twice during the cropping year (late November 2021 and late April 2022), field measurements of surface saturated hydraulic conductivity (K_{fs}) were made using an infiltrometer (SATURO, Meter Group, Pullman, WA, USA). Measurements were made twice per plot in the 2021 measurements and once per plot in the 2022 measurements. The point of measurement was the inter-row position, equidistant from plants in the interior of each plot (Fig. 2-2). During the harvest period (27 April 2022) undisturbed surface soil samples (excluding mulch material) were taken at 8 randomly chosen locations in each plot. Distances from plantain pseudostems were randomized once for each of the 8 samples and kept constant across plots. These samples were used to determine gravimetric soil water content and porosity. In addition, at harvest, undisturbed soil samples (three per plot) were taken at 20 cm and 50 cm depths to be used to determine porosity and inferred θ_s (soil water content at saturation).

Data analyses

Analysis of crop growth, porosity, surface soil water content, and infiltration rate

Measures of agronomic performance (crop height, CCI, canopy density, sucker production, percentage flowering, fruiting, and yield), porosity, surface soil water content, and infiltration rate were analyzed by a linear mixed-effects model. A repeated structure (plot) was used for all variables except porosity and surface soil water content, which were only measured once (at 369 DAP). Covariance structures for repeated measures models were chosen according to the corrected Akaike information criterion (AICC). Infiltration data from April 2022 was not analyzed due to unacceptably high variances within measurement runs and flux rates exceeding the requirements of the device, according to the SATURO manual. Replicate blocks were treated as a random effect. Significant ($\alpha = 0.05$) effects were further investigated with Tukey's HSD post-hoc testing. All statistical analyses described were performed in R (v4.2.3, R Core Team, Vienna, Austria, 2025; Hothorn et al., 2008; Pinheiro et al., 2022).

Autocorrelation length of volumetric water content

Time-series data of soil volumetric water content (θ) were subjected to several analysis steps. After quality assurance/quality control of the data, the dataset was trimmed to encompass the dates of 10 August 2021 to 8 April 2022 (start of harvesting) to avoid any missing values and the compounding effects of harvest on soil water content. As an initial examination of the temporal structure of θ in each plot, the autocorrelation function from each plot at each depth (20 and 50 cm) was calculated. Autocorrelation functions express the autocorrelation coefficient (the correlation coefficient of a variable with itself) of the measured variable at successive lags (h) from the origin in space or time (in this case, lags were 15 minutes). In each case, the

autocorrelation length (λ) was calculated and recorded. In this variable, a long λ would be associated with stronger buffering against change in the hydrological condition at that depth. Thus, deeper soils would generally be expected to have longer λ, as would higher clay content soils that may retain moisture longer. Autocorrelation lengths (λ) represent the distance (in lags) from an origin at which measurements are no longer autocorrelated (i.e., the autocorrelation coefficient is not significantly different from zero). Autocorrelation length is typically expressed in the autocorrelation function line (Eq. 1):

$$r(h) = e^{-(\frac{h}{\lambda})}$$

where *r(h)*, the autocorrelation coefficient at lag *h*, is equal to e^{-1} (Nielsen and Wendroth, 2003). Once λ was calculated for each sensor depth in each plot, these values were subjected to linear mixed effects modeling as described in above for agronomic variables to determine any significant treatment effects on autocorrelation length.

Delineation of rain events

In order to distinguish discrete rain events in the precipitation dataset, an R function was created to use the 15-minute precipitation observations and delineate them according to the standard parameters of minimum rainless event time (MIT) and a minimum threshold observation for what is considered genuine precipitation. Irrigation events, typically daily, were not included in this analysis because of a lack of any observable response in the soil water content data to irrigation – likely due to the interrow position of the soil water content sensors being outside of the wetting front. Because manipulating these input parameters significantly changes the output of what is considered a rain event, care must be taken to select appropriate input parameters (Dunkerly, 2022). Generally, it is advisable to select an MIT value to allow for

maximum independence of events while minimizing intra-event variability containing long periods of zero-rain observations. Long periods of 24 h or more are sometimes used but typically exhibit high intra-event variability. Molina-Sanchis et al. (2016) propose that an MIT as short as 1 h would allow for acceptable independence due to macropore drainage. For our analysis, we employed the more commonly used 6 h MIT, which is suggested as a balance between high intra-event rainfall intermittency and low independence (Dunkerly, 2015). For the minimum observation of precipitation, a value of 0.63 mm h^{-1} was used, which was reported as the minimum evaporation rate for a wet canopy at night in a Puerto Rican forest (Holwerda et al., 2012). This delineation function used calculates "storm parameters" for each rain event in terms of total precipitation accumulation (mm), average intensity (mm h^{-1}), maximum intensity (mm h^{-1}), event duration (h).

Temporal analysis of soil wet-up responses

Because many delineated rain events nevertheless do not always result in a measurable soil water content response, an analysis of the soil wetting response to delineated rain events was conducted to investigate the effects of treatment on this process. In the 6 h following the end of a delineated rain event (the maximum time allowable to ensure independence from any other delineated event), if the final value of measured θ from a sensor was at least 0.01 cm^3 cm^{-3} greater than the starting value, it was considered to be a wet-up response. This threshold was chosen because it is the maximum accuracy of the TEROS 10 sensor in mineral soil. From this, the proportion of rain events resulting in a wetting response was calculated for each sensor in each plot.

Using the set of all rain events resulting in a soil wetting response, statistics regarding the time delays between precipitation and θ were calculated to provide measures of the time lag by event, depth, and mulch treatment. These statistics included the wet-up magnitude (total increase of θ from first observation to maximum θ in the delineated wet-up event), wet-up duration (time from minimum θ value at the start of the wet-up event to maximum θ value), time from the start of a rain event to peak θ, time from the peak rain observation to peak θ, and time from the centroid of rain observations to peak θ. These measures of lag times were taken from those carried out by Hood et al. (2007) in hydrograph responses of watersheds to precipitation events. The results of this analysis were also subjected to linear mixed-effects modeling.

To determine the influence of rain event parameters (i.e., total accumulation, average intensity, maximum intensity, and duration) and mulch treatments on whether a soil wet-up occurred at each depth, we performed binomial regressions on the binary response variable of "true" or "false" wet-up events, following DeGuzman et al. (2023). In this regression, the primary interest is in the significance of the interaction between a rain event parameter and the mulch treatment, which indicates whether a mulch treatment affects how a particular rain event parameter influences the soil wet-up response. In addition, the overall strength of the main effect of a rain event parameter can be used to classify the overall importance of each of the rain event parameters in determining whether a wet-up response occurs.

Cross-correlation analysis

Cross-correlation analyses were also used in conjunction with the time lag method above (following Hood et al., 2007) to compare results from each technique of the temporal relationship between precipitation and θ response and the relationship between θ at both 20 and

50 cm depths. The cross-correlation function computes cross-correlation coefficients $r_c(h)$ for one time series against a second time series at positive and negative lags *h*. As the distance in both directions increases, $r_c(h)$ falls below the critical value *t* at some lag, given in the equation (Eq. 2):

$$t = r_c \sqrt{\frac{n-2}{1-r_c}}$$

where *t*, the test statistic, is compared to critical values of *t* in a t-distribution for $n - 2$ degrees of freedom, and *n* is the number of observations in the dataset (Nielsen and Wendroth, 2003). This allows any value of r_c at a given lag *h* to be compared to the critical value of *t*, to establish the significance of the cross-correlation at that lag distance.

Cross-correlations between precipitation and soil moisture data at 20 cm and 50 cm depths were performed individually, as were cross-correlations between soil moisture at 20 cm and 50 cm. To compute the maximum period in time for which the conceptually "leading" variable (precipitation) remains correlated with its "following" variable (θ), the lag *h* in that direction was recorded where it fell below the critical value. This was taken as the "length" of correlated time between the leading and following variables, or cross-correlation length, reported in hours for direct comparison with the lag time analyses. If the maximum value of r_c was observed on the other side of zero from expected, it would be taken as a signal that the first variable does not temporally lead the second variable. Once these critical lags were recorded, they were subjected to linear mixed effects modeling by treatment for each variable pair (rainfall with 20 cm moisture, rainfall with 50 cm moisture, and 20 cm moisture with 50 cm moisture).

Soil hydraulic simulations in HYDRUS-1D

External estimation of soil hydraulic parameters in HYDRUS-1D

We used HYDRUS-1D (v4.17; Šimůnek et al., 2005) direct simulation to calculate water fluxes through the one-dimensional soil profile of each plot for comparisons by treatment. HYDRUS-1D is a numerical simulation of one-dimensional water flow in the vadose zone using the Richards equation (Šimůnek et al., 2005). To obtain reasonable initial estimates of soil hydraulic parameters (θ_s, θ_r, α, n, and K_s, of the van Genuchten function; van Genuchten, 1980) for each plot, we began with a pedotransfer function relating particle size fractions to θ_r, α, n, and K_s (Rawls and Brakensiek, 1989). As described above, θ_s was taken to be equivalent to field-measured porosity at harvest time, and particle size fractions of sand and clay are inputs to the pedotransfer function. The resulting values of the soil hydraulic parameters were then used in HYDRUS-1D simulations with two defined layers: 1–30 cm and 31–100 cm, corresponding to typical depths of topsoil and the carbonate subsoil of the calciustsoll at the site. HYDRUS-1D simulations used atmospheric boundary condition data (from the on-site weather station) for precipitation and meteorological variables (for evapotranspiration calculations by the Penman-Monteith method; Allen et al., 1998), and crop growth data by plot, including surface cover fraction, for estimations of root growth and crop water uptake, based on the Feddes et al. (1978) model. Simulations used no hysteresis, free drainage, and allowed runoff.

For all plots, we compared the performance of model runs according to the overall root mean square error (RMSE) between the θ values at both depths predicted by HYDRUS-1D and the observed sensor values. For the hydraulic parameters α, n, and K_s, we used an external optimization process in R using the 'optim' optimization function to sequentially estimate values for these parameters at 20 cm, 50 cm, and again at 20 cm (for computational parsimony) in each plot, optimizing the RMSE. The multi-dimensional optimization method used was 'Nelder-

Mead,' with a convergence tolerance in the RMSE of 0.03 (in units of θ; $cm^3\ cm^{-3}$). Initial estimates passed to the optimization function were taken from the plot with the best-fitting RMSE score, and the upper and lower bounds of optimization were chosen according to ranges of van Genuchten parameters reported elsewhere (Bai et al., 2022; Wang et al., 2014). We used linear mixed-effects modeling as described above to rule out any treatment-associated differences in soil physical properties expressed as hydraulic parameters ($p \geq 0.05$).

Estimation of combined canopy and mulch interception by regression

To estimate the potential contribution of mulch interception to observed differences in soil water response (and in the absence of any other differences in soil hydraulic parameters), we used a method based on Acharya et al. (2020) to use near-surface soil water content data to infer the total interception storage of the crop canopy, groundcover, and the upper layer of soil above the sensor. First, we selected all rain events that resulted in a soil "wet-up" response at 20 cm and had more than 36 h separation from the previous event (in order to exclude any soil moisture responses that may have occurred with an interception storage already partially filled). Among these, to have sufficient data points for linear regression, we pooled rain events across replicates (justified by the lack of soil hydraulic differences among plots) to plot the total accumulation of these soil-wetting rain events (mm) over magnitude ($cm^3\ cm^{-3}$) of soil-wetting response (control $n = 7$; hay $n = 11$; callisia $n = 9$). The resulting y-intercept of linear regression for each treatment can then be taken as an estimate of the necessary threshold of interception storage plus upper soil water storage, which must be overcome to produce a soil-wetting response at the sensor depth. Increases in this y-intercept over the total storage for the no-mulch control treatment were taken to be the additional interception storage provided by the mulch treatment (hay and living mulch).

To produce an estimate of *a* (the interception constant passed to HYDRUS-1D), however, it is also necessary to estimate the actual canopy interception of the plantain crop, so that the additional interception storage provided by mulch (and estimated by differences in the y-intercepts of the regression described above) can be given absolute meaning for soil hydrological simulations. The total canopy interception storage *I* is described by van Dam et al. (1997) as the product of LAI and *a*, and Jiménez and Lhomme (1994) provide an estimated interception storage *I* of a banana crop of 1.9 mm with an LAI of 2 m^2 m^{-2}. We used this published estimate as the starting point, giving 0.95 (1.9 / 2) as the value for *a* in the no mulch control. We used average LAI in each of the two mulch treatments (calculated from surface cover fraction), and for total interception storage *I*, we used the sum of 1.9 and the additional estimated interception storage *I* from the difference in y-intercepts described above. Thus, a value for the interception constant *a* was calculated for each mulch treatment as *I* / LAI to pass to HYDRUS-1D for direct simulations.

Direct simulation of soil water balances in HYDRUS-1D

To provide a simulated water budget by mulch treatment for our experiment, we performed direct simulations in HYDRUS-1D according to the soil hydraulic parameters and interception constants selected above, using an average among replicates for soil hydraulic parameters. Using the weather record for the experimental period, we calculated water fluxes in runoff, interception, evapotranspiration, and deep drainage. The results of this simulation were not statistically compared, as the soil hydraulic parameters were already shown to have no systematic treatment differences, and estimated interception constants could not be generated per plot. Instead, the results of these direct simulations were used to provide additional contextual

information for differences in directly observed behaviors of soil water in response to mulch treatment.

Results

Crop growth, porosity, surface soil moisture, and infiltration rate

The first signs of flowering were observed in the field on 19 January 2022 (271 days after planting; DAP). During the growing season, no statistically significant differences among the mulch treatments were found in any of the repeated measures variables (plant height, leaf chlorophyll, canopy cover, sucker number, and proportion in fruit or flower), indicating mulch had no effect on these plant growth traits (Table 2-3). Similarly, although total plantain yield under hay mulch was 12.2% greater than the control and 38.8% greater than callisia, these differences were not statistically significant ($p = 0.202$). Average bunch weight was also not significantly different by mulch treatment. Because yield was averaged across the season, a single plot-wide measure of yield was used in these statistics (i.e., $n = 12$), potentially contributing the failure to detect a significant effect.

Infiltrometer-measured saturated conductivity (K_{fs}) and surface soil porosity also show no significant differences by treatment. The average porosity of 0.66 cm^3 cm^{-3} is noted to be within expectations for this soil type after tillage based on data from previous experiments (unpublished). Surface gravimetric soil water content, however, measured near the end of the cropping season (369 DAP) was significantly different by treatment ($p = 0.029$), with the control (no mulch) cover having lower surface soil water than the mulched treatments (Table 2-3).

Temporal statistical results

Autocorrelation analysis

The autocorrelation length λ at 20 cm was 9.3 days experiment-wide, on average; no statistically significant differences were detected by treatment (Table 2-4). At 50 cm depth, λ was 11.6 days on average across treatments; no treatment effect was detected in this variable either. The lower values of autocorrelation lengths in the shallower depths indicate that these depths are less buffered against hydrological input and output.

Soil wet-up response to delineated rain events

Across the observation period, 124 rain events were delineated, and of these, 20 events were associated with a detected wet-up anywhere in the experiment (Fig. 2-3). No significant differences according to linear mixed-effects modeling were detected in terms of the fraction of rain events producing a wet-up response by treatment at either depth, nor total magnitude of the θ increase, nor the duration of the increase period (Table 2-4).

However, among the lag times calculated for the delay of rainfall to soil wetting responses, significant differences by treatment were found in all measures of time lag from precipitation to θ response at 20 cm (Table 2-4). In all these cases, the temporal lag of callisia living mulch was significantly greater than that of the no mulch control and the hay mulch cover.

No other measure of cross-correlation was found to be significant except for the cross-correlation (CC) length between 20 cm and 50 cm θ, where the CC length in callisia was greatest at 101.3 days, followed by hay mulch at 59.9 days, which was itself significantly longer than that of the no mulch control at 19.2 days (Table 2-4).

Binomial regression of wet-up response on rain event parameters and mulch treatments

Of the 8 total binomial regression models (for four rain event parameters at two depths), we detected a significant interaction between the rain parameter and the mulch treatment in two, both at 20 cm: total precipitation accumulation ($p = 0.0006$) and maximum precipitation intensity ($p = 0.0366$). In both cases, hay mulch exhibited a different behavior compared to callisia living mulch and the no mulch control, being more responsive in general to total precipitation and maximum precipitation intensity in terms of the probability of resulting in soil wetting, indicating greater responsiveness to these rain parameters (Fig. 2-4).

HYDRUS-1D simulation

Results of van Genuchten parameter external optimizations

After external optimization of fitting parameters α, n, and hydraulic conductivity (K_s), no significant differences by treatment were found in linear mixed-effects modeling, though the effect of depth was significant in all five selected van Genuchten parameters (Table 2-5). The RMSE, which was calculated for both sensor depths simultaneously, was minimized to between 0.021 and 0.023 $cm^3\ cm^{-3}$ after all sequential optimizations were complete. Lines of best fit for each treatment showed a general tendency for the model to overestimate θ in the dry range and to underestimate θ in the wet range (Fig. 2-5). Observed deviations from the 1:1 representing perfect simulation sometimes took a vertical shape (indicating a modeled soil wet-up where none was really recorded) or horizontal (when a soil wet-up was recorded but none was modeled; Fig. 2-5).

Combined canopy and mulch interception estimates

Linear regression of rain events resulting in 20 cm depth soil wet-up more than 36 hours apart provided an estimate of combined canopy, mulch, and upper soil water storage for each treatment, or the water storage that must be satisfied to lead to soil wet-up at 20 cm (Fig. 2-6). If the intercept value for the no mulch control (9.4 mm; $R^2 = 0.75$) is taken as the baseline storage value for crop canopy, residue, and the upper 20 cm of soil, an increase in the value for each mulch can be taken as an estimate of the interception storage I provided by the mulch cover. Thus, I for hay was estimated at 3.4 mm ($R^2 = 0.68$), and I for callisia living mulch was estimated as 12.9 mm ($R^2 = 0.30$). It should be noted however, that any water uptake by callisia, which was not directly modeled, would also contribute to the I term in this analysis.

Results of direct simulation of soil water balances

Soil water balances simulated for each of the three mulch treatments demonstrated the role of the changed interception constant in altering the water balance. Evaporation and transpiration varied little across the treatments, with the combined average ET simulated at 36% of total rainfall, or 185 mm during the measurement period, and drainage (mean 92 mm or 18%) was also similar (Fig. 2-7; note also that this comprises only precipitation, whereas irrigation, having no observed effect on soil water data, was not considered in the simulation. As a result, true ET would also include the irrigation water). Error (water still unaccounted for after all water balance terms were summed) was also similar across treatments, at 3.6% on average. The total interception predicted by the model, however, was proportional to the different interception constants estimated above: 2.4% under no mulch (12 mm), 4.7% under hay mulch (24 mm), and 9.2% under callisia living mulch (47 mm).

Discussion

The overall lack of mulch treatment differences in plantain crop growth and yield (Table 2-3) contrasted with expectations, especially in light of other studies documenting increases in banana biomass production with mulching (McIntyre et al., 2000; Santosh and Tiwari, 2019). However, a key difference between our study and these is the length of the cropping period. In this study, only the plant crop was harvested with no ratoon crops, due to the detection of *Fusarium* in the field, which necessitated the termination of the experiment. In contrast, McIntyre et al. (2000) conducted a study for 4.5 years and saw an overall 30% increase in biomass under mulch, along with higher soil porosity, soil water content, and crop water uptake. Similarly, Santosh and Tiwari (2019) reported reduced irrigation demand under black plastic mulch in a field study that lasted four years, with a plant crop and two ratoon crops. In addition, no difference in surface porosity was detected between our mulches, despite such a difference being reported in McIntyre et al. (2000), though the soil physical effects of mulch would be expected to increase over the total time of application (Fér et al., 2022).

However, it is still notable that surface soil gravimetric water content, measured at the same time as porosity, did demonstrate a significant increase in soil moisture under mulch. The lack of observable differences in soil water content overall at the 20 cm and 50 cm volumetric water content sensor depths may indicate that the mulch treatments, only established over a period of months, did not sufficiently alter soil physical properties to lead to observable effects on the degree of soil wetness at depth. Because banana and plantain rooting systems generally have an “effective” rooting depth of 0.4–0.6 m (Carr, 2009; Fogain and Gowen, 2005; Irizarry et al., 1981), the soil water difference observed only at the surface most likely reflects the

insufficient time for soil physical effects of mulching to lead to appreciable increases in soil water at depth, and therefore to lead to increased growth or yield.

The soil water response to rainfall was apparently affected by the mulch covers, however (Fig. 2-4). Binomial regression revealed that hay mulch was significantly more likely to lead to soil wetting at 20 cm in response to rain event size (mm) and intensity (mm h^{-1}). This result apparently conflicts with the lack of any differences in measured field-saturated hydraulic conductivity. However, the SATURO device cannot record a measurement in the presence of large macropores (when the maximum flux rate of the device is exceeded by the soil hydraulic conductivity), and this was observed numerous times under hay mulch. This possibly indicates that the hay mulch cover was helping preserve surface macropores, especially artifacts of roto-tilling, from crusting or compaction, which may explain the increased wet-up likelihood (Ma et al., 2022).

To the degree that the same effect was not observed in the other mulch treatment (callisia), this could be related to the longer establishment time of the living mulch, which has been noted elsewhere (Puertas et al., 2008), or could be related the larger interception storage or water uptake of the fully established living mulch. Finally, other research has shown a significant degree of spatial variation and non-uniformity of throughfall distribution under banana canopies owing to the long, broad architecture of banana leaves (Zhang et al., 2021), in addition to the intrinsic variability of rainfall at point or plot scales (Kundu and Siddani, 2011). Thus, the architecture of the hay mulch structure could have served to more evenly distribute incoming rainwater across the soil surface, similar to what was observed by Zengui et al. (2023) under a straw mulch, and supported by the observed lower variance (Fig. 2-3) in soil water measurements among the replicate plots of hay as compared to the other two treatments (0.015

$cm^3\ cm^{-3}$ mean standard error in no mulch control, 0.010 $cm^3\ cm^{-3}$ in callisia, and 0.007 $cm^3\ cm^{-3}$ in hay).

External optimization of van Genuchten's soil hydraulic parameters showed no significant differences among treatments (Fig. 2-5; Table 2-5), which permitted summarizing these parameters across treatment, an approach similar to that used by Andrews et al. (2020). Verifying a lack of variation was important in particular because of other studies (e.g. Herbst et al., 2006; Wang et al., 2014) that have noted the possibility of a high degree of spatial variation in soil hydraulic parameters, which we were able to address through the external optimization process.

In the absence of differences by treatment in soil hydraulic properties, it is likely that the observed longer lag time (Table 2-4) in soil wetting response to rainfall under callisia mulch was driven by higher interception storage (Cook et al., 2006; Fér et al., 2022). This is supported by the regression analysis of rain events separated by 36 hours or more (Fig. 2-6). Although the selection of only rain events with >36 hours of inter-event time created a limited number of points for regression, and subsequently a weak R^2 particularly in callisia, there remains a need to use only rainfall that would occur absent any water stored in the canopy at the start of the event (Dunkerly, 2008). The abbreviated study period, caused by the detection of *Fusarium*, necessitated the analysis being performed with limited qualifying storm events.

Indeed, in McIntyre and colleagues' (2000) mulch study, a faster soil water recharge, the opposite of our observation, was observed under mulch covers, but again, this is most likely due to the longer study period of 4.5 years, allowing changes in soil physical properties that would outweigh the effect of increased interception storage. The baseline interception reported for a plantain canopy (at 2 $m^2\ m^{-2}$ LAI) reported by Jiménez and Lhomme (1994), was given at 1.9

mm, rendering the estimate for the addition interception provided by the callisia mulch as 12.9 mm. The high value, compared to that estimated for hay (3.4 mm), could be most directly explained by the physical architecture of the callisia canopy, which features leaves with a slightly cupped shape, and many dense, branching clusters compared to hay, which is composed of long, thin stalks that could provide a direct pathway for raindrops to pass through the mulch layer to the soil surface. The rooting structures of the callisia, additionally, could be providing additional "interception" storage in this case if they slow the water movement or fill macropores.

The simulated water balance (Fig. 2-7) based on the estimated soil hydraulic parameters and interception storage was especially notable for the near-total lack of simulated runoff from any treatment. Although runoff is a serious problem in the Caribbean region generally, it is highly episodic in nature, generated especially from rocky, steep soils of mountainous areas (whereas the study area is on a carbonate plain), and during intense tropical waves. The lack of flooding and runoff elsewhere in the area and on the island during the study period of 2021–22 accords with the prediction that runoff was not generated at scale, regardless of soil surface treatments. Deep drainage, or potential groundwater recharge, was also not apparently affected by the mulches in the simulation, reflecting the lack of soil hydraulic differences in the parameterization.

The process of deriving soil hydraulic parameters from inverse fitting has been used successfully and with acceptable accuracy for water balances (Andrews et al., 2020, Graham et al., 2018, Ries et al., 2015), though Andrews et al. note a consistent disagreement between lab-measured values of soil hydraulic parameters and those from inverse fitting. In any case, though the water balance from this approach should be considered only with appropriate caveats, our results confirm that reasonable, especially comparative, estimates can be made to characterize

water relations of agricultural management practices using high-frequency soil water content and meteorological data. In tropical soils in particular where standard pedotransfer functions may not be reliable (Hodnett and Tomasella, 2002), an inverse estimation approach can help provide insights into soil water relations in understudied tropical agroecosystems.

Conclusion

The lack of mulch effects on soil water storage (other than interception and time lags) and plantain yield in the first year indicates, at a minimum, that beneficial soil physical results from mulching require adequate time, especially if soil physical changes to increase soil water content are expected to outweigh added interception losses. This is particularly the case with a living mulch cover that requires initial time to establish beneath a shaded canopy. Further study would be required to confirm how these benefits might interact with the increased interception storage of mulches, in terms of runoff prevention, but also soil water recharge and crop growth.

Tables and Figures

Table 2-1. Pre-experiment soil profile depths at five sampling sites, with Munsell color classes and gravimetric soil water content θ_g

Sample site	Depth [cm]	θ_g [g g^{-1}]	Munsell class
1	0–18	0.206	10YR 2/2
1	19–28	0.212	10YR 4/1
1	29–100	0.201	7.5YR 8/2
2	0–18	0.233	10YR 2/2
2	19–35	0.215	10YR 3/3
2	36–100	0.134	7.5YR 8/2
3	0–22	0.242	10YR 2/2
3	23–36	0.198	10YR 7/4
3	37–100	0.184	7.5YR 8/2
4	0–18	0.195	10YR 3/3
4	19–28	0.203	10YR 7/4
4	29–100	0.187	7.5YR 8/2
5	0–20	0.210	10YR 2/2
5	21–35	0.218	10YR 3/2
5	36–100	0.190	7.5YR 8/2

Table 2-2. Mean particle size fractions across mulch treatments (callisia is a living mulch) at two depths, displayed with standard error uncertainty.

Particle	Depth [cm]	No mulch	Hay mulch	Callisia
Sand	20	37.3 ± 3.4	38.5 ± 4.0	36.5 ± 2.0
Silt		11.0 ± 1.2	13.5 ± 1.3	11.3 ± 1.1
Clay		51.8 ± 3.7	47.0 ± 3.8	52.3 ± 1.0
Sand	50	53.8 ± 2.6	46.5 ± 2.7	48.0 ± 4.7
Silt		12.0 ± 0.4	15.0 ± 1.4	14.3 ± 1.3
Clay		34.3 ± 2.3	38.5 ± 2.5	37.8 ± 3.6

Table 2-3. Summary of agronomic results by mulch treatment (callisia is a living mulch). Means of plantain plant height, leaf chlorophyll (chlorophyll content index), canopy cover, number of suckers, percent fruiting or flowering, surface gravimetric water content (θ_g), surface porosity, surface field saturated hydraulic conductivity (K_{fs}), total plantain yield, and bunch weight are displayed with standard error uncertainty at the time they were measured in the cropping season (days after planting; DAP). Variables with statistically significant differences by treatment are in bold.

	DAP	Unit	No mulch	Hay mulch	Callisia
Height	320	[m]	3.4 ± 0.1	3.5 ± 0.0	3.3 ± 0.1
Chlorophyll	294	[CCI]	15.7 ± 0.7	13.6 ± 1.0	15.6 ± 2.2
Canopy	320	[%]	88.8 ± 1.9	89.4 ± 0.8	89.9 ± 2.5
Suckers	320	[plant^{-1}]	2.18 ± 0.12	2.94 ± 0.21	2.09 ± 0.14
Fruiting/flowering	334	[%]	52.0 ± 4.1	58.0 ± 4.8	48.0 ± 1.7
θ_g	**369**	**[g g^{-1}]**	**0.22 ± 0.01^{b*}**	**0.25 ± 0.01^{a}**	**0.24 ± 0.01^{a}**
Porosity	369	[cm^3 cm^{-3}]	0.65 ± 0.01	0.67 ± 0.01	0.67 ± 0.01
K_{fs}	213–222	[cm h^{-1}]	24.2 ± 6.1	20.5 ± 1.8	17.3 ± 4.2
Yield	total	[t ha^{-1}]	18.8 ± 1.6	21.1 ± 1.9	15.2 ± 0.6
Bunch weight	average	[kg]	32.4 ± 1.9	33.1 ± 0.5	35.0 ± 2.9

*Letter superscripts not shared by two treatments indicates statistical significance in post-hoc testing ($\alpha = 0.05$)

Table 2-4. Temporal results of volumetric soil water content (θ) data by soil depth and mulch covers (callisia is a living mulch). Compares: fraction of rain events resulting in soil wet-up, defined as an increase of >0.01 $cm^3\ cm^{-3}$ over a rain event; magnitude of wet-up events; duration of wet-up events (time from minimum to maximum θ during rain event); lag between start of rain event and peak θ; peak of rain event and peak θ; centroid of rain event and peak θ; temporal lag of peak precipitation cross-correlation (CC) with θ values; temporal lag of peak 20 cm θ cross-correlation with θ values at 50 cm; cross-correlation length of precipitation with θ values; cross-correlation length of θ at 20cm with θ values at 50 cm, and autocorrelation length λ. Variables with statistically significant differences by treatment within depths are in bold. Inapplicable cells are denoted with dashes.

		20 cm			50 cm		
		No mulch	Hay mulch	Callisia	No mulch	Hay mulch	Callisia
Rain events wetting soil	[%]	5.2±0.7	7.3±1.7	4.8±0.3	2.0±0.2	3.2±0.9	2.0±0.2
Wet-up magnitude	[$cm^3\ cm^{-3}$]	0.08±0.01	0.07±0.00	0.06±0.01	0.06±0.02	0.05±0.01	0.04±0.01
Wet-up duration	[h]	7.7±0.6	8.6±1.1	9.5±0.4	9.7±1.6	9.8±2.5	12.2±2.6
Rain start to peak θ	[h]	**9.6±0.9^{b*}**	**8.9±1.0^{b}**	**11.5±0.8^{a}**	10.1±2.0	10.6±1.9	12.5±2.8
Rain peak to peak θ	[h]	**5.3±0.5^{b}**	**4.8±0.9^{b}**	**7.0±0.5^{a}**	7.0±1.3	6.0±1.3	7.4±1.2
Rain centroid to peak θ	[h]	**5.3±0.6^{b}**	**4.7±0.9^{b}**	**7.3±0.5^{a}**	6.1±1.8	5.7±1.8	7.7±2.0
CC peak lag, rain	[h]	**8.1±5.0^{b}**	**5.7±1.3^{b}**	**18.5±2.1^{a}**	9.1±2.9	11.7±3.3	8.3±3.9
CC peak lag, 20 cm θ	[h]	--	--	--	9.2±5.3	4.5±1.0	3.9±1.4
CC length, rain	[d]	8.6±3.0	11.9±0.7	9.4±3.1	7.5±4.5	5.4±5.4	8.6±4.9
CC length, 20 cm θ	[d]	--	--	--	**19.2±7.6^{c}**	**59.9±19.8^{b}**	**101.3±2.9^{a}**
θ autocorrelation λ	[d]	8.2±2.4	7.5±1.2	11.9±1.8	8.1±3.0	15.3±6.2	11.5±3.1

* Letter superscripts not shared by two treatments indicates statistical significance in post-hoc testing ($\alpha = 0.05$)

Table 2-5. Optimized values of van Genuchten soil hydraulic parameters from observed data (saturated water content; θ_s), pedotransfer function (residual water content; θ_r), and external optimization process (α, a fitting parameter; n, a fitting parameter; and saturated hydraulic conductivity, K_s), minimizing root mean squared error (RMSE); the RMSE in units of volumetric water content ($cm^3\ cm^{-3}$) is displayed by treatment. No significant ($\alpha = 0.05$) differences by treatment were detected in any parameter.

		20 cm			50 cm		
		No mulch	Hay mulch	Callisia	No mulch	Hay mulch	Callisia
θ_r	[$cm^3\ cm^{-3}$]	0.128 ± 0.002	0.133 ± 0.001	0.134 ± 0.001	0.112 ± 0.004	0.124 ± 0.002	0.121 ± 0.004
θ_s	[$cm^3\ cm^{-3}$]	0.587 ± 0.004	0.588 ± 0.003	0.587 ± 0.002	0.624 ± 0.007	0.629 ± 0.004	0.631 ± 0.003
α	[cm^{-1}]	0.054 ± 0.001	0.079 ± 0.058	0.089 ± 0.056	0.034 ± 0.010	0.040 ± 0.027	0.054 ± 0.040
n	[-]	1.21 ± 0.02	1.20 ± 0.01	1.20 ± 0.03	1.28 ± 0.02	1.28 ± 0.01	1.33 ± 0.02
K_s	[$cm\ h^{-1}$]	9.47 ± 6.98	6.83 ± 0.26	7.81 ± 1.92	15.32 ± 0.48	14.99 ± 0.39	19.25 ± 2.91
RMSE	[$cm^3\ cm^{-3}$]	0.023 ± 0.002	0.021 ± 0.002	0.022 ± 0.002	0.023 ± 0.002	0.021 ± 0.002	0.022 ± 0.002

Fig. 2-1. Callisia repens groundcover after establishment under plantain canopy.

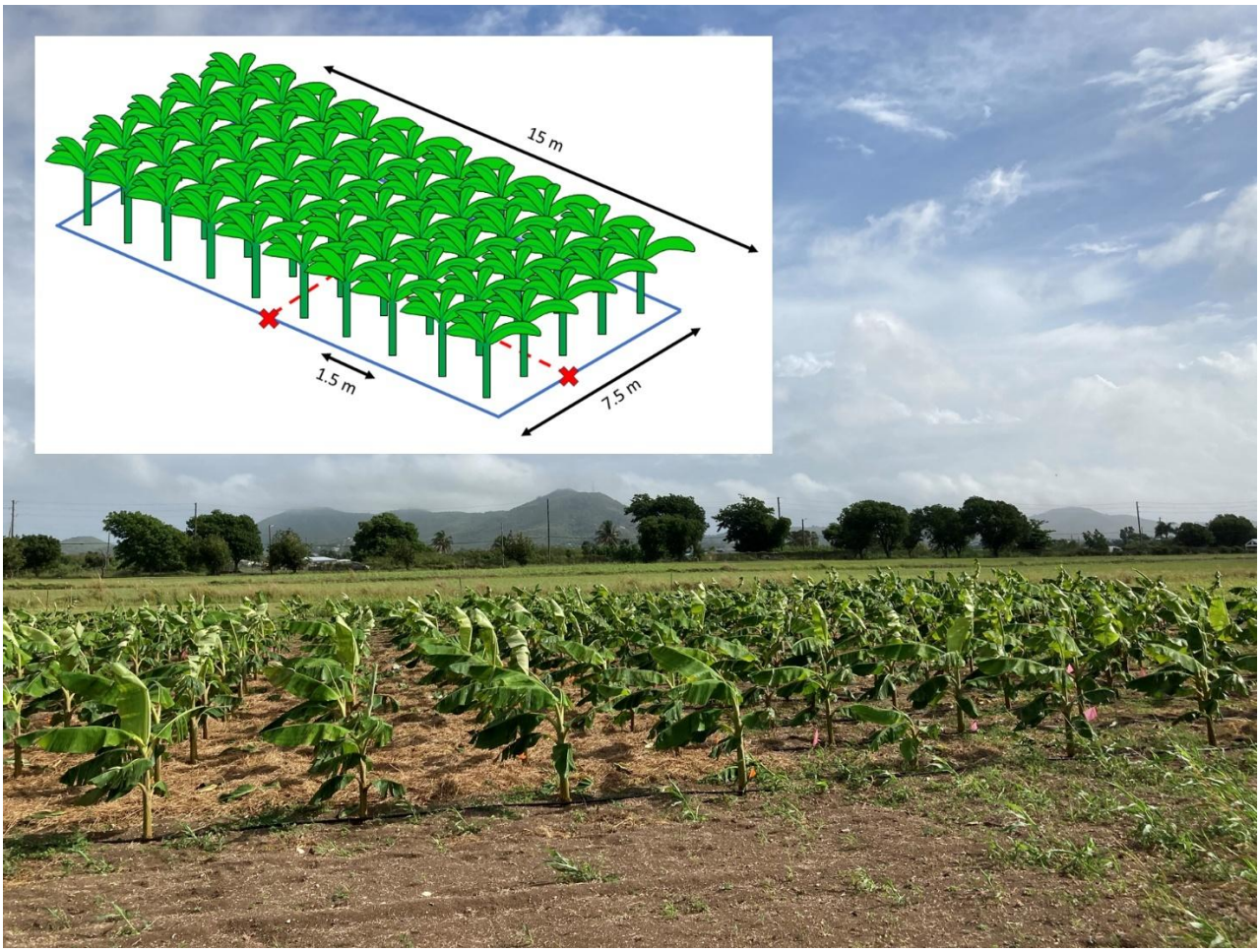

Fig. 2-2. Plantain crop shortly after establishment with hay mulch visible on the left and bare soil on the right. Schematic in upper left inset depicts the positioning within one plot of soil water content sensor installation (intersection point of two red dashed lines); soil physical measurements, e.g., infiltration and bulk density, were made at similar interrow positions elsewhere in the center of the plot. Schematic is not drawn to scale.

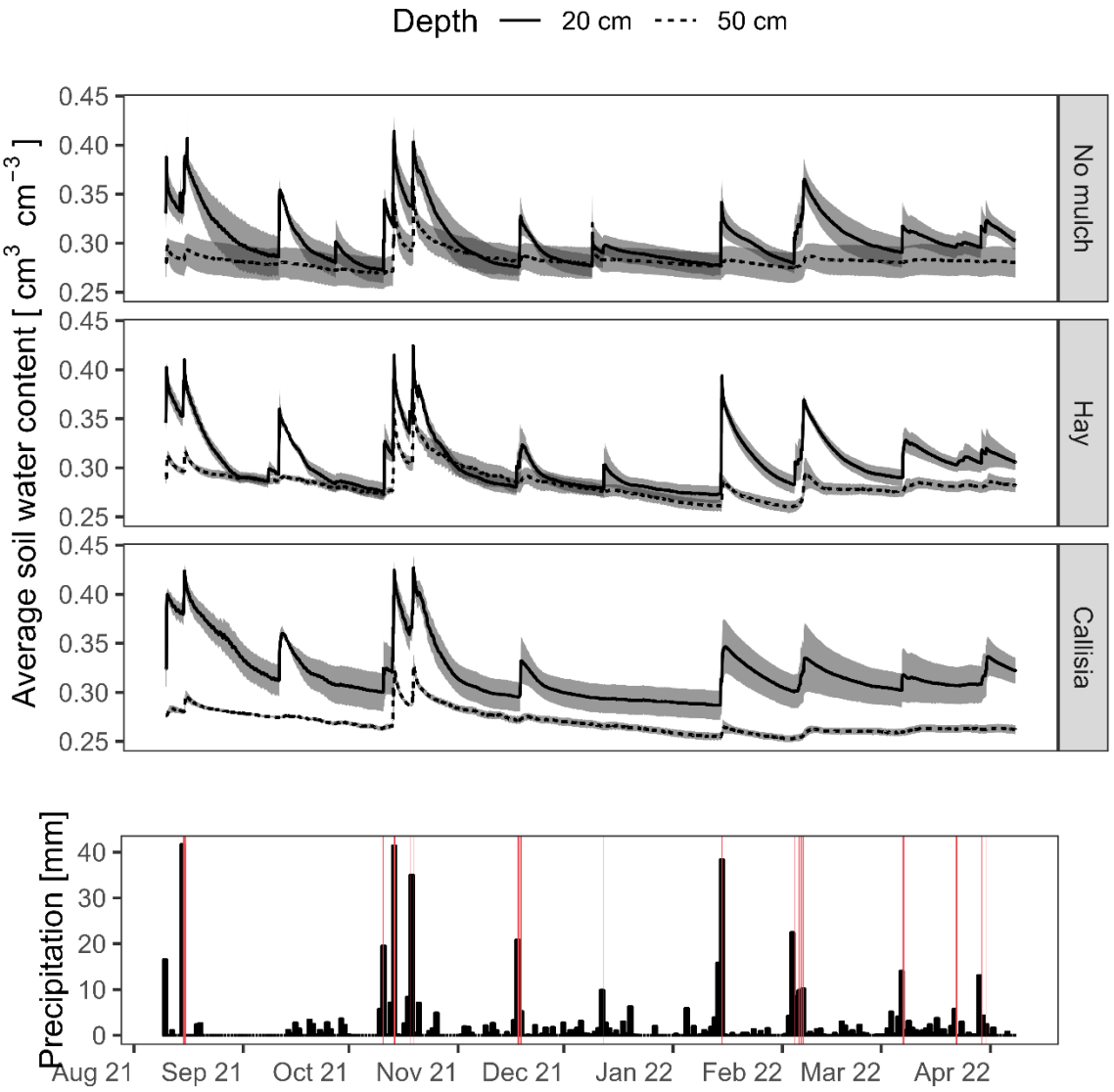

Fig. 2-3. Time series plot of soil volumetric water content at two depths (20 and 50 cm) across three mulch cover treatments in plantain (no mulch, hay mulch, and callisia living mulch), and daily precipitation plotted with delineated rain events resulting in soil wetting response in red. Gray bands in soil water content plots represent standard error across replicates.

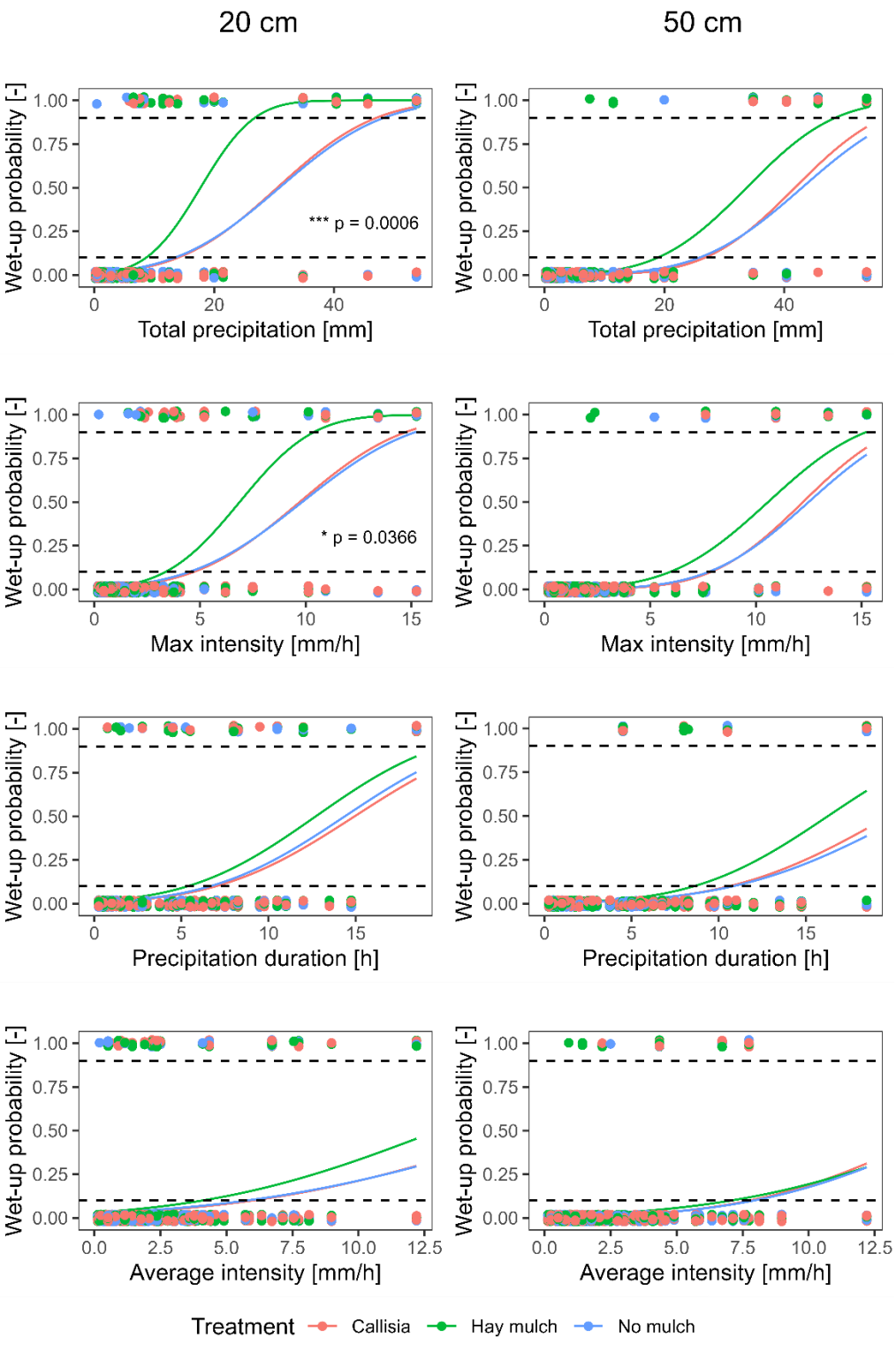

Fig. 2-4. Binomial regression of probability of a soil wet-up response on single parameters of rain events and mulch cover treatments (callisia is a living mulch) in plantain at 20 and 50 cm soil depths. Plots in which a significant interaction between the rain event parameter and the mulch treatment was detected are marked by asterisks and the p-value. Dashed horizontal lines denote a 10% and a 90% chance of a wet-up occurring.

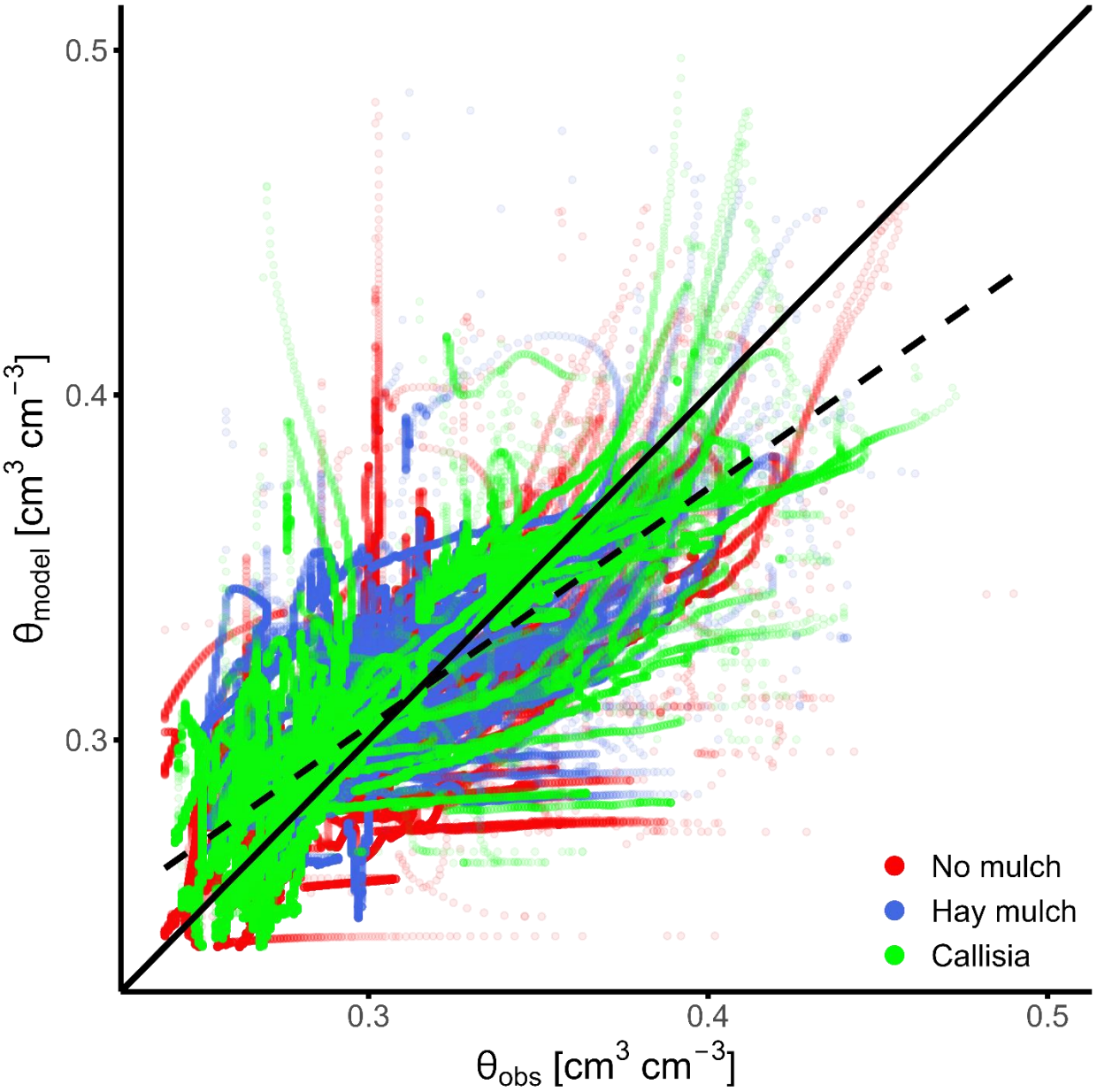

Fig. 2-5. Predicted (θ_{model}) vs. actual (θ_{obs}) soil water content, ($cm^3\ cm^{-3}$) by mulch treatments: no mulch, hay mulch, and callisia living mulch. Solid black line depicts a 1:1 relationship; dashed black line depicts line of best fit for all data points.

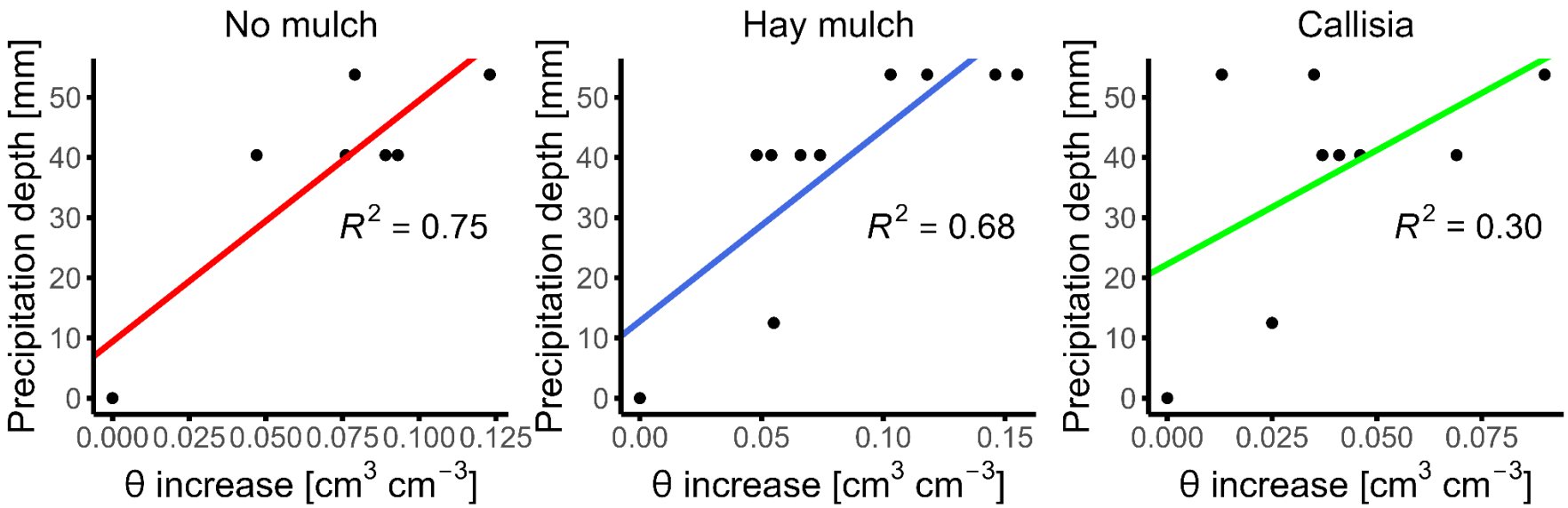

Fig. 2-6. Linear regression of precipitation depth on resulting increase of soil water content (θ) at 20 cm depth in three mulch cover treatments: no mulch, hay mulch, and callisia living mulch. Points represent single rain events with >36 h time separation from the previous rain event.

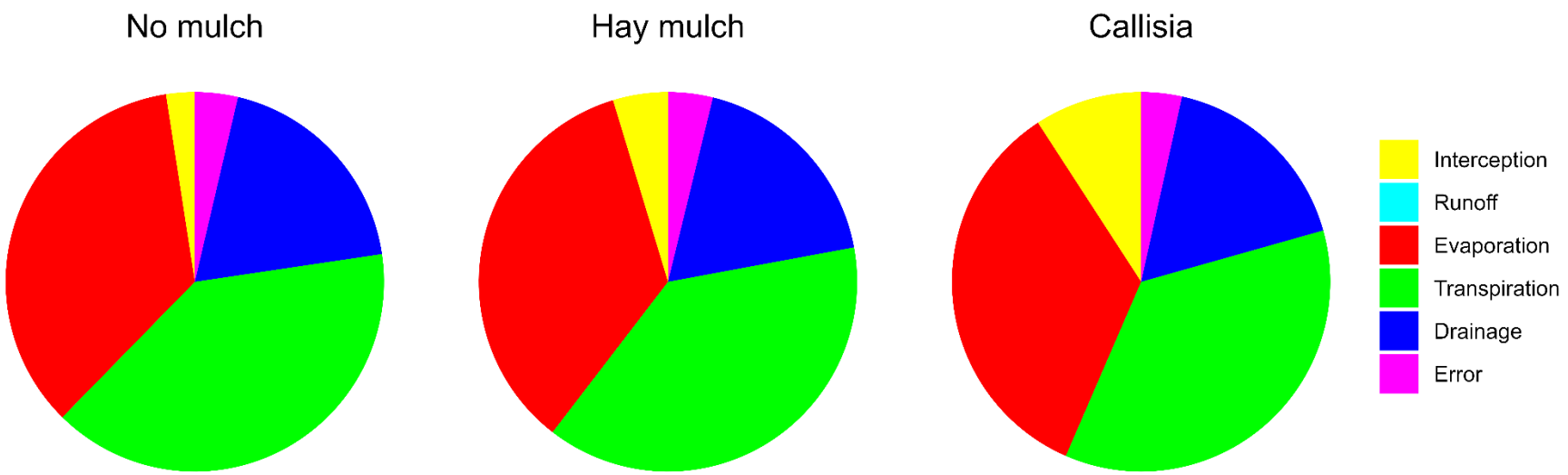

Fig. 2-7. Simulated water balance as a fraction of total precipitation under no mulch, hay mulch, and callisia living mulch. "Error" represents recorded precipitation remaining unaccounted for in water balance components interception, runoff, evaporation, transpiration, and deep drainage.

Chapter 3
Runoff Generation in Ephemeral Streams of the Virgin Islands
The Case of Salt River, St. Croix

Abstract

Small islands worldwide have limited water resources and an increased need to understand the mechanisms underlying island water budgets, but they also usually lack adequate data. Our study focused on the Salt River watershed on the island of St. Croix in the Virgin Islands, which is an ephemeral stream network comprising both volcanic and carbonate hydrogeology. We used hydrometeorological and soil moisture data at upstream and downstream sites (chosen by geospatial topographic and soil information) to characterize thresholds for runoff generation and to analyze the disrupted connectivity of the ephemeral stream network. We found evidence of runoff thresholds, in line with work in similar catchments elsewhere. Connectivity from headwaters to lowland areas was uncommon, and saturation-excess overland flows and subsurface stormflow appeared to dominate runoff events. The upstream subcatchment (with volcanic hydrogeology) was much more responsive (runoff coefficient = 0.237) than the entire catchment (with partly carbonate hydrogeology; runoff coefficient = 0.086). The transition between these hydrogeologic zones may disrupt connectivity and play an important role in aquifer recharge while buffering the marine environment from water quality problems. For resource managers, this study offers the possibility of identifying sensitive groundwater recharge zones and provides insight into the frequency of ridge-to-reef flow events.

Introduction

Processes governing runoff generation in island watersheds hold particular importance for island communities worldwide (Amadio, 2014; Hemmings et al., 2015; van der Velde et al., 2007). Two primary concerns, often especially important for small islands, demonstrate the importance of characterizing runoff generation: water security and downstream water quality (Nemeth and Platenberg, 2007; Robins, 2013). Water security is of obvious importance for remote islands where precipitation inputs of water into islands' hydrology account for the entirety of the available water supply outside of expensive desalination efforts, and the socio-economic development of island states is directly linked to the successful management of water resources (Falkland, 1999; Gheuens et al., 2019). Runoff in these islands' watersheds represents the loss of rainwater to the sea in an island's water budget (Robins and Lawrence, 2000). Downstream water quality affects both the health and utility of freshwater resources in streams, ponds, reservoirs, etc., but also affects marine water quality in areas where runoff discharges directly into the sea (Rogers and Ramos-Scharrón, 2022). In the Caribbean, these concerns are shared region-wide (Crisman and Winters, 2023; Mycoo and Roopnarine, 2024), particularly by small, water-limited islands with economies dependent on the health of the coastal ecosystem (tourism and fishing) and agriculture (Lancellotti and Hensley, 2024), and increasingly as concerns mount that annual precipitation may become increasingly unreliable in the Caribbean region because of climate change (Bowden et al., 2021; Crisman and Winters, 2023). Thus, surface hydrology and runoff generation processes are critically important issues in the region. Here, we begin by conducting a brief review of surface hydrology and runoff generation, followed by a regional contextualization that provides the motivations for this study.

Surface hydrology and runoff generation

Runoff (or stormflow) is generally governed by three processes: infiltration-excess overland flow (or "Hortonian" flow, caused by precipitation intensity greater than infiltration capacity), saturation-excess overland flow (caused by precipitation while soil pores are saturated), and subsurface stormflow (where water is directed to stormflow through shallow, subsurface flow pathways; Mirus and Loague, 2013). Although runoff is typically envisioned as overland flow only (Beven, 2021), subsurface flows (sometimes called subsurface stormflows to distinguish them from baseflow; Mirus and Loague, 2013) are acknowledged to constitute a significant proportion of streamflow, especially in steeper, rockier areas (Gutiérrez-Jurado et al., 2019; Mirus and Loague, 2013). In reality, it is important to acknowledge that observed streamflow can be a combination of different kinds of runoff (Zhang et al., 2025).

Global generalization of hydrological processes, including runoff generation, has historically been a difficult process in hydrology (Beven, 2000; Sultan et al., 2022). Nevertheless, runoff thresholds have been identified in many places across the world, though the thresholds themselves are defined in terms of numerous different metrics (Giani et al., 2022; Ross et al., 2021; Tarasova et al., 2018). The relationship between soil moisture and runoff generation is also a common theme, and soil hydrological dynamics (e.g., macroporosity, preferential flow, permeability, porosity, etc.), often influenced by land use/land cover, are widely acknowledged as playing a central role in the mechanisms of runoff generation (James and Roulet, 2007; Singh et al., 2021; Yonaba et al., 2021; Zhang et al., 2025), though rainfall characteristics are obviously critical as well (Nicolini et al., 2016; Peña-Angulo et al., 2021; Tao et al., 2021). In ephemeral stream networks, processes similar to those that govern runoff generation may also govern hydrologic connectivity (Gomi et al., 2008; James and Roulet, 2007).

In ephemeral stream systems, runoff generation studies are often typified by their semi-arid climates (e.g., the Sahel and East Africa: Mounirou et al., 2021; Sultan et al., 2022; or the Mediterranean basin: Gutiérrez-Jurado et al., 2019; Serrano-Notivoli et al., 2022). However, others caution that ephemeral systems in dry tropical forests, where subsurface and saturation excess flows have been identified as drivers of runoff generation (Farrick and Branfireun, 2014b; Farrick and Branfireun, 2015), should not be compared directly to semi-arid systems (Farrick and Branfireun, 2014a). This points to the difficulties of generalization, or Beven's (2000) "uniqueness of place," but a near-universal conceptual model for runoff generation, the "fill-and-spill" concept, has been proposed (McDonnell et al., 2021). This concept argues that different runoff processes operate at different scales (Mounirou et al., 2020; Mounirou et al., 2021) and in different landscapes, but that some landscape storage unit must "fill" before runoff is generated, which agrees with the widespread findings of runoff thresholds in many parts of the world (DeGuzman et al., 2023; Ross et al., 2021). This highlights both the continuing need for regional studies in hydrology, while permitting some useful comparison between landscapes. Our study, focused on the Virgin Islands archipelago of the northeastern Caribbean, is designed to address a regional knowledge gap in runoff generation.

Regional information

The Virgin Islands is an archipelago in the Lesser Antilles of the northeastern Caribbean, consisting of inhabited islands politically divided into the British Overseas Territory of the British Virgin Islands, the unincorporated American territory of the U.S. Virgin Islands, and islands controlled by the Commonwealth of Puerto Rico (Fig. 3-1). Nine islands in this

archipelago have significant land area and population, though all are small overall on a global scale (e.g., St. Croix is the largest island by land area at 218 km^2).

The Virgin Islands are subject to scattered, unpredictable rainfall due to their geography, relatively low topography, and localized weather patterns. The islands of the northeastern Caribbean, as opposed to the islands of the eastern Caribbean further down the Lesser Antilles island chain, are small and normally have an east-west or rounded orientation (compared with a typical north-south orientation in the eastern Caribbean). This contributes to reduced convection in this sub-region (Jury and Bernard, 2021). Here, we define the northeastern Caribbean as the island chain of some 20 islands extending from Vieques in the west to Montserrat in the east, excluding notably Puerto Rico and Guadeloupe, which are much larger islands that receive more rainfall. Catchment areas in the Virgin Islands are inherently small due to the limited land area, and distances from headwaters to marine ecosystems are often very short (Lancellotti and Hensley, 2024). Runoff generation processes in these conditions are important for the dual objectives of conserving water resources on land and protecting downstream terrestrial and marine habitats from the effects of nonpoint source pollution carried by runoff. The economy of the Virgin Islands relies heavily on tourism, which is primarily centered around the marine ecosystem (Culbertson et al., 2020). However, the tourism industry itself also places major demands on freshwater resources (Francois et al., 1983), highlighting the importance of runoff generation in Virgin Islands watersheds from both economic and environmental perspectives. Also, although agriculture has decreased in importance over the last century, community members and political leaders routinely express interest in expanding this sector to diversify the economy, which would ultimately rely on groundwater resources and, thus,

successful management of runoff generation in Virgin Islands watersheds (Agricultural Plan Task Force, 2021).

Despite the importance of runoff generation in the Virgin Islands, these processes have not been well-documented. In the 1960s and 70s, preliminary investigations by hydrologists at the U.S. Geological Survey made estimates of island-wide runoff coefficients (Jordan, 1975), and over three decades, studies by Ramos-Scharrón and others described the effect of roadways on Virgin Islands runoff generation (a review of this work can be found in: Ramos-Scharrón et al., 2023). A catchment-scale investigation of runoff generation processes, however, has not been attempted in the Virgin Islands. It is therefore useful to review studies of runoff generation within the region, as well as for small islands globally.

The climate and hydrological situation of small islands is governed by several geographic factors such as latitude, areal extent, elevation, orientation, and proximity to continents (Peña-Angulo et al., 2021). For this reason, although some studies of runoff generation have been done in Puerto Rico (Rossi et al., 2016; Schellekens, 2000), we consider them less applicable to the small islands of the northeastern Caribbean. Unfortunately, there are very few published studies of runoff generation within the northeastern Caribbean specifically (though one study by Stapel [2023] found some indications of preferential flow in soils of Sint Eustatius, as well as the role of a restricting bedrock layer in promoting saturation-excess flow).

Studies of small island hydrology tend to be scattered in general, at least partly because of the many logistical and practical difficulties involved in carrying out field monitoring campaigns that are common across small islands (Hughes, et al., 2022; Khan and Mohamed, 2022). Other than the difficulties of measurement, a few themes from this limited literature do emerge, though. First is the heterogeneity among and within islands (in Mallorca, Spain; Peña-

Angula et al., 2021; in St. Vincent; Phillips et al., 2024). Despite this, another theme among several subdisciplines is the importance of cyclonic precipitation or other major storm events for both groundwater recharge and runoff, as opposed to ordinary orogenic or convective precipitation (Dores et al., 2020; Jones and Banner, 2003; Nicolini et al., 2016; Peña-Angula et al., 2021). Schellekens (2000) points out the need to consider subsurface lateral flow in a steep forested catchment of Puerto Rico, and Hughes et al. (2022) notes that changing land use can have a major effect on the water budget of a small island (Norfolk Island, Australia), which agrees with hypotheses made in the Virgin Islands by Jordan (1972; 1975). Other authors note the need for subdaily data monitoring, since island catchments usually respond to rainfall within a few hours (in Puerto Rico and Hawaii, respectively; Hall et al., 2022; Huang et al., 2021). In most of these cases, a general paucity of available data was noted.

Because of the importance of runoff generation processes to the Virgin Islands, where existing information is limited, we carried out this study to address some of these gaps in regional hydrological understanding. In particular, the mechanism of runoff generation, which is important for pollutant fluxes and groundwater interactions, should be identified. Our study consisted of three objectives for this purpose: 1) to identify runoff thresholds and mechanisms of runoff generation in a Virgin Islands watershed; 2) to develop a descriptive relationship between hydrometeorological/soil conditions and runoff magnitudes/coefficients; and 3) to analyze ridge-to-reef streamflow connectivity mechanisms and describe the frequency and duration of such events.

Methods

Site description

Our study of runoff generation focuses on the Salt River Bay watershed on the island of St. Croix in the Virgin Islands (17.7572° N, 64.7794° W; Fig. 3-1). Salt River Bay is an embayment (which covers 0.75 km^2) and submarine canyon on the north-central coast of St. Croix. It has received significant research attention from the marine sciences over the years (Hubbard, 1986; Shepherd and Dill, 1977), and is partially within Salt River Bay National Historical Park and Ecological Preserve, administered by the U.S. National Park Service (Kendall et al., 2005). Sugar Bay, connected to the larger Salt River Bay, is a long, narrow water body fringed by mangrove forests (Kendall et al., 2005; Fig. 3-1). Sugar Bay connects at its upper portion to the mouth of the primary stream channel network of the watershed, hereafter called "Salt River" (in some places called "Salt River Gut," as "gut" is the local word for a stream). Our study focused on the primary stream network of Salt River, based on the assumption that major runoff flux into the marine zone can occur through the mouth and Sugar Bay (Pait et al., 2020). The Salt River catchment is the second largest on the island of St. Croix (10.01 km^2). The watershed has an upper headwaters known as Canaan Valley (subcatchment area of 1.57 km^2), where the stream network originates in the mountainous Northside Range of St. Croix, including Blue Mountain (337 m elevation). From there, the stream flows southward along with numerous tributaries but turns east-northeast in the lowlands of St. Croix's Central Valley, finally transitioning into a sheet-flow dominated swamp area that gives way to the Sugar Bay mangrove forest. The average slope of the catchment is 39.4%, while the average slope of Canaan Valley is 57.4% (USDA-NRCS, 2022; Fig. 3-2).

Geologically, the Virgin Islands are the eastern end of the Greater Antilles, part of the Puerto Rico platform, except for St. Croix, which is on its own geologically distinct microplate

(Speed, 1989). Separated from the northern islands by the Virgin Islands trough, St. Croix is the above-water part of the St. Croix Ridge, which forms the southern boundary of the trough (Gill et al., 1997). The geology of St. Croix consists of three geomorphic zones. The first two, the mountains of the Northside Range and the East End Range, are uplifted Cretaceous sedimentary and volcaniclastic formations; these are the steepest topography of the island (Speed, 1989). Between these two mountainous areas is the Central Valley, a plain underlain by Neogene limestone formations. This was formed when the area between the Northside Range and the East End Range was a seaway that hosted coral reefs and estuarine environments, promoting carbonate deposition (Nagle and Hubbard, 1989). Today, Quaternary alluvial sediments overlie much of the limestone formation in the Central Valley (Gill et al., 1997).

These two distinct geological formation phases inform the primary distinction in the hydrogeology of Salt River. The headwaters of Salt River are underlain by the Cretaceous formations, with limited groundwater storage in fractured joints and faults (Miller et al., 1999). The permeability of these rock features is low compared to the limestone Central Valley. The Central Valley, with much more rock permeability, is associated with the Kingshill Aquifer, the most significant groundwater feature in all of the Virgin Islands (the other islands do not have the volcanic/carbonate hybrid geology of St. Croix; Robinson, 1972). The Kingshill Aquifer provides wells with significantly higher yields than those found in upland mountainous zones (Cederstrom, 1950; Torres-Gonzales and Rodriguez-del-Rio, 1990). Most watersheds of St. Croix, in common with Salt River, rise in the Northside Range and flow south, interfacing with the Central Valley limestone hydrogeology at the foothills (Jordan, 1975). This interface between the volcanic headwaters area and the limestone plains of the Central Valley has been suggested as an important zone of groundwater recharge on the island (Gill et al., 1997). Soils within the

catchment are broadly of two types: those overlying the Cretaceous-age rocks of the Northside Range (with depths mapped as 43 cm to >203 cm) and those overlying more recent depositional formations in the Central Valley (soil depths mapped as >152 cm to >224 cm; USDA-NRCS, 2024). The characteristic soils of the mountainous Cretaceous area are Inceptisols, found on hillslopes, and Mollisols, located on valley floors (USDA-NRCS, 2024). In the Central Valley, soils overlying the post-Cretaceous limestone formations primarily include Mollisols found on limestone hills and calcareous valley floors, as well as non-calcareous soils on alluvial plains (USDA-NRCS, 2024).

The climate of the area is classified as "tropical savanna" with dry winters (Köppen climate classification "*Aw*"; Beck et al., 2018). Rainfall typically occurs in short, intense bursts with uneven spatial distribution. A pronounced dry season, lasting from January through April, is typically followed by a weak wet period in May, then a mid-summer dry period in July and August. This dry period precedes the primary wet season, which begins in September and continues through December, coinciding with the Atlantic hurricane season (Giannini et al., 2001). Significant fractions of the total annual precipitation (1000 mm annually; Kendall et al., 2005) result from tropical waves and storms during this period. However, within individual rain events — whether short convective showers or major tropical waves — precipitation is spatially distributed in a relatively stochastic manner. An orographic effect of the Northside Range is discernible over longer timescales, with greater average rainfall falling in the mountainous area compared to the southern plains (Menne et al., 2012). In the modern era, the intense periods of rainfall experienced during the wet season are reported to be the only episodes in which freshwater flows through the entire Salt River watershed and into Sugar Bay (Kendall et al.,

2005; Shepherd and Dill, 1977). Historically, though, the stream was perennial, as documented in the early 20th century and earlier periods (Lancellotti and Hensley, 2024).

Of this precipitation, historical reports estimated a groundwater recharge rate of 3% for St. Croix as a whole. No runoff coefficient has been reported for Salt River, but Jordan (1975) gives general estimates of 1–9% for the island. It should be noted that no reliable streamflow data exists for this catchment at any point in the historical record (Lancellotti and Hensley, 2024). With average monthly temperatures ranging from 26–30 °C (Kendall et al., 2005), evapotranspiration is the most significant fraction of the annual water budget, an estimated 88–96% of total annual rainfall (Jordan, 1972). Much of the variation in runoff is attributable to interannual variability in stormflow and precipitation within a given catchment; it is not uncommon in St. Croix for some 25% of annual precipitation at a site to be received during a single storm event (Jordan, 1975).

Land use within the Salt River watershed, like much of St. Croix, has undergone significant change in historical times. After European contact in 1493 but before major European colonization efforts (ca. 1700), the island was covered with mature tropical hardwood forests, which gave way to plantation agriculture over the course of the 18th century under the colonial rule of Denmark (Lancellotti and Hensley, 2024). Danish colonial and early American records of the sugarcane estates in the Salt River watershed indicate that, from 1803 (when cultivation records began) to 1924, an average of 75% of the total land area was either planted to sugarcane or used as pasture (G.F. Tyson, unpublished data). Beginning in the mid-20th century, most of this agricultural land was abandoned and reverted to secondary forest (Atkinson and Marín-Spiotta, 2014). The growth of housing development has characterized land use change across the Virgin Islands in contemporary times. Homesites have been developed on steep hillsides within

the Salt River watershed, with concomitant road development, both paved and unpaved. Major housing developments have also been constructed within the Central Valley area, particularly at the outlet of the Canaan Valley headwaters subcatchment (IRF, 1993). After repeated flooding, the U.S. Army Corps of Engineers constructed a flow mitigation structure in 2004, effectively diverting the stream to the north around the residential area of Mon Bijou with a 23 m wide artificial channel underlain by stone gabions to a typical channel depth of ~6 m (IRF, 1993; USACE, 1987).

Data collection

Weather data

We installed two weather stations (ATMOS 41, Meter Group, Pullman, WA, USA) to measure precipitation, temperature, wind speed, solar radiation, and barometric pressure at 15-minute intervals at a height of 2 m. We installed one station within the headwaters subcatchment on 13 September 2022 (17.7595 °N, 64.7982 °W), and the other was installed downstream in the central plains on 13 July, 2021 (17.7553 °N, 64.7795 °W; Fig. 3-1). We chose these locations to provide precipitation time series data at a location about 1.2 km upstream from the stream gauges, or near to the centroid of the contributing area of the measurement outlet (220 m from centroid at SR1; 450 m from centroid at SR2). The conceptual workflow of our data collection and analyses is presented in Fig. 3-3.

Stream gauges

The weather stations corresponded to two stream gauging stations. The upstream gauge (SR1) was located at the mouth of the headwaters valley (subcatchment area of 150 ha; 17.7533°

N, 64.7926° W), or 220 m upstream from the point of soil transition from upland soils (with volcanic parent material) to lowland soils (calcareous or alluvial), which correspond with the watershed's two hydrogeologic zones (Fig. 3-2). The downstream gauge was sited near the mouth of the main stream channel at Sugar Bay, just before the channel loses definition and transitions to an estuarine swampy area (SR2; catchment area of 860 ha; 17.7599° N, 64.7646° W; Fig. 3-4b). We outfitted each gauging station with a HOBO U-10 water level logger (Onset, Bourne, MA, USA), installed in the thalweg to record water depth at 10-minute intervals (but converted to 15-minute intervals for inter-operability with the other time-series datasets). In both cases, we chose the reach for the sensor deployment based on the criteria of a relatively well-defined, uniform channel geometry of the maximum feasible straight length. These began recording data on 24 and 21 November 2021 (SR1 and SR2 respectively).

Soil moisture measurements

Also associated with each gauging station (SR1 and SR2) were two soil moisture monitoring sites (Fig. 3-1), measuring volumetric soil water content ($cm^3\ cm^{-3}$) in 15-minute intervals at four depths: 10, 30, 50, and 100 cm (TEROS 10, Meter Group, Pullman, WA, USA). This follows the approach of Farrick and Branfireun (2014b) in a tropical dry forest catchment in Mexico. One of these sites was chosen on a convex hillslope with typical forested vegetation cover approximately 200 m laterally upslope of the stream channel ("hillside"). We selected these sites to provide maximum comparability with the convex hillside sites described by Farrick and Branfireun (2014b), and for maximum representativeness, they were also sited on the most prevalent hillside soil series in both the upland (SR1) and lowland (SR2) zones. We then installed another soil moisture monitoring station on a concave toeslope immediately adjacent to

the streambanks near the gauge ("streambank"; Fig. 3-1); these sites were selected to be as close as possible to the stream gauges. In a radius of 30 m at each of these sites, we measured surface volumetric water content to confirm the representativeness of the location chosen at the microsite scale. In all four cases, the chosen location was under a forest canopy.

Streamflow measurements

To calculate streamflow (discharge), it was also necessary to develop rating curves for both sites since no previous hydrological monitoring has taken place at these locations. For this, we used a SonTek FlowTracker2 acoustic doppler velocimeter (Xylem, Inc., Washington, DC, USA) to measure flow velocity according to USGS practices (i.e., at least 15 cross-sectional flow segments measured at 0.6 water column depth; Grant and Dawson, 1997). Because flow events are flashy and generally rare, only 10 and 6 valid data points were useable for the construction of a rating curve at SR1 and SR2 (respectively), but these discharge estimates still produce more plausible discharge figures than those produced by the Manning equation (Grant and Dawson, 1997). The rating curves used in our study are displayed in Fig. 3-5 and Table 3-1. These flow measurements were collected between September 2022 and August 2024. When possible, an effort was made to collect flow measurements sequentially after little change in gauge height had occurred to confirm the accuracy of the meter and discharge estimation method, as well as to improve the fit of the rating curve with low *n*.

The water level sensor at SR2 was situated in a slight depression, which formed a still pool of water at lower water levels associated with zero flow. We therefore physically measured the gauge of zero flow (*GZF*) in the field at 27 cm to constrain the SR2 rating curve. This measurement was confirmed by field observations as the gauge height at which observable flow

occurred. We then calculated the rating curve using the method described by Kennedy (1984) for rating curves in channels with $GZF > 0$. Also, on 6 May, 2024, following the high flow event of 3 May, we collected a transect of 12 surface water samples to measure salinity (ppt) from the Sugar Bay mangrove lagoon to a distance of 575 m, which we compared with salinity readings taken near the entrance to the bay, where the surf enters from the Caribbean Sea.

Soil physical properties

Using a bulk density soil sampler (AMS, Inc., American Falls, ID, USA) and auger, we sampled undisturbed soil adjacent to each soil moisture monitoring site at 10, 30, 50, and 100 cm depths to calculate porosity from the mass of the oven dry sample, known volume of the sample cylinders, and particle density of 2.65 g cm^{-3}. In order to provide field-validated estimates of soil particle size distributions, we tested the particle size data given by the U.S. Soil Survey (USDA-NRCS, 2024; Table 3-2) against measurements by the PARIO automated hydrometer and wet-sieving method (Meter Group, Pullman, WA, USA). Sixteen samples were taken from each location-depth (SR1 hillside and streambank, SR2 hillside and streambank, at 10, 30, 50, and 100 cm). These consisted of aggregated samples from two auger holes made within 10 m of the actual soil moisture sensor site. Samples were air-dried, weighed, and passed through a 2 mm sieve; the sample remainder was kept to be washed, oven-dried, and weighed to determine the rock fraction by mass (R_w). From the < 2 mm sample, a subsample was taken for oven-drying to determine the dry mass of that portion of the sample and to calculate R_w. Because of a shortage of hydrogen peroxide, not all 16 samples (four locations, four depths) were able to be tested in this laboratory process. Of the 16 samples, 4 were used for PARIO analysis (Table 3-3). These samples were treated with hydrogen peroxide (30% solution) to remove organic material until

effervescence was no longer observed in a water bath at 80 °C. Once the oxidation process was complete, samples were treated with a chemical dispersant (sodium hexametaphosphate, 5 g L^{-1}) and placed on a laboratory shaker for 24 h for mechanical dispersal. After removal of organic matter and aggregate dispersal, the samples were diluted to a volume of 1 L and particle deposition rates were measured using a PARIO automated particle size analyzer (Meter Group, Pullman, WA, USA), including wet sieving of the coarse fraction and oven drying of effluent for the fine fraction, to calculate particle size fractions of sand (> 50 µm), silt (2–50 µm), and clay (<2 µm). Based on the average over- and under-estimation of clay and sand, respectively, from the analyzed samples, and particularly based on the close agreement between this over- and under-estimation (+15.9% and –16.3%), we corrected the soil survey particle size data by the mean of these correction factors (16.1%) to produce particle size distribution estimates for all soil moisture sites, and for further use in the pedotransfer function used for 10 cm depth soil to estimate soil surface K_{sat}. Particle size fractions and K_{sat} values resulting from this method are shown in Table 3-3.

During sampling on 29 November, 2023 near the streambank site of SR1, a saturated water table was observed at a depth of 83 cm below ground surface. Subsequent surveying from this point confirmed the depth of this water table at 111 cm below the surface at the soil moisture sensor site and 334 cm above the water level observed at the stream gauge downstream at the same date and time (lateral distance of 78 m downstream). Images of this observation are shown in Fig. 3-4a.

Data processing

Quality assurance/control

Before further processing or analysis, we subjected all time series data (precipitation, streamflow, and soil moisture) to a quality assurance/control (QA/QC) process to address data gaps, erroneous values, and to ensure consistency among sites and sensors. First, in order to capture the period in which all sensors at both sites (SR1 and SR2) were active, the dataset used in this study was trimmed to data between 15 June 2022 and 10 September 2024. For the period before the SR1 weather station was installed, we used weather data from the SR2 station for SR1. The SR2 weather station is located 1.83 km from the SR1 gauge, compared to 1.13 km for the SR1 weather station. In all time-series data, gaps less than one hour long were filled by simple interpolation.

Gaps longer than 1 hour in precipitation, when they occurred in a context where no other nearby ATMOS 41 station (a network of 4 across St. Croix) and no other daily gauge data (combination of GHCN, CoCoRaHs, and RAWS rain gauges across the island; Menne et al., 2012; Reges et al., 2016) recorded any rainfall (< 3 mm d^{-1}), were zeroed. The remaining gaps were visually inspected against neighboring rainfall records and were zeroed if appropriate (i.e., no rainfall occurred within a reasonable buffer of the gap). Additionally, periods in the rainfall record that significantly diverged from neighboring daily and subdaily rain gauges were systematically visually inspected, and if signs of erroneous data in the rainfall record were found, these, along with remaining unfilled gaps, were marked for rainfall interpolation. The SR2 weather station began experiencing recurring apparent equipment malfunctions in its precipitation estimates in the later months of 2024, which resulted in the use of this blending technique several times during that period. The chosen interpolation technique used the timings of the hyetographs of the nearest two subdaily rain gauges (upwind and downwind) and created a

relative blend of the rainfall timings of the two based on the distance from the weather station in question. This relative hyetograph was then used to convert the nearest daily rain gauge total into a subdaily hyetograph, which was used to fill the persisting gap or quality-flagged segment of the rainfall record. This interpolation method of relying on neighboring gauges (nearest neighbor for daily total and nearest two subdaily neighbors for blended relative hyetograph) was selected after evaluating its performance against several other proposed techniques, including the direct use of GPM IMERG satellite estimated precipitation at a 30-minute timestep, the use of Daymet data (Thornton et al., 2022) to interpolate daily precipitation total, and kriging interpolation for daily precipitation total from all nearby available daily gauges. The use of neighboring gauges rather than gridded datasets such as GPM IMERG was further supported by the findings of Bathelemy et al. (2022), who evaluated gridded datasets for the Caribbean archipelago, and found that although some datasets perform reasonably at the daily timescale, RMSE remained high for gridded data at the subdaily scale.

In streamflow measurements, there were generally no gaps longer than 1 hour that required any form of interpolation, but several equipment failures did necessitate the use of weather station barometric pressure to calculate water level, which was done using a correction in elevation difference to estimate atmospheric pressure at the stream gauge location (following Panek and Sorrells, 1996). Furthermore, at SR1, streambed scouring and shifting micro-topography (an acknowledged issue in stream hydrology in this region; e.g., Li et al., 2022) caused the original sensor deployment to be located outside of the thalweg beginning 14 November, 2023, such that a new sensor was deployed some 2 m away in the new thalweg. The altitude difference between these two points of measurement was surveyed in the field at 13 cm and used to correct the stream gauge record from 27 October, 2023 to 14 November, at which

point the new sensor's data was used going forward. The flow event encompassing this event was not used for analysis since the discharge calculation was unknown with the changing streambed topography. At SR2, a temporary battery power failure necessitated the deployment of a backup data logger 1 m away from the original, with a 3.5 cm altitude difference surveyed in the field and used as the hydrograph data from 15 August 2024 to the end of the dataset. It should also be noted that a major flood event occurred at SR2 on the night of 3 May, 2024, and the stream was over its banks during the peak. As a result, the discharge calculated during that period (of ~1 hour) is likely underestimated and erroneous.

In soil moisture data, gaps greater than 1 hour were only interpolated if they occurred while receiving less than 6 mm of precipitation. The threshold of 6 mm was chosen as a reasonable value (based on Acharya et al., 2020) below which soil moisture status at depths of 10 cm and greater would not be expected to be substantially affected. Above this value, the soil moisture could be expected to exhibit changes that could not be captured by interpolation, and these gaps were left as empty data where they occurred.

In all variables, after the above QA/QC processes were used, data was also subjected to visual inspection to correct obvious data errors or outliers, such as readings logged during instrument handling or deployment. A full record of alterations made to the raw data was kept. These gap-filling and data-cleaning procedures are similar to those carried out by other researchers (Pappas et al., 2014; Serrano-Notivoli et al., 2022; Varadarajan et al., 2022). Additionally, we performed a cross-validation check of random daily sampling with the same extent (i.e., duration and frequency) as actual QA/QC procedures, checking gap-filled or interpolated values against observed data (precipitation R^2 at SR1 = 0.962; at SR2 = 0.993; streamflow R^2 at SR1 = 0.999; no interpolation took place at SR2; soil moisture R^2 at SR1 =

1.000; at SR2 = 1.000). All data processing and analysis were performed in R (v4.2.3, R Core Team, Vienna, Austria, 2025).

Rain event delineation

We delineated discrete rain events from the weather record at both SR1 and SR2 weather stations for further processing. A minimum inter-event time (MIT) of 6 hours was used as the primary parameter for delineation (Dunkerly, 2015; Knappenberger et al., 2017). In event delineation, longer MITs are associated with increasing intra-event variability (i.e., multiple peaks within an event), while shorter MITs are associated with event interdependence, which is problematic for most statistical analyses (Dunkerly, 2022). We chose the MIT of 6 h to minimize intra-event variability while still permitting significant infiltration between events and ensuring streamflow responses have sufficient time to respond to rainfall and be effectively paired with rainfall (Hall et al., 2022; Molina-Sanchis et al., 2016). To account for trace, non-zero quantities of precipitation recorded by the sensors, only 15-minute rainfall observations exceeding 0.1575 mm were used to define the end of a rainless period. This threshold is based on research in Puerto Rico (Holwerda et al., 2012) that determined a minimum canopy evaporation rate of 0.63 mm h^{-1}, converted to a 15-minute equivalent. Any observed precipitation below this value was assumed to be intercepted and therefore not involved in soil hydrological processes.

Baseflow separation

Using the resulting hydrographs, we performed baseflow separation using Duncan's (2019) physically-based technique. We selected this technique because it was demonstrated to produce plausible results even for highly ephemeral flow systems. Unlike most separation

methods, this method allows baseflow recharge during flow events, in addition to fitting to the recession curve after rain events by adapting the widely used digital filter technique of Lyne and Hollick (1979). We fit the baseflow recession curve fitting parameter *k* according to Duncan's recommendations (0.87 at SR1 and 0.85 at SR2, based on daily timesteps), and *c*, the constant flow term, was set to 25% of the mean flow for each site as a negative value, or -0.0058 m^3 s^{-1} at SR1 and -0.0118 m^3 s^{-1} at SR2. The negative values reflect the physically-based approach and represent a constant water loss to the hyporheic zone in a losing stream, whereas positive values are often used to represent snowmelt.

Flow event delineation, event pairing, and runoff coefficients

To delineate separate streamflow events, we used a combination of the "peaks-over-threshold" approach and the baseflow-proportion approach (Wasko and Guo, 2022). We chose this method to balance the need to maintain event independence (by focusing on quickflow) with the recognition that baseflow thresholds alone are insufficient for hydrograph separation in small, forested catchments, as argued by Hewlett and Hibbert (1967). The approaches we used are common in other rainfall-runoff studies, despite requiring some judgment of the appropriate method to use (Giani et al., 2021; Ross et al., 2021). A new event was initiated when streamflow increased by more than 0.01 m^3 s^{-1}, and the event was continued until quickflow fell below 0.003 m^3 s^{-1}. To ensure event independence, we merged delineated events if the quickflow at the start of a new event exceeded 0.01 m^3 s^{-1} (i.e., prior to the required new flow spike of > 0.01 m^3 s^{-1}). We then paired these streamflow events with rain events, proceeding sequentially from the most recent flow event to the earliest. For each flow event, we selected the initiating rain event as the one that was either ongoing or had ended within the minimum inter-event time (MIT)

before the flow event began. This rain event, plus all subsequent rainfall within the flow event (except for rain already paired to the subsequent flow event), was considered as part of the rainfall for that flow event. The MIT of 6 h is often used for event delineations of this kind (and for rain events as above; Dunkerly, 2015; Knappenberger et al., 2017). Still, we calculated the first-order autocorrelation of time intervals between flow events for a range of MIT values (1 to 24 h) to quantify the temporal dependence of events under different values of this parameter. Generally, event delineation was relatively insensitive to changes in MIT (autocorrelation coefficients ranged from 0.107 to 0.131 at SR1 and -0.075 to 0.080 at SR2; coefficients at the chosen 6 h MIT were 0.127 and 0.027 at SR1 and SR2, respectively). We calculated event runoff coefficients by dividing the total event quickflow (converted to mm based on catchment or subcatchment size) by the total precipitation associated with the flow event.

Data analyses

Soil saturation and antecedent soil water

Using porosity data derived from bulk density measurements and time-series soil moisture measurements at depth, we calculated the soil water storage and unsaturated pore space (in mm) for the 1 m soil profile. Sensor measurements were treated as midpoints of soil strata (i.e., 0−20 cm, 20−40 cm, 40−75 cm, and 75−100 cm). The total soil water storage (in mm) at the beginning of rainfall for a given flow event was recorded as the antecedent soil water (*ASW*) for that event at the respective soil moisture site (hillside or streambank). We calculated unsaturated soil pore space as the difference between total porosity and volumetric water content ($cm^3\ cm^{-3}$), multiplied by the soil profile thickness, following the methods used by Farrick and Branfireun (2014b). Based on the work of Singh et al. (2021) and Tymchak and Torres (2007),

we also calculated the wetting front velocity from soil moisture data at each site to provide insight into subsurface flow. This is calculated by dividing the depth of the soil moisture probe by the time between the start of a rain event and a soil moisture response. Soil moisture response is defined as an increase greater than the standard deviation of the soil moisture values measured in the 4 hours previous to the rain event (Tymchak and Torres, 2007), or the instrument error ($0.03\ cm^3\ cm^{-3}$), whichever was greater. Additionally, downward preferential flow can be detected by deeper moisture probes responding to precipitation before shallower ones (Singh et al., 2021).

Piecewise regression modeling of runoff thresholds

To model runoff responses (i.e., event quickflow), we performed a piecewise regression analysis (a "broken stick" model), a common approach in estimating runoff thresholds (Farrick and Branfireun, 2014b; Ross et al., 2021), where the sum of event precipitation (*P*) and pre-event soil water (*ASW*) were taken together as the predictor (*ASW+P*). For each soil moisture station (hillside and streambank) at both SR1 and SR2, we fit a piecewise linear model in R using a function that takes a suggested visual breakpoint and performs Brent optimization of the root mean squared error (RMSE) to locate the threshold where the linear equations fit best on either side of the threshold. Then, the intersection of these two lines was taken as the runoff threshold of the model, where the combined quantity of pre-event soil water and precipitation begins to linearly predict additional quickflow. For SR2, where only 11 flow events were available, this fitting process was unstable, so we assumed a slope of 0 for the linear equation to the left of the breakpoint to permit a fit of the linearly increasing part of the runoff response.

Dimensionless characterization of runoff events (Dunne-plot)

To characterize runoff events and provide comparisons of events between sites, we created a dimensionless "Dunne-like" diagram of flow events following Mirus and League's (2013) method, based on the original "Dunne" diagram (1978). This plot is dimensionless on both the x- and y-axis, where the x-axis is precipitation intensity over surface saturated hydraulic conductivity, K_{sat} (mm h^{-1}/mm h^{-1}), and the y-axis is precipitation depth over unsaturated soil storage (mm/mm). The hillside values of these soil variables were used to best represent the center of the catchment, following the approach used by Mirus and League (2013). To estimate surface K_{sat} at these locations, we used a pedotransfer function to convert particle size fractions to a K_{sat} estimate. Because many pedotransfer functions are not well suited for tropical soils and were calibrated in soils with generally low clay content (Tomasella and Hodnett, 2004), we chose the "WMF330" pedotransfer function developed by Ottoni et al. (2019), which performed well in Brazilian as well as European soils to calculate K_{sat} (cm d^{-1}) and only required particle size fractions of silt and clay (%) and matrix bulk density (BD_m; g cm^{-3}) as inputs (Eq. 3-1):

$$K_{sat} = 1266\ (0.582 - 0.00216\ silt - 0.00232\ clay - 0.203\ BD_m)^{1.853}$$

However, when soils were extremely stony (i.e., rock mass fraction > 30%), we also applied the pedotransfer function described in Nasri et al. (2015) to modify the matrix bulk density of stony soil by the rock mass fraction (R_w) and overall sample bulk density (BD; g cm^{-3}), which helps account for the skeletal structure rocky soils can create, preventing additional compaction (Eq. 3-2):

$$BD_m = BD\ (1 - 1.67\ {R_w}^{3.39})$$

We plotted flow events as well as rain events that did not produce runoff flows in this way for further analysis.

Connectivity and lag times

To assess the temporal runoff response of the catchment, we calculated the time lag between the onset of precipitation and the initiation of flow. This metric proved more useful than other standard measures of lag times, such as peak rainfall to peak flow or centroid of rainfall to peak flow (Black et al., 2021; Sultan et al., 2022). This was preferable because of significant variability in recorded flow event durations (typical of an ephemeral system), whereas the start of flow in ephemeral systems provides a more consistent and meaningful indicator for analyzing runoff generation. We used a one-way ANOVA to confirm an effect of site on this lag time metric ($\alpha = 0.05$). All statistical analyses and data visualizations were performed in R (packages 'dplyr', 'ggplot2', 'glmnet', 'scales', 'viridis', 'zoo' were used: Friedman et al., 2010; Garnier et al., 2024; R Core Team, 2025; Wickham, 2016; Wickham et al., 2023a; Wickham et al., 2023b; Zeileis and Grothendieck, 2005)

To investigate the degree of connectivity between streamflow at SR1 and SR2, we classified the hydrograph of both sites according to five connectivity categories: 1) "gaining" connectivity when streamflow downstream was greater than streamflow upstream; 2) "losing" connectivity when streamflow upstream was greater than streamflow downstream; 3) only downstream flowing; 4) only upstream flowing; and 5) no flow at either site. We also separated the data record into three periods, one comprising "connected" conditions (i.e., scenario #1 and #2 above), "disconnected" conditions (#3 and #4), and "no flow" (#5) conditions. We added buffers to the transitions between flow states by excluding data from periods within one average lag time (calculated above) of a flow-state transition, to exclude transitional periods. We then used these three states as the categorical variable in a one-way ANOVA (in R) on soil water

content at 100 cm at the SR2 streambank to analyze a possible physical indicator of connectivity thresholds (α = 0.05).

Results

Runoff thresholds and environmental conditions

Average annual rainfall across the Virgin Islands (from NOAA GHCN gauges; Menne et al., 2012) was 597 mm in 2021, 1101 mm in 2022, 609 mm in 2023, and 1630 mm in 2024 (calendar years; 2024 was the third rainiest year in the Virgin Islands in the previous 100 years) with the rainfall in 2022 associated largely with two major events, Tropical Storm Fiona (September 2022) and a subsequent major precipitation event in November. The pronounced dry period in 2021 and prior to September 2022, part of a recent trend of drying (Fig. 3-6) is evident in the soil water content data at the beginning of our study (Fig. 3-7), followed by a year-on-year increase as this dry period was alleviated by the rainfall of late 2022. Actual observed rainfall at the two weather stations during the study was 3031 mm at SR1 and 2388 mm at SR2, highlighting the variability among locations. Streamflow followed this pattern, with initial flow in 2022 caused by the initial pulse of rainfall and more consistent flows beginning in the 2023 rainy season, eventually leading into the exceptionally wet year of 2024 (Fig. 3-7). A total flow of 878,403 m^3 (SR1) and 892,448 m^3 (SR2) was recorded for the duration of this study, of which 54% was separated as baseflow at SR1 and 21% at SR2. The processes of baseflow separation, hydrograph separation, and rainfall event delineation described above resulted in 49 delineated flow events at SR1, and 11 flow events at SR2 over 3182 h of flow occurring at SR1, and 1199 h at SR2. These flow events are summarized in Table 3-4. The peak flow and largest flow event in the study period occurred on 8 May, 2024 at both SR1 (Fig. 3-8) and SR2 (Fig. 3-4).

For the SR1 upstream subcatchment, piecewise linear regression modeling identified a runoff threshold (Fig. 3-9) at 362 and 309 mm of combined pre-event soil water and precipitation for the hillside and streambank locations, respectively (RMSE = 0.32 and 0.34 mm). After the runoff threshold was satisfied, a slope of 0.658 (hillside) and 0.572 (streambank) characterized the linear rise of quickflow with $ASW+P$ (Fig. 3-9). At SR2, RMSEs for piecewise regressions were larger (hillside RMSE = 1.57 mm; streambank RMSE = 0.96 mm), owing to the reduced number of total events (n = 49 for SR1, while n = 11 for SR2). Runoff thresholds in SR2 were 270 mm (hillside) and 363 mm (streambank) with slopes of 0.181 and 0.189 (Fig. 3-9). In wetting front velocities, we observed a trend of increasing mean wetting front velocity with depth in all but one site (SR2 hillside; Table 3-5). Preferential flow was not detected according to our analysis of soil moisture data at any time during the study period.

Runoff coefficients and runoff generation

The runoff coefficient for the SR1 subcatchment was 0.237, while for the entire catchment (i.e., SR2) it was 0.086, indicating that the headwaters valley was significantly more productive in generating runoff compared to the catchment as a whole. We computed these study-wide runoff coefficients with total flow (including baseflow). Meanwhile, event runoff coefficients at SR1 had a maximum of 0.387 (mean = 0.046), whereas the maximum event runoff coefficient at SR2 was 0.165 (mean = 0.065). Event runoff coefficients at SR1 were partially explained by both precipitation intensity over hillside K_{sat} (i.e., the Fig. 3-10 x-axis) with a negative reciprocal relationship (Fig. 3-11a; R^2 = 0.50) and by simple rainfall, with a positive linear relationship (Fig 3-11b; R^2 = 0.53). At SR2, precipitation intensity over K_{sat} had a strong

reciprocal relationship (Fig 3-11c; R^2 = 0.88), while simple rainfall was not explanatory (Fig 3-11d; R^2 = 0.03).

When runoff events are plotted logarithmically in a Dunne-like diagram with runoff coefficient as a third dimension, a visible effect of precipitation intensity on runoff coefficient emerges (Fig. 3-10a). This distribution of events shows that higher runoff coefficients are driven by saturation excess overland flow and/or subsurface stormflow, as opposed to Hortonian overland flow. In addition, flow events at SR2 are driven more by saturation excess overland flow than by subsurface stormflow, as compared to those at SR1. Comparatively few runoff events are driven more by Hortonian flow at either site (though more at SR2), and the runoff coefficients from these events are low. The role of subsurface flow at SR1 is supported by the observation of a water table perched above the level of streamflow in the streambank zone on 29 November 2023 (Fig. 3-4a) and by increased wetting front velocities at depth (Table 1). Rain events that did not result in streamflow are also plotted in Fig 3-10b. Across both sites, a preference for runoff generation with increasing saturation excess was notable, with some Hortonian flow events as noted above. Rain events that failed to generate runoff were observed to have lower y-axis values (driven mostly by lower rainfall accumulations), but also demonstrated the lower limits of subsurface stormflow pathways in both catchments (Fig. 3-10b).

It should also be noted that although values on the dimensionless axes of Fig. 3-10 above and below the thresholds of 10^0 would, in theory, represent thresholds between Hortonian vs. non-Hortonian flow (on the x-axis) and saturation excess overland flow vs. subsurface stormflow (on the y-axis), significant simplifications and assumptions intrinsic to the plot (e.g., assuming uniform K_{sat} throughout the catchment) imply Fig. 3-10 should only be conservatively

interpreted in terms of different runoff generation types, more as a spectrum than as categorical shifts. This is in addition to reasonable caveats stemming from the method of K_{sat} estimation (the pedotransfer functions) and unsaturated storage volume (porosity measures).

Connectivity

Lag time, or catchment response time, from the start of precipitation to the first streamflow response, varied by site. Upstream (SR1), streamflow lag time was 3.9 h (± 1.0, standard error), whereas lag time downstream (SR2) was 10.1 h (± 3.1), which was significantly different according to the results of the one-way ANOVA ($p = 0.014$). The larger of these two mean lag times, 10.1 h, was used for the buffering of flow-state transitions (discussed in 2.4.4 and below in this section).

Connectivity flow-states are plotted in Fig. 3-12 against soil water content ($cm^3\ cm^{-3}$) at 100 cm depth at the SR2 streambank. The presence of the typical dry seasons at the beginning of the dataset (summer 2022) and through spring and summer 2023 are marked by a lack of flow during most of that period. In contrast, the wet periods during the latter months of 2022 and 2023 correspond to the typical rainy season. However, the extraordinarily wet year of 2024 disrupted this pattern, with no significant dry period occurring early in the year. The longest observed period of "gaining" connectivity (when the flow rate is greater at the catchment outlet than upstream) was recorded in 2024 (Figs. 3-8; 3-12).

The hypothesized relationship between deep soil moisture at the SR2 streambank and connectivity is confirmed by the results of the ANOVA between "connected," "disconnected," and "no flow" flow states, where Tukey's HSD post-hoc testing detected a significant difference ($p < 0.05$) in the mean 100 cm soil water content among all three states (Fig. 3-13). The highest

moisture levels correspond to the connected (mean = 0.34 ± 0.03 cm^3 cm^{-3}) and disconnected flow states (mean = 0.34 ± 0.03 cm^3 cm^{-3}), while drier conditions (mean = 0.27 ± 0.03 cm^3 cm^{-3}) related to no flow. The statistically significant difference between connected and disconnected states most likely owes to a wider distribution of moisture values in the disconnected state (and a large number of total observations; Fig. 3-13).

Conditions in Sugar Bay (the embayment nearest the mouth of the Salt River watershed outlet and part of the larger Salt River Bay) may be taken as an indicator of connectivity between the channel network of the Salt River drainage basin and the marine environment. In normal conditions, salinity levels in Sugar Bay are comparable to those of the rest of Salt River Bay and to the surf outside the bay in the Caribbean Sea (e.g. 33–38 ppt). Even shortly after rainy periods (e.g. 29 November, 2022), salinity in Sugar Bay was observed at normal marine levels (mean 33.4 ppt observed throughout Sugar Bay on that date). This is despite the presence of streamflow at SR2 on the same date, 29 November. Hence, streamflow at SR2 in itself is not necessarily sufficient to establish surface connectivity between Sugar Bay and the terrestrial stream network. This is due to the presence of a flat swampy area between SR2 and the Sugar Bay mangrove where the stream channel loses definition and gives way to sheet flow, effectively buffering Sugar Bay from discharge from the watershed (Fig. 3-14) except in exceptionally saturated conditions (Fig. 3-15). In fact, field observations from within the swampy area confirmed that even during rainy periods, surface water was usually absent, confirmed by the lack of a salinity signal in Sugar Bay (Figs. 3-14; 3-15).

However, consistent with the behavior of the catchment as a whole, sufficient saturation of the lowland zone can lead to complete ridge-to-reef connectivity and direct surface discharge through this swampland to the Sugar Bay mangroves and beyond. On 6 May, 2024, following the

study-wide flow peak of 3 May, we measured salinity in a linear transect from the edge of the mangrove forest furthest landward point in Sugar Bay where outfall would be expected, and confirmed the presence of freshwater and estuarine conditions in Sugar Bay extending to at least 575 m from the edge of the mangrove swamp (Fig 3-16). This is in line with historical observations of freshwater in Salt River Bay, but it is still unknown how frequent these events are today in comparison to the past, though commentators usually presume they have become less frequent (concomitant with the overall trend of reduced streamflows; Lancellotti and Hensley, 2024).

Discussion

Thresholds and runoff generation

Several lines of evidence support the existence of runoff generation thresholds in the Salt River watershed, in addition to existing theoretical support for the concept in the literature across various catchment types, including ephemeral systems (Ross et al., 2021; Saffarpour et al., 2016; Serrano-Notivoli et al., 2022). The piecewise regression modeling shown in Fig. 3-9 displayed apparent threshold behavior, with thresholds ranging from 270 to 363 mm $ASW+P$. These values are consistent with the threshold of 289 mm $ASW+P$ reported by Farrick and Branfireun (2014b). Their study was methodologically similar to ours and was also performed in a tropical dry forest. Threshold behavior in pre-event soil water and precipitation has also been found at the plot- and catchment scale by other researchers (DeGuzman et al., 2023; Wang et al., 2022) and across different climatic zones (Penna et al., 2011). Although the number of flow events was low for SR2, causing some uncertainty in the actual value of the thresholds, the behavior of non-runoff-

generating rain events versus runoff events (Fig. 3-10b) indicated a “fill-and-spill” behavior that is consistent with the existence of a threshold.

The slopes of the rising limbs of piecewise regression (Fig. 3-11), ranged from 0.658 to 0.181 (despite acknowledged uncertainty; viz., DeGuzman et al., 2023) of additional quickflow (mm) per additional soil water and rainfall (*ASW+P*, mm). This suggests that, above the runoff threshold, not all additional water contributes directly to quickflow. Instead, portions are likely abstracted into other forms of storage or impoundment, such as deeper soil infiltration or temporary surface storage. This aligns with findings from several researchers of island hydrogeology (O’ahu Island: Dores et al., 2020; Barbados, Guam, and Puerto Rico: Jones and Banner, 2003; Lifu Island, New Caledonia: Nicolini et al., 2016) who agree that large storm events (e.g., 200 mm), rather than ordinary convective showers, account for the groundwater recharge of island aquifers, which is also supported to a limited degree by the groundwater level record in Fig. 3-17. The variability of the slopes of the piecewise regression (Fig. 3-9) meanwhile may stem largely from error related to the spatial heterogeneity of rainfall in the region (Hernandez et al., 2000; Varadarajan et al., 2022). However, the lack of any runoff events in which rainfall exceeded the available soil pore storage space and the high wetting front velocities at depth (Table 1) in three of the soil measurement locations supports the possible importance of subsurface flow (Singh et al., 2021), particularly at SR1, where the behavior was stronger. This also supports the general theory that steeper catchments with shallower soils would exhibit a preference for subsurface flows (Gutiérrez-Jurado et al., 2019; Mirus and Loague, 2013).

The fact that *ASW+P* explained runoff generation better than rainfall alone may also point to the importance of pre-event soil water in the hydrograph, transported often through

subsurface flow, which other studies (e.g. Farrick and Branfireun, 2015) have noted can be a major component of runoff and streamflow in some catchments. Indeed, Beven (2021) argues against using the term "runoff" for this reason while nevertheless being distinct from baseflow. In ephemeral stream systems, Gutiérrez-Jurado et al. (2019) found that depth to groundwater is a key control on streamflow activation when subsurface and saturation-excess flows are dominant, as they appear to be in Salt River. This aligns with several of our lines of evidence: that streamflow is controlled by a combination of rainfall quantity and pre-event soil water (Fig. 3-9); that saturated groundwater was actually observable near the surface during a period of sustained flow (Fig. 3-4a); and that stream connectivity was related to soil water at depth (Figs. 3-12 and 3-13). The combination of soil water and precipitation ($ASW+P$) being the controlling factor for runoff generation thresholds is also supported by the higher event runoff coefficients related to saturation-excess-type runoff events (Fig. 3-10a).

The apparent dominance of subsurface stormflows and saturation-excess overland flow observed in our study initially seems to contrast the most significant body of hydrologic literature for the Virgin Islands, in which Ramos-Scharrón and LaFevor (2016; 2018) make a strong argument in favor of Hortonian (infiltration-excess) overland flow being an important component of the hydrograph in watersheds of St. John (see also Ramos-Scharrón et al., 2023). Their research attributes this to the widespread construction of paved and unpaved roadways in steep parts of these catchments over the past half-century, driven by land development and tourism growth. Ramos-Scharrón and LaFevor (2018) show that rainfall intensities as low as 10 mm h^{-1} in catchments on St. John can initiate streamflow. However, the authors also note that in the absence of road networks, a total rain depth of 10–78 mm would be required to generate flow and that these catchments would likely exhibit subsurface/saturation-excess overland flow as the

dominant mechanism, which is common in forested tropical watersheds (Farrick and Branfireun, 2014b; Huang et al., 2021). They also highlight that the most important contributions to runoff from Hortonian road runoff would be in small rain events (Ramos-Scharrón and LaFevor, 2016), which does not necessarily conflict with our findings, nor those of researchers elsewhere (Zhang et al., 2025). It is also the case that smaller catchment sizes (Cerdan et al., 2004) in St. John would magnify the importance of short-scale runoff generation from Hortonian events on unpaved roadways that, in the larger watershed of Salt River, would be less relevant.

Our finding of the relative rarity of Hortonian flow events is largely based on our estimates of K_{sat}. The absolute physical relevance of a value of one for the ratio of rainfall intensity over K_{sat} should be interpreted with caution though, as noted above. Infiltration capacity, which is often governed by the unsaturated hydraulic conductivity rather than K_{sat}, varies with moisture conditions. A preferred method for quantifying infiltration capacity at all times in unsaturated conditions is to use the soil hydraulic parameters of the van Genuchten (1980) equation, but these were not available for the soils in our study. Thus, the x-axis in Fig. 3-10 should be considered a simplification since the infiltration rate in unsaturated conditions depends on the hydraulic gradient at the wetting front rather than on K_{sat}. It is more useful to conceive of the meaning of the Fig. 3-10 x-axis as a relative rather than an absolute metric. Still, our estimate of K_{sat} for SR1 (hillside) was 39.4 mm h^{-1}, compared to the value (23.0 mm h^{-1}) reported by Ramos-Scharrón and LaFevor (2016) for the same soil type (Victory-Southgate) found both in St. John and St. Croix. However, it is lower than the value estimated by the U.S. Soil Survey for the same soil (67.2 mm h^{-1}; USDA-NRCS, 2024). A study by Juliá et al. (2021) of field-measured K_{sat} in Puerto Rico soils compared to U.S. Soil Survey data found that the soil survey consistently underestimated measured field-measured values. This discrepancy aligns

with infiltrometer data from a St. Croix soil (Sion clay), which showed a measured surface K_{sat} of 200.7 mm h^{-1} (Hensley et al., in review), compared to the Soil Survey value of 24.1 mm h^{-1}. Based on these findings, we consider it likely that the K_{sat} values used in this study for Fig. 3-10 are most likely underestimates, further disfavoring Hortonian flow as a dominant runoff mechanism, though these caveats must be kept in mind.

The apparent contradiction with the work of Ramos-Scharrón and LaFevor (2016; 2018) may be resolved by their finding that the topographic position and orientation of St. John's road networks significantly influence their contribution to the hydrograph (Linh et al., 2024; Ramos-Scharrón and LaFevor, 2018). This could help explain the apparently lower importance of these road networks in Salt River. Other factors accounting for the different findings may relate to key differences between Salt River (and similar watersheds on the island of St. Croix), compared with those of St. John where Ramos-Scharrón and colleagues conducted their research. For example, compared to St. Croix, St. John catchments are generally steeper and smaller, with shorter losing streambeds, and anthropogenic impoundments (check dams, ponds, and various legacy stormwater infrastructure; IRF, 1993) are less common in St. John. Finally, their work on unpaved roads was primarily focused on sediment production (a major problem for water quality, both freshwater and marine, across the Virgin Islands). While we found that streamflow discharge from the Salt River mouth into Salt River Bay was relatively rare, sediment plumes have been repeatedly observed by residents and bay users. This raises the possibility that water quality impairment could often occur through nearshore stormwater flows (potentially from nearshore unpaved road networks like those Ramos-Scharrón and colleagues describe), rather than from the primary channel network. An important implication of this would be that water

quality protection measures are significantly more important in smaller, steeper watersheds more typical of St. Thomas and St. John, as opposed to St. Croix.

Disruptions to connectivity

The lower study-wide runoff coefficient at SR2 (0.086) compared to SR1 (0.237) is to be expected, as larger catchments generally have lower runoff coefficients (Cerdan et al., 2004; Gomi et al., 2008; Mounirou et al., 2020; Mounirou et al., 2021). Though these values may be higher than normal for St. Croix (Jordan, 1975) due to the rainy year of 2024, they are nevertheless in line with runoff coefficients reported for relevant catchments elsewhere (~0.05–0.35 in Mallorca: Peña-Angula et al., 2021; 0.04–0.12 on Norfolk Island: Hughes, et al., 2022; 0.05–0.31 in a Mexican tropical dry forest; Farrick and Branfireun, 2014b). The runoff coefficient can be interpreted at the highest level as a "spill" of the "fill-and-spill" concept (McDonnell et al., 2021), i.e., the logical result of an unusually rainy period during our study. We also observed a seasonal or year-over-year effect of increasing flows (potentially due to groundwater storage), which is consistent with a system dominated by saturation-excess and subsurface flow. This followed the initial major streamflow activation event of September 2022, an effect also observed by Gutiérrez-Jurado et al. (2019) in an ephemeral system. In terms of the connectivity of the stream network, this indicates a requirement for some combination of: 1) sufficiently saturated soil to promote saturation-excess runoff and subsurface flow; and 2) sufficient recent streamflow for various stream impoundments or storage structures to remain full so that connectivity can be maintained. The relatively large alluvial lowland area of the Salt River watershed (around SR2) overlying the Kingshill Aquifer (Miller et al., 1999) appears to act as a significant buffer against discharge from the headwaters to the bay unless sufficient

saturation has been reached (Figs. 3-12 and 3-13). The lowland reaches of the stream network otherwise act as losing streams at almost all times, serving to disrupt connectivity. These lowland reaches, like ephemeral streams elsewhere (Al-Amri et al., 2023), may also recharge the aquifer during periods of high flow, based on data from a monitoring well 6.7 km from SR2 (Fig. 3-17; USGS, 2024), where a higher groundwater table was associated with flow periods at SR2 (one-way ANOVA; $p < 2 \times 10^{-16}$). Our results also appear to support the hypothesis of Gill et al. (1997; a similar concept also given by Tombs and Barton, 1979) that groundwater recharge zones exist at the interface between the volcanic upland geology of the Northside Range and the alluvial and carbonate lowland geology of the Central Valley.

Besides this natural geomorphic buffer against frequent discharge to the sea and the various small-scale impoundments and dams along the stream channel (IRF, 1993), a major disruption to connectivity between SR1 and SR2 is the U.S. Army Corps of Engineers (USACE) flood control structure, installed in 2004 (USACE, 1987). This structure diverts the flow of the stream and significantly broadens the channel, permitting increased infiltration along its 1.8 km course. This structure is thought to further disrupt the connectivity between the headwaters and the coast (Lancellotti and Hensley, 2024). Thus, identifying an apparent threshold of soil water content in the streambank zone related to connectivity along the entire course of Salt River is important for predicting and modeling watershed connectivity in Salt River and similar catchments in the Virgin Islands. The high but variable wetting front velocity at 100 cm in the streambank soil of SR2 is a further indication of the potential importance of this metric because it demonstrates the potential for significant subsurface flows either to or from lowland streamflow under the right soil moisture conditions (James and Roulet, 2007; Singh et al., 2021). Although watersheds with a larger alluvial area preceding coastal discharge are much more

common in St. Croix than in the rest of the Virgin Islands, alluvial fans of at least some size are a common feature of catchments across the archipelago, pointing to this geomorphic feature as a likely control on ridge-to-reef connectivity. This suggests a broader potential for management and monitoring of ridge-to-reef runoff and groundwater recharge by focusing on such regions of islands in the northeastern Caribbean, and implies more intensive runoff management would be required in watersheds with a smaller or shorter coastal alluvial area before reaching the sea.

In past years, observers at Salt River Bay have reported reduced salinity levels, and in 1977, a "freshwater wedge" associated with inputs from the stream network (Shepherd and Dill, 1977; Kendall et al., 2005; Pait et al., 2020). More recently, though, Kendall et al. (2005) referenced data showing declining turbidity in Sugar Bay from 1981–94, even after the significant loss of mangroves following Hurricane Hugo in 1989. They attributed this decline in turbidity to reduced stream discharge into the bay during that period, which is consistent with reports from across St. Croix and other parts of the Virgin Islands in the second half of the 20th century about declining streamflow and reduced connectivity (Lancellotti and Hensley, 2024). These declines predate the construction of the USACE flood control project in 2004, making it more likely that a falling groundwater table over that period, coupled with declining rainfall (Fig. 3-6) contributed to this decrease. This interpretation is further supported by our findings, which highlight the multi-year impacts of changing hydrometeorological conditions on streamflow. Rainfall in the Virgin Islands appears to follow long-term oscillations (Fig. 3-6), possibly driven by oceanic or atmospheric cycles in the Atlantic basin, which indicates that streamflow regimes and runoff coefficients are likely to also shift over the years, and are sensitive to the effects of recent years. Climate change, which may only increase the annual precipitation variability, may produce (as in 2024) major wet periods that make saturation-excess flow and large runoff

coefficients commonplace, even as other years may see extreme dryness with very rare flows dominated by Hortonian processes.

Conclusions

As an ephemeral stream, runoff generation in Salt River is highly dependent on rainfall. However, pre-event soil water content is equally important as a predictor of flow, and soil water content at depth is a helpful predictor of watershed connectivity. Runoff at SR1 displayed qualities of both saturation-excess overland flow and subsurface flow. At SR2, the dominance of saturation-excess overland flow and longer lag times to initiate streamflow is best explained by the low topography and deeper soils of the Central Valley. The deep water table of the Kingshill Aquifer (normally some 6–12 m below ground level), as opposed to relatively shallow water tables that can develop over bedrock in the headwaters zone, best explains the much more episodic, flashy nature of streamflow observed at SR2 near the catchment outlet (Fig. 3-7).

Baseflow and subsurface flows can be sustained for longer periods in the headwaters valleys that overlay volcanic geology, even while surface connectivity becomes disrupted in the lowland zone. This confirms earlier work speculating that the interface between these two hydrogeologic zones may serve as a natural recharge area on the island of St. Croix. The Kingshill Aquifer is the most significant source of freshwater in the entire Virgin Islands archipelago, so this additional evidence for important geographic zones of groundwater recharge has socioeconomic implications as the Virgin Islands pursues diversification from tourism by promoting agriculture and industry, which implies continuing demands on freshwater resources. Groundwater level and deep soil water content, meanwhile, have predictive potential for ridge-to-reef connectivity and lowland streamflow. This possibility of prediction could be important as

managers attempt to balance marine water quality and island water security concerns against riparian ecology and stormwater management. Our findings also confirm that discharge events to the bay were relatively rare during the study period despite continuing reports of impaired marine water quality. This suggests that nearshore stormwater management and water quality issues may sometimes outweigh catchment-wide management and stream discharge inputs as controls on marine water quality and ecosystem health. As land use continues to shift across the Virgin Islands, from reforesting of abandoned agricultural land to the spread of impervious surfaces and invasive species with unknown ecohydrological impacts, our results contribute to an improved understanding of runoff generation processes in the Virgin Islands, providing new streamflow datasets to the hydrologically understudied region of the northeastern Caribbean.

Tables and Figures

Table 3-1. Actual measured streamflow rates in Salt River at various gauge heights.

Site	Gauge [m]	Discharge [m^3 s^{-1}]
SR1	0.01	0.002088
SR1	0.01	0.003399
SR1	0.10634	0.026507
SR1	0.111523	0.053
SR1	0.118505	0.061
SR1	0.125565	0.01693
SR1	0.18221	0.215183
SR1	0.1913	0.175
SR1	0.202252	0.1774
SR1	0.34782	0.235
SR2	0.27	0
SR2	0.3399	0.0027
SR2	0.37	0.007
SR2	0.628208	0.269
SR2	0.645092	0.302
SR2	0.73212	0.39297

Table 3-2. U.S. Soil Survey data of sand and clay fraction and saturated hydraulic conductivity (K_{sat}) for selected soil series and map units, St. Croix, USVI

Depth [cm]	Variable	Arawak	Carib	Cramer	Glynn	Hessel-berg	Jeal-ousy	Maho Bay	Para-sol	Sandy Point	Sion	Soli-tude	South-gate	Victory	ArD	CaA	CvD	VsF
10	Clay [%]	25.0	32.5	35.0	33.5	55.0	35.0	25.0	30.0	25.0	45.5	17.5	18.5	18.5	26.9	32.3	28.1	20.6
	Sand [%]	37.2	34.7	26.5	35.3	17.1	33.3	38.5	33.5	57.0	24.2	63.1	43.0	43.0	36.1	36.1	33.4	41.4
	K_{sat} [mm h^{-1}]	100.8	32.4	54.0	94.9	3.6	79.2	172.8	25.2	18.0	3.24	403.2	100.8	32.4	95.6	41.3	56.5	67.2
30	Clay [%]	25.0	32.5	50.0	42.0	55.0	38.0	22.5	30.0	30.0	47.3	15.0	18.5	18.5	27.4	32.9	35.8	21.4
	Sand [%]	37.2	34.7	22.1	34.7	17.1	29.0	39.8	33.5	35.8	48.8	65.4	43.0	43.0	36.1	35.8	31.3	41.0
	K_{sat} [mm h^{-1}]	151.2	25.2	32.4	9.7	6.5	43.2	151.2	25.2	7.2	10.6	403.2	151.2	180.0	136.9	30.6	87.8	150.3
50	Clay [%]	25.0	32.5	-	37.5	37.3	38.0	-	38.5	30.0	27.5	15.0	-	18.5	26.2	32.1	23.5	21.1
	Sand [%]	37.2	34.7	-	32.2	41.0	29.0	-	27.8	35.8	55.1	65.4	-	43.0	37.1	35.9	39.2	41.1
	K_{sat} [mm h^{-1}]	9.72	25.2	9.7	54.0	0.04	43.2	9.7	18.0	7.2	100.8	403.2	9.7	180.0	11.4	35.6	61.6	88.2
100	Clay [%]	25.0	29.0	-	40.0	19.5	30.0	-	30.0	0.0	20.5	20.0	-	-	25.5	27.7	30.0	30.0
	Sand [%]	37.2	50.0	-	33.3	64.8	33.5	-	50.0	0.0	42.0	50.2	-	-	38.4	46.4	50.0	38.2
	K_{sat} [mm h^{-1}]	9.72	32.4	3.6	9.7	403.2	9.7	3.6	32.4	360.0	100.8	64.8	3.6	9.7	29.4	50.3	8.3	7.2

Table 3-3. Summary of soil physical characteristics in Salt River at upstream (SR1) and downstream (SR2) sites in hillside and streambank locations with U.S. Soil Survey map units: R_w (rock fraction by mass), sand, silt, and clay fractions from soil survey data as modified by correction factor from PARIO measurements, *BD* (raw bulk density), ρ (porosity), BD_m (matrix bulk density for stony soils or $R_w > 0.3$, computed from the Torri relation in Nasri et al., 2015), K_{sat} (saturated hydraulic conductivity computed by pedotransfer function from Ottoni et al., 2019), and K_{sat}-*SS* (computed from soil survey map units). Rows in italics were subjected to PARIO measurements.

Site	**Location**	**Depth**	**Map Unit**	R_w	**Sand**	**Silt**	**Clay**	***BD***	ρ	BD_m	K_{sat}	K_{sat}-*SS*
		[cm]		[-]	[%]	[%]	[%]	[g cm^{-3}]	[cm^3 cm^{-3}]	[g cm^3]	[mm h^{-1}]	[mm h^{-1}]
SR1	Hillside	10	VsF	0.35	57.5	38	4.5	1.25	0.47	1.19	39.6	67.3
SR1	Hillside	30	VsF	0.33	57.1	37.6	5.3	1.30	0.49	1.24	36.3	150.3
SR1	Hillside	50	VsF	0.12	57.2	37.8	5.0	1.37	0.52	1.37	29.5	88.2
SR1	Hillside	100	VsF	0.09	54.3	31.8	13.9	1.35	0.51	1.35	28.3	7.2
SR1	Streambank	10	CvD	0.66	49.5	38.5	12.0	1.27	0.48	0.75	63.42	56.5
SR1	Streambank	30	CvD	0.77	47.4	32.9	19.7	1.29	0.48	0.40	89.5	87.8
SR1	Streambank	50	CvD	0.59	55.3	37.3	7.4	1.29	0.49	0.93	55.1	61.6
SR1	Streambank	100	CvD	0.68	66.1	20.0	13.9	1.70	0.64	0.93	63.1	8.3
SR2	Hillside	10	ArD	0.11	52.2	37.0	10.8	1.30	0.49	1.30	29.9	95.6
SR2	Hillside	30	ArD	0.12	52.2	36.5	11.3	1.19	0.45	1.19	36.0	136.9
SR2	Hillside	50	ArD	0.16	53.2	36.7	10.1	1.33	0.50	1.33	28.9	11.5
SR2	*Hillside*	*100*	*ArD*	*0.22*	*54.5*	*36.1*	*9.4*	*1.21*	*0.46*	*1.21*	*36.5*	*29.4*
SR2	Streambank	10	CaA	0.15	52.2	31.6	16.2	1.40	0.53	1.40	24.7	41.3
SR2	*Streambank*	*30*	*CaA*	*0.18*	*51.9*	*31.3*	*16.8*	*1.34*	*0.51*	*1.34*	*27.4*	*30.7*
SR2	*Streambank*	*50*	*CaA*	*0.34*	*52.0*	*32.0*	*16.0*	*1.41*	*0.53*	*1.35*	*27.2*	*35.6*
SR2	*Streambank*	*100*	*CaA*	*0.15*	*62.5*	*25.9*	*11.6*	*1.57*	*0.59*	*1.57*	*22.3*	*50.4*

Table 3-4. Summary of flow events in Salt River (SR1; upstream, SR2; downstream) by event duration, antecedent soil water (*ASW*) at hillside (HS) and streambank (SB) locations, precipitation, lag time from precipitation start to flow start, total event flow, total event quickflow, peak flow, and runoff coefficient (*RC*).

Site	Start	Duration	*ASW* (HS)	*ASW* (SB)	Rain-fall	Rainfall intensity	Lag	Total flow	Quick-flow	Peak flow	*RC*
		[h]	[mm]	[mm]	[mm]	[mm h^{-1}]	[h]	[mm]	[mm]	[m^3 s^{-1}]	[-]
SR1	2022-06-30 02:00	1.00	198.7	153.1	9.6	1.04	8.25	0.02	0.02	0.02	0.003
SR1	2022-07-02 06:15	3.25	198.5	159.3	17.3	1.61	1.50	0.07	0.07	0.02	0.004
SR1	2022-07-14 11:45	4.25	202.2	158.9	13.9	2.22	0.25	0.12	0.12	0.03	0.009
SR1	2022-07-21 02:45	65.25	202.6	156.3	33.3	0.58	5.75	1.24	1.18	0.03	0.036
SR1	2022-07-30 01:15	52.50	206.8	155.3	21.2	1.93	3.25	0.98	0.87	0.05	0.041
SR1	2022-08-20 01:45	1.750	201.2	149.7	6.0	4.83	0.25	0.04	0.04	0.02	0.006
SR1	2022-08-20 22:45	20.50	201.4	150.7	13.0	1.04	3.00	0.40	0.40	0.03	0.030
SR1	2022-08-22 22:15	4.75	202.2	157.3	5.8	11.59	0.25	0.07	0.07	0.02	0.013
SR1	2022-08-24 11:45	12.25	203.0	156.1	3.4	4.58	0.50	0.15	0.15	0.01	0.043
SR1	2022-08-26 00:00	38.25	203.2	155.3	4.9	0.22	1.00	0.72	0.62	0.01	0.127
SR1	2022-08-27 14:30	59.25	203.0	155.0	13.4	0.25	6.50	1.16	0.88	0.02	0.066
SR1	2022-09-05 18:30	96.50	201.6	152.0	44.1	1.00	0.00	1.92	1.53	0.02	0.035
SR1	2022-09-17 04:45	269.00	202.8	154.4	201.0	0.72	28.75	33.19	18.91	0.18	0.094
SR1	2022-09-29 18:00	188.50	307.4	229.8	64.2	0.54	0.75	29.43	9.15	0.17	0.142
SR1	2022-10-09 22:30	1.500	310.6	229.9	10.4	2.31	3.75	0.26	0.04	0.08	0.004
SR1	2022-10-26 02:15	9.00	277.2	196.2	5.5	2.74	–0.25	0.66	0.14	0.08	0.025
SR1	2022-11-07 10:30	7.00	338.7	298.8	1.5	2.99	0.25	0.06	0.06	0.01	0.037
SR1	2022-11-07 18:00	6.75	337.3	296.4	6.6	13.19	0.00	0.06	0.06	0.02	0.009
SR1	2022-11-08 01:15	20.00	341.0	305.8	29.5	3.03	0.50	1.31	1.30	0.28	0.044
SR1	2022-11-11 11:15	23.00	332.6	289.9	4.1	0.91	3.50	0.52	0.52	0.02	0.126
SR1	2023-06-29 03:30	28.25	202.3	-	87.9	5.33	0.50	0.55	0.55	0.03	0.006
SR1	2023-08-20 11:30	0.25	210.2	-	22.6	1.03	8.50	0.01	0.01	0.01	0.000
SR1	2023-08-22 16:00	3.75	216.8	185.3	35.1	28.1	0.25	0.19	0.19	0.04	0.005
SR1	2023-09-13 04:45	0.25	206.7	160.8	21.2	16.96	1.00	0.02	0.02	0.03	0.001
SR1	2023-09-19 15:45	0.50	206.8	160.6	7.5	9.97	0.25	0.02	0.02	0.03	0.003
SR1	2023-10-03 21:15	91.00	206.0	160.1	92.9	1.34	16.00	8.42	8.31	0.11	0.089
SR1	2023-10-11 12:15	8.25	266.2	240.6	8.6	5.74	0.00	0.24	0.24	0.08	0.027
SR1	2023-10-11 21:00	3.50	267.9	248.5	5.1	4.05	0.00	0.25	0.25	0.07	0.050
SR1	2023-10-20 03:30	4.00	-	211.6	9.6	1.74	4.50	0.14	0.14	0.04	0.014
SR1	2023-10-24 04:15	5.00	-	200.6	4.3	0.90	0.00	0.16	0.16	0.04	0.038
SR1	2023-10-27 00:00	4.25	-	193.6	23.4	4.94	2.25	0.41	0.41	0.08	0.018
SR1	2023-10-27 16:15	764.75	-	217.7	311.1	0.42	0.25	255.41	120.52	0.50	0.387
SR1	2024-02-06 21:30	520.25	227.9	-	154.8	0.31	1.00	14.20	7.42	0.19	0.048
SR1	2024-03-15 01:15	83.25	251.0	-	20.0	0.96	4.25	1.61	1.12	0.03	0.056
SR1	2024-04-08 11:30	13.00	220.9	-	19.3	1.15	0.25	0.17	0.17	0.07	0.009
SR1	2024-04-11 16:30	45.75	223.9	-	33.4	1.03	1.00	0.56	0.56	0.03	0.017
SR1	2024-04-19 12:15	3.50	232.2	-	4.4	2.20	0.00	0.12	0.12	0.06	0.026
SR1	2024-04-20 14:45	385.25	231.2	-	165.4	0.43	2.75	57.69	33.34	0.41	0.201
SR1	2024-05-07 03:00	7.00	331.2	295.8	7.4	1.23	5.00	0.44	0.14	0.03	0.019
SR1	2024-05-08 10:30	26.75	340.6	298.1	19.7	11.25	0.25	3.28	2.15	0.57	0.109
SR1	2024-05-10 11:00	7.75	337.8	301.4	11.2	1.18	8.50	0.55	0.20	0.06	0.018
SR1	2024-05-22 19:30	19.75	299.7	257.7	21.3	1.42	5.75	0.86	0.60	0.06	0.028
SR1	2024-06-16 13:45	19.25	290.2	205.4	12.9	1.84	1.00	0.96	0.85	0.09	0.066
SR1	2024-06-17 09:15	7.00	328.8	243.4	3.5	0.86	3.75	0.19	0.14	0.02	0.041
SR1	2024-06-21 13:30	3.00	336.5	267.7	9.5	1.19	7.00	0.06	0.04	0.02	0.004
SR1	2024-07-19 14:45	0.50	-	-	13.7	1.08	7.50	0.01	0.01	0.01	0.001
SR1	2024-07-31 16:30	6.25	-	174.7	49.4	9.89	1.00	0.33	0.33	0.08	0.007
SR1	2024-08-13 21:00	234.75	246.8	200.4	138.3	0.65	17.00	16.42	10.95	0.24	0.079
SR1	2024-09-02 06:15	0.75	265.2	210.2	17.0	0.93	6.75	0.05	0.02	0.03	0.001
SR2	2022-09-29 20:45	3.00	219.0	319.6	53.2	9.83	2.75	0.02	0.02	0.02	0.000
SR2	2022-11-05 14:45	140.25	218.7	319.3	173.8	1.19	8.25	23.87	23.39	7.56	0.135
SR2	2023-06-29 17:30	0.50	130.8	228.9	47.8	2.53	14.75	0.00	0.00	0.01	0.000
SR2	2023-10-03 22:00	2.25	140.2	226.6	60.3	2.19	22.50	0.04	0.04	0.10	0.001
SR2	2023-10-27 23:30	6.75	172.2	253.0	55.6	3.04	7.50	0.06	0.06	0.12	0.001
SR2	2023-11-10 03:45	30.75	234.3	347.7	55.4	6.21	0.75	6.34	6.33	2.62	0.114
SR2	2024-02-07 11:30	34.50	166.8	239.2	143.2	3.23	14.25	4.83	4.82	6.50	0.034
SR2	2024-04-21 12:45	6.75	174.0	250.8	43.0	1.15	32.5	0.02	0.02	0.02	0.000
SR2	2024-04-21 20:00	398.50	217.5	294.2	183.9	0.43	4.50	23.71	23.11	20.12	0.126
SR2	2024-05-08 10:45	411.00	266.9	338.0	56.4	0.14	0.50	11.80	8.00	3.89	0.142
SR2	2024-08-13 21:45	164.75	185.9	231.9	48.0	0.25	2.75	8.55	7.91	2.84	0.165

Table 3-5. Mean wetting front velocities (with standard errors) at four soil depths across hillside and streambank deployment positions in SR1 (upstream subcatchment) and SR2 (downstream catchment).

	Hillside		Streambank	
Depth [cm]	**SR1 [mm h^{-1}]**	**SR2 [mm h^{-1}]**	**SR1 [mm h^{-1}]**	**SR2 [mm h^{-1}]**
10	72 ± 20	53 ± 16	75 ± 20	49 ± 15
30	129 ± 32	99 ± 36	233 ± 88	117 ± 42
50	206 ± 64	167 ± 54	229 ± 90	322 ± 177
100	427 ± 153	150 ± 91	300 ± 96	671 ± 330

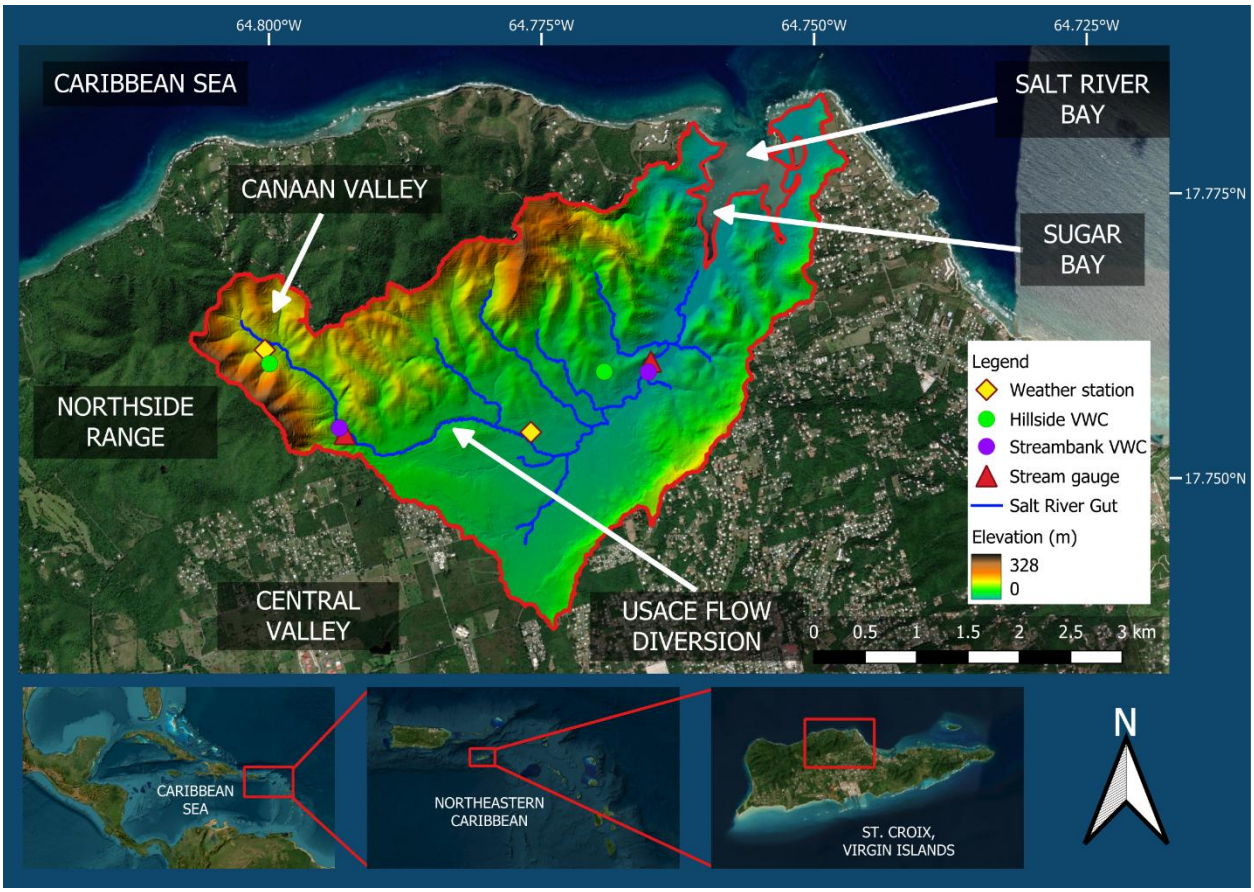

Fig. 3-1. The Salt River Bay watershed study area on the island of St. Croix in the northeastern Caribbean, with study sites marked (weather stations, stream gauges, and soil volumetric water content (VWC) stations, and topographic map.

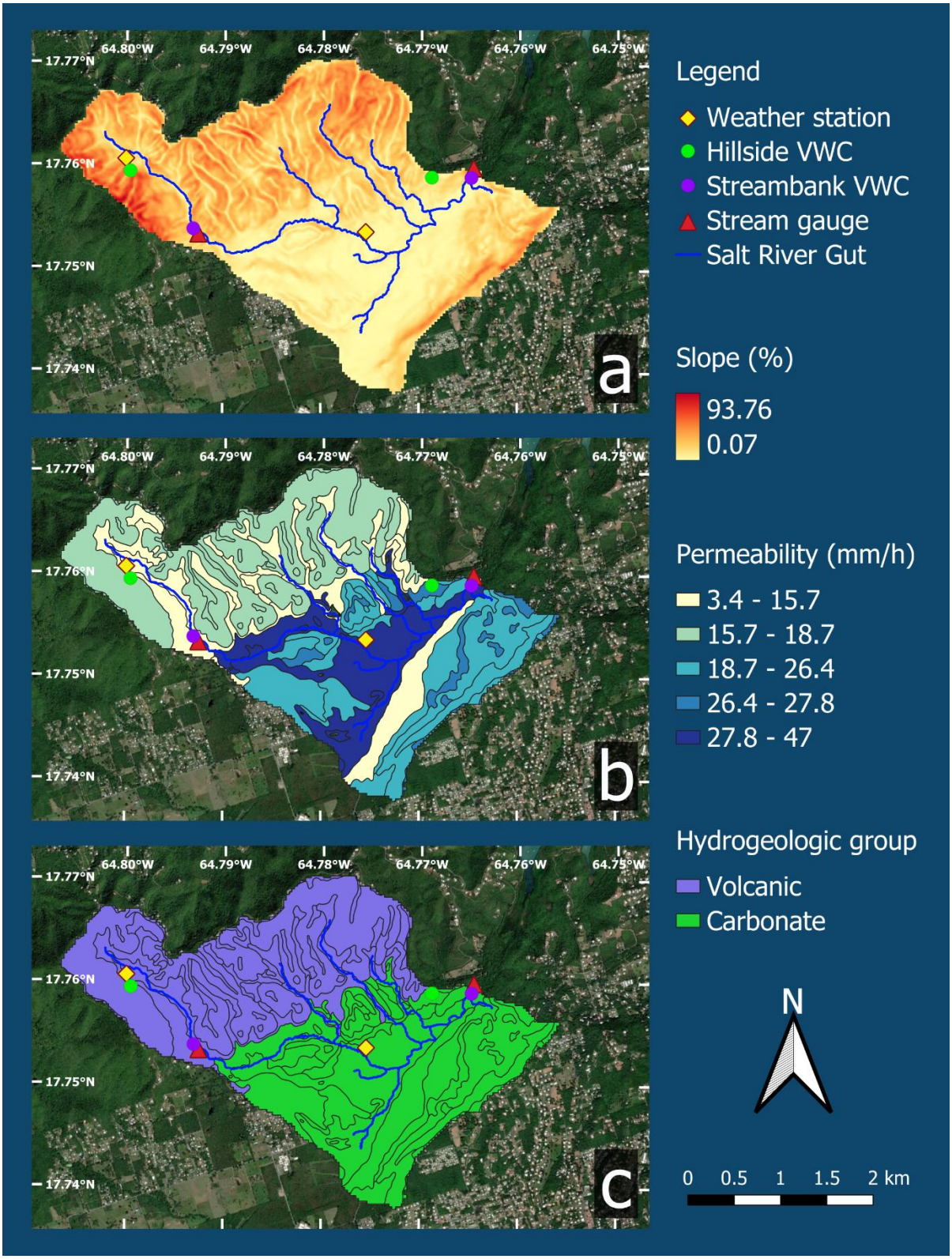

Fig. 3-2. (a) Slope (%), (b) permeability (mm h^{-1}) and (c) hydrogeologic soil group of the SR2 (downstream Salt River) catchment, with study sites marked (weather stations, stream gauges, and soil volumetric water content (VWC) stations).

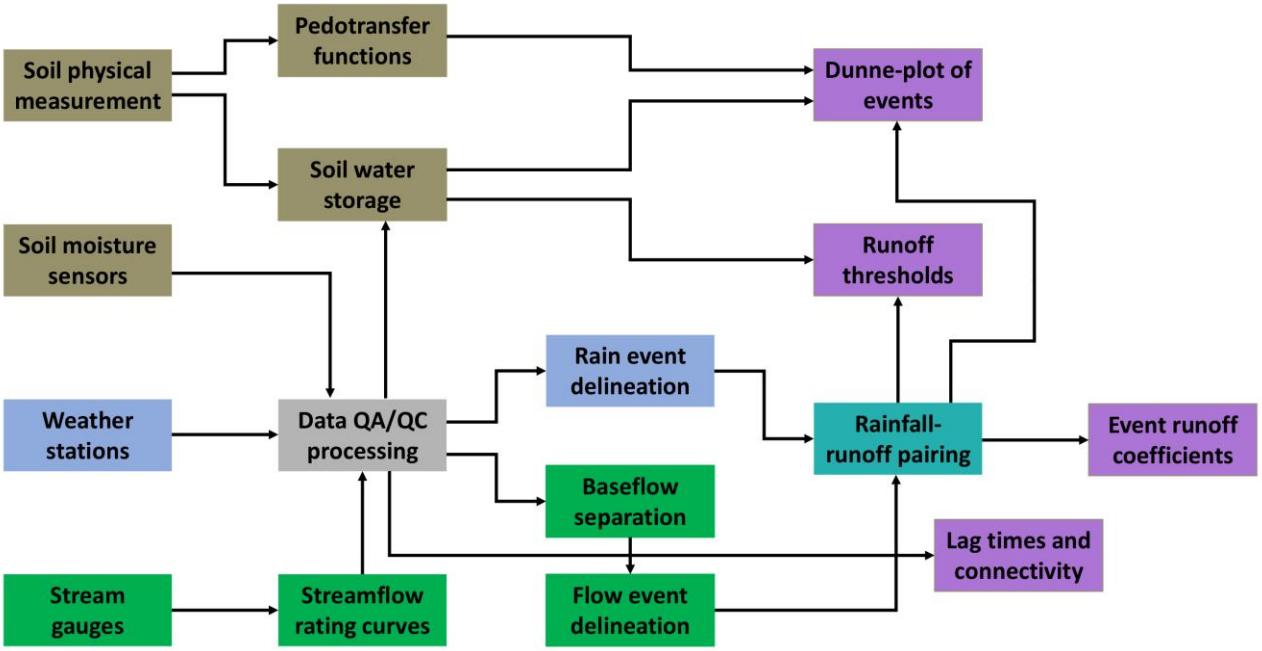

Fig. 3-3. Conceptual workflow of data collection, processing, and analysis. Streamflow related items marked in green, soil moisture related items in brown, precipitation items in blue, and analysis products in purple.

Fig 3-4. (a) Observed saturation in borehole at 83 cm depth near SR1 (upstream gauge) on 29 November, 2023. (b) Salt River Gut high flow on 8 May, 2024 near SR2 (downstream gauge).

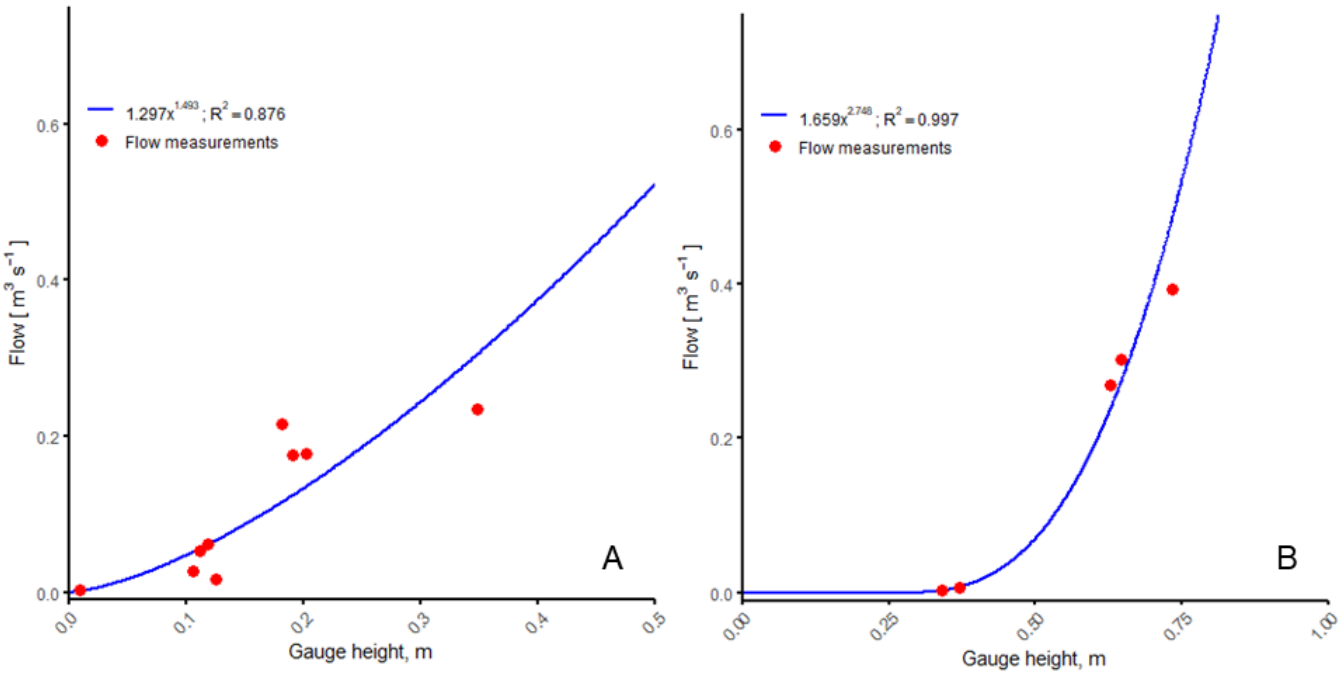

Fig. 3-5. (a) Rating curve at SR1, upstream subcatchment; (b) rating curve at SR2, downstream site (entire catchment).

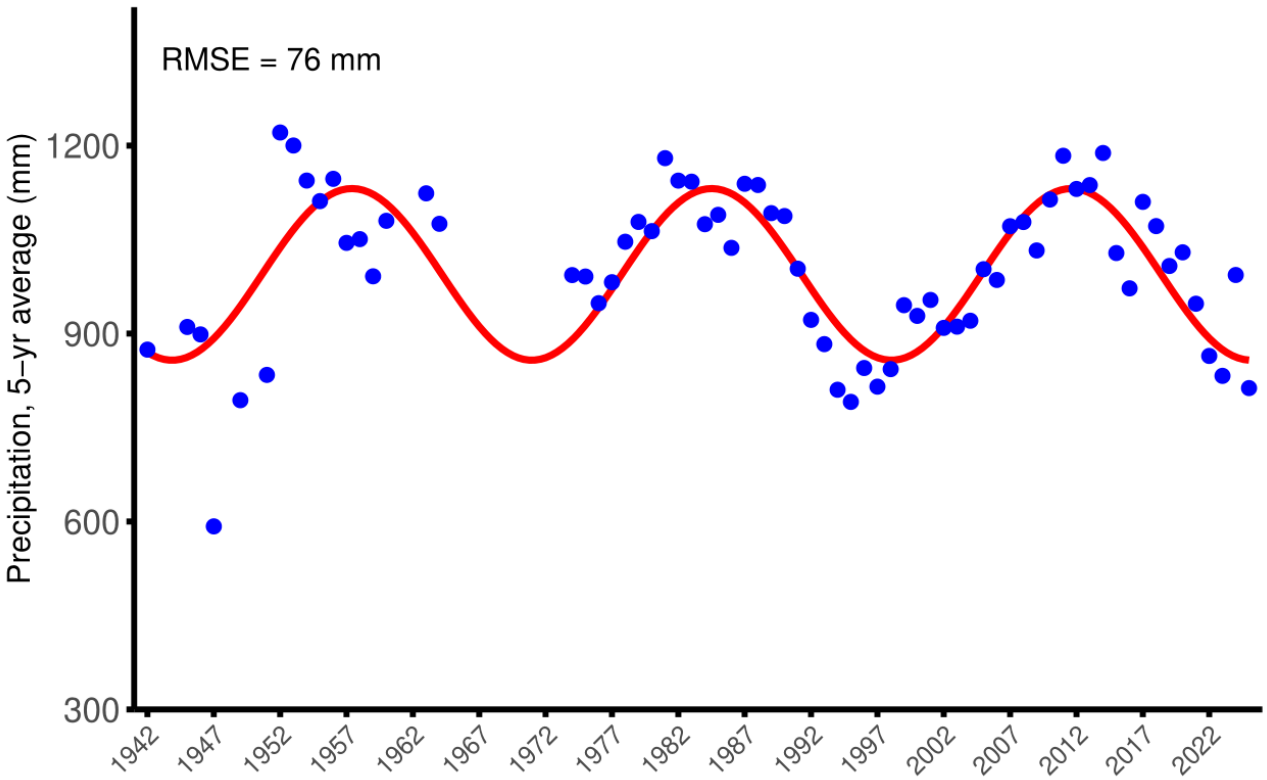

Fig. 3-6. Five-year rolling average of annual precipitation records across the Virgin Islands with sinusoidal model, 1938–2024.

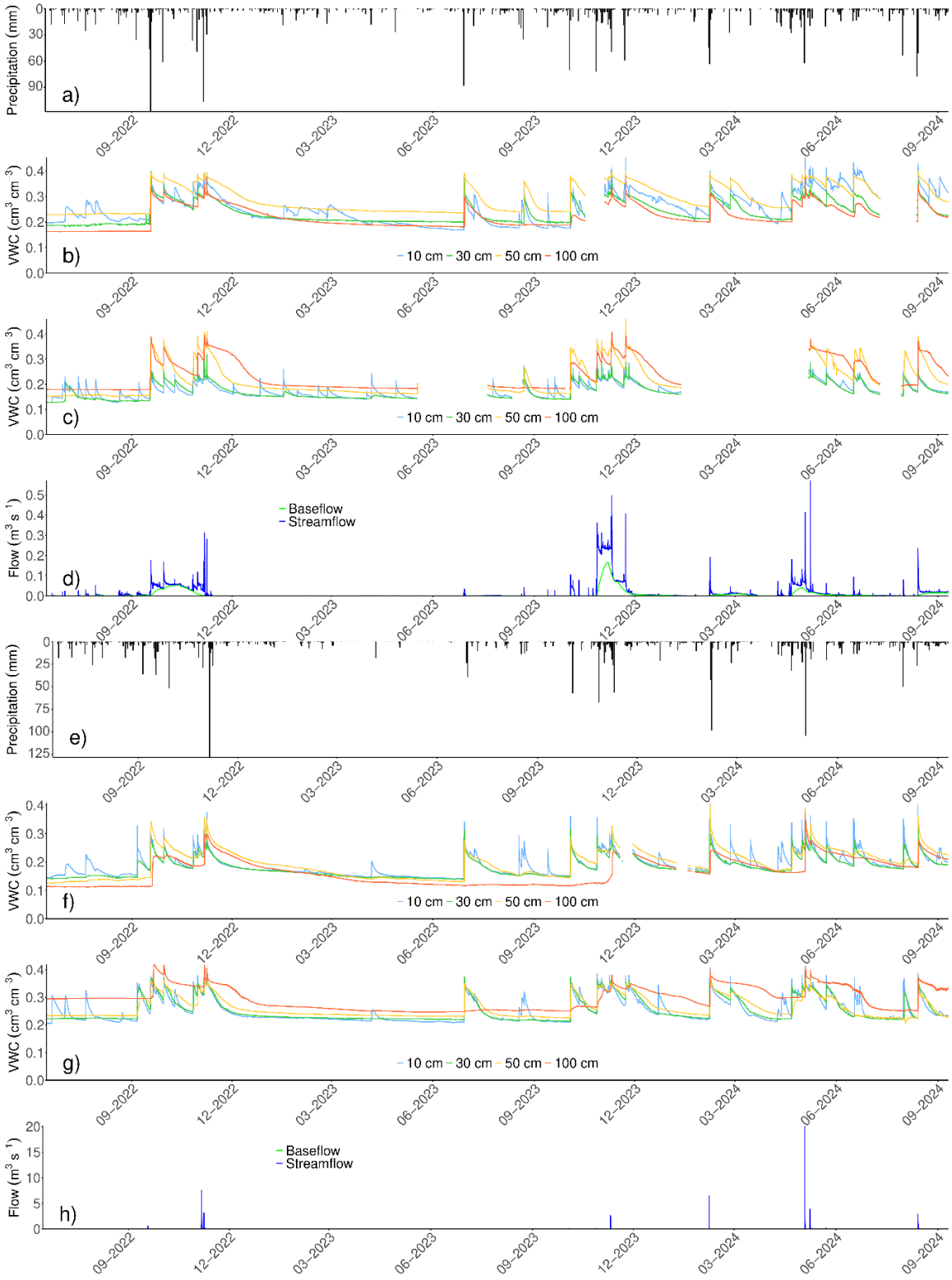

Fig. 3-7. (a) Precipitation at upstream subcatchment (SR1). (b) hillside soil water content (cm^3 cm^{-3}) at SR1. (c) streambank soil water content at SR1. (d) streamflow at SR1 (m^3 s^{-1}). (e) precipitation at downstream catchment (SR2). (f) hillside soil water content (cm^3 cm^{-3}) at SR2. (g) streambank soil water content at SR2. (h) streamflow at SR2 (m^3 s^{-1}).

Fig. 3-8. High flow event of 8 May, 2024 at SR1.

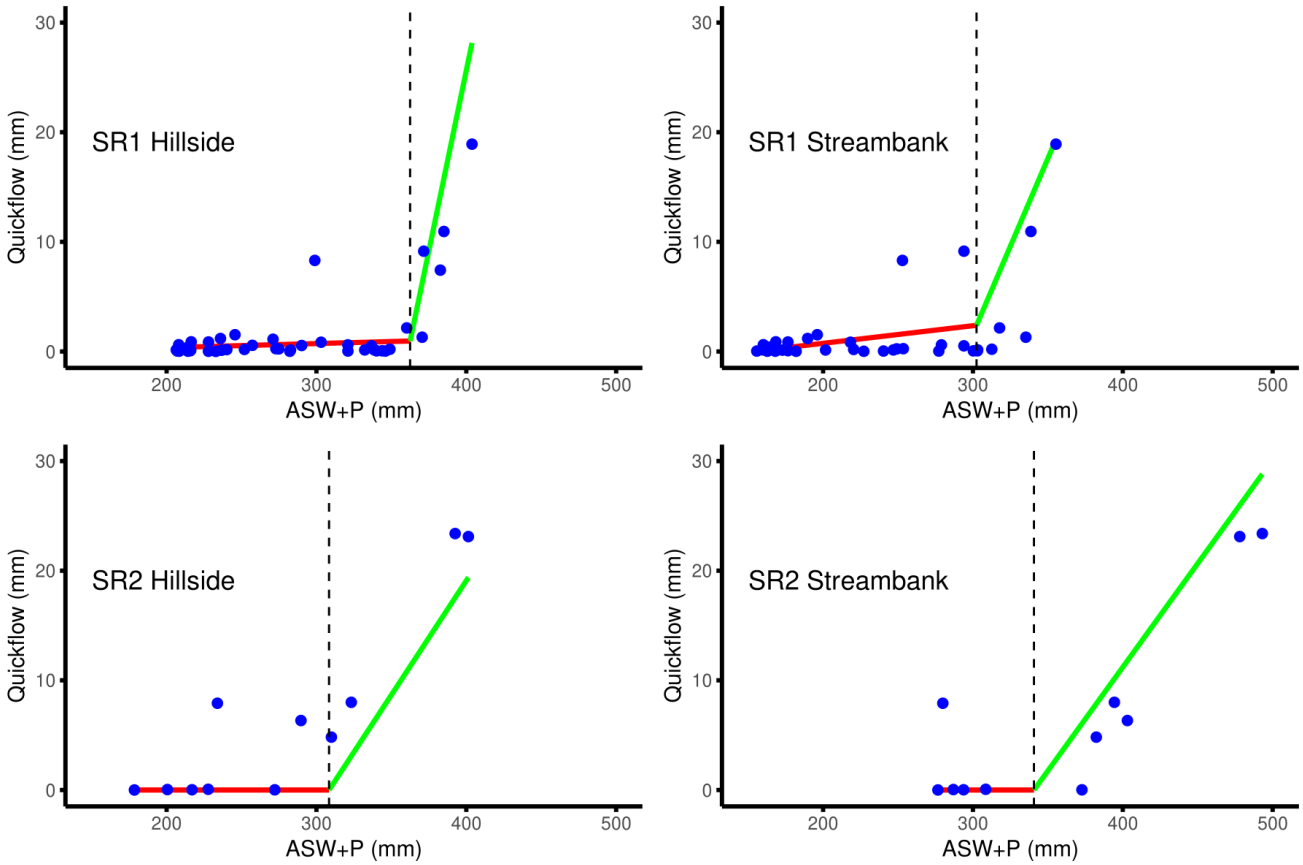

Fig. 3-9. Piecewise linear regression of runoff generation thresholds, event antecedent soil water (ASW) plus precipitation (P; mm) on event quickflow (mm) in the upstream subcatchment (SR1) and the downstream catchment (SR2) for two soil moisture sensor deployment locations, hillside and streambank.

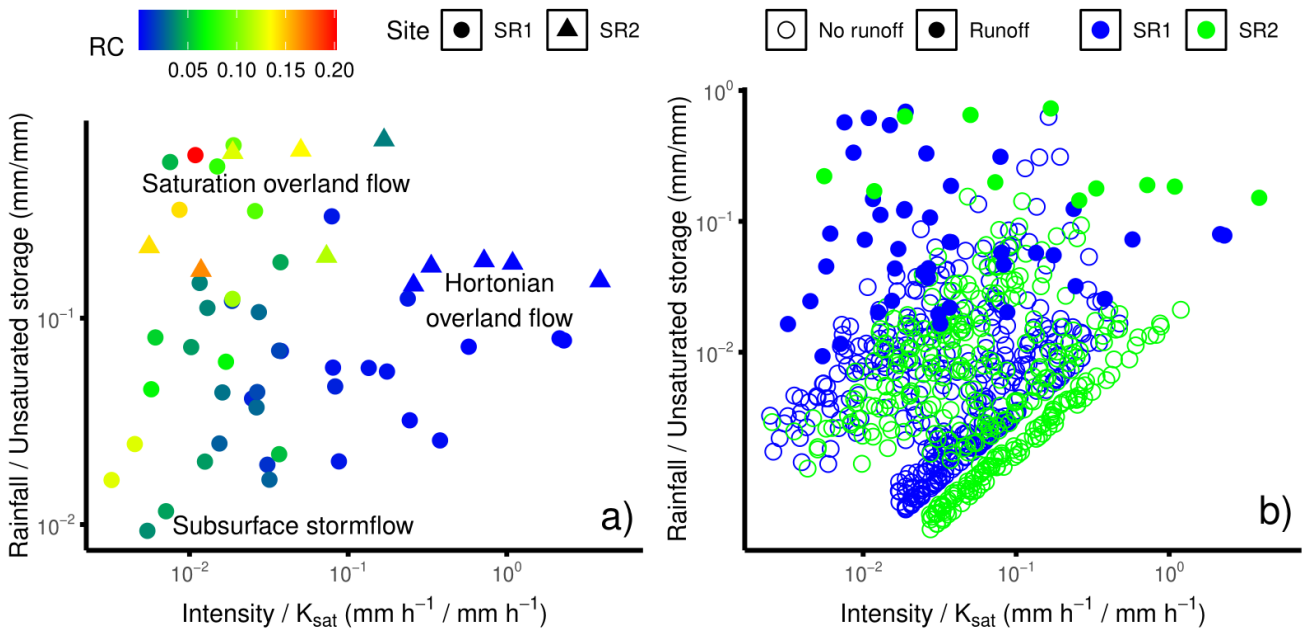

Fig. 3-10. Dimensionless plots of runoff events, event intensity over hillside surface saturated hydraulic conductivity K_{sat} (mm h^{-1} / mm h^{-1}) and event precipitation over hillside soil unsaturated storage space (mm / mm). (a) Flow events by site (SR1 and SR2) and event runoff coefficient (RC). (b) Flow events and other rain events by site and whether runoff was initiated.

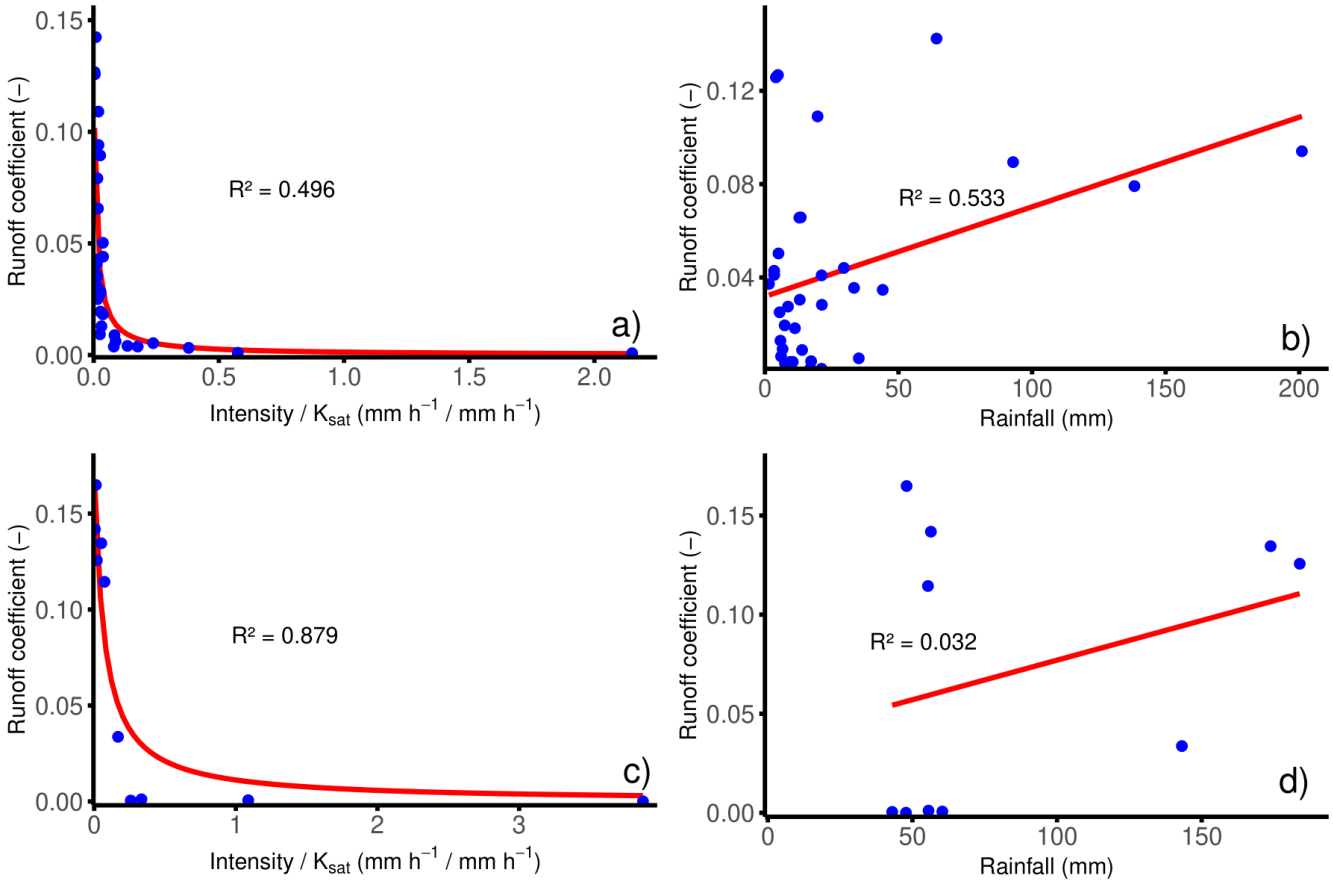

Fig. 3-11. (a) Reciprocal model of runoff coefficient (event quickflow over event precipitation; mm mm^{-1}) by precipitation intensity over hillside surface saturated hydraulic conductivity K_{sat} (mm h^{-1} / mm h^{-1}) at SR1. (b) linear model of runoff coefficient by event precipitation at SR1. (c) reciprocal model of runoff coefficient by precipitation intensity over hillside surface saturated hydraulic conductivity K_{sat} at SR2. (d) linear model of runoff coefficient by event precipitation at SR2.

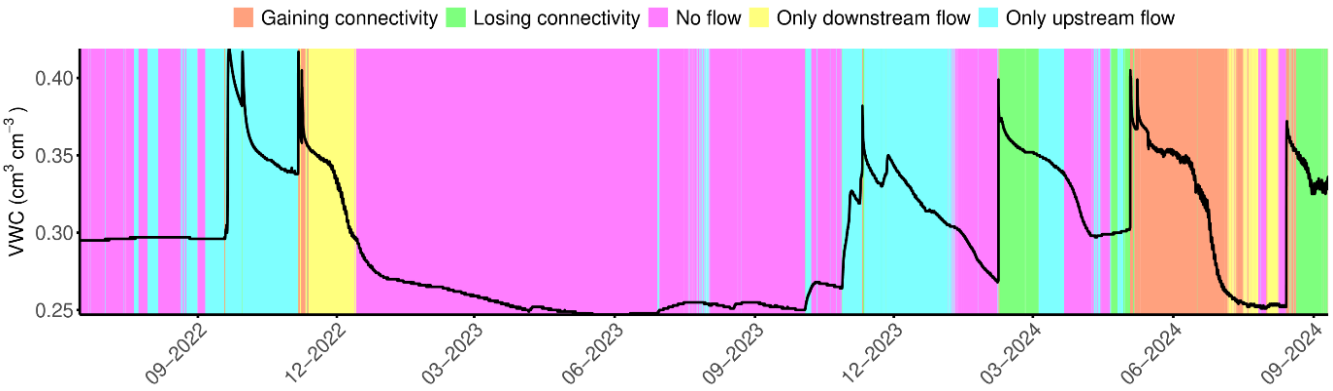

Fig. 3-12. Time series of soil volumetric water content (VWC; $cm^3\ cm^{-3}$) at the streambank of the downstream site (SR2) at 100 cm depth according to five connectivity classes, referring to streamflow at the upstream site (SR1) and downstream (SR2).

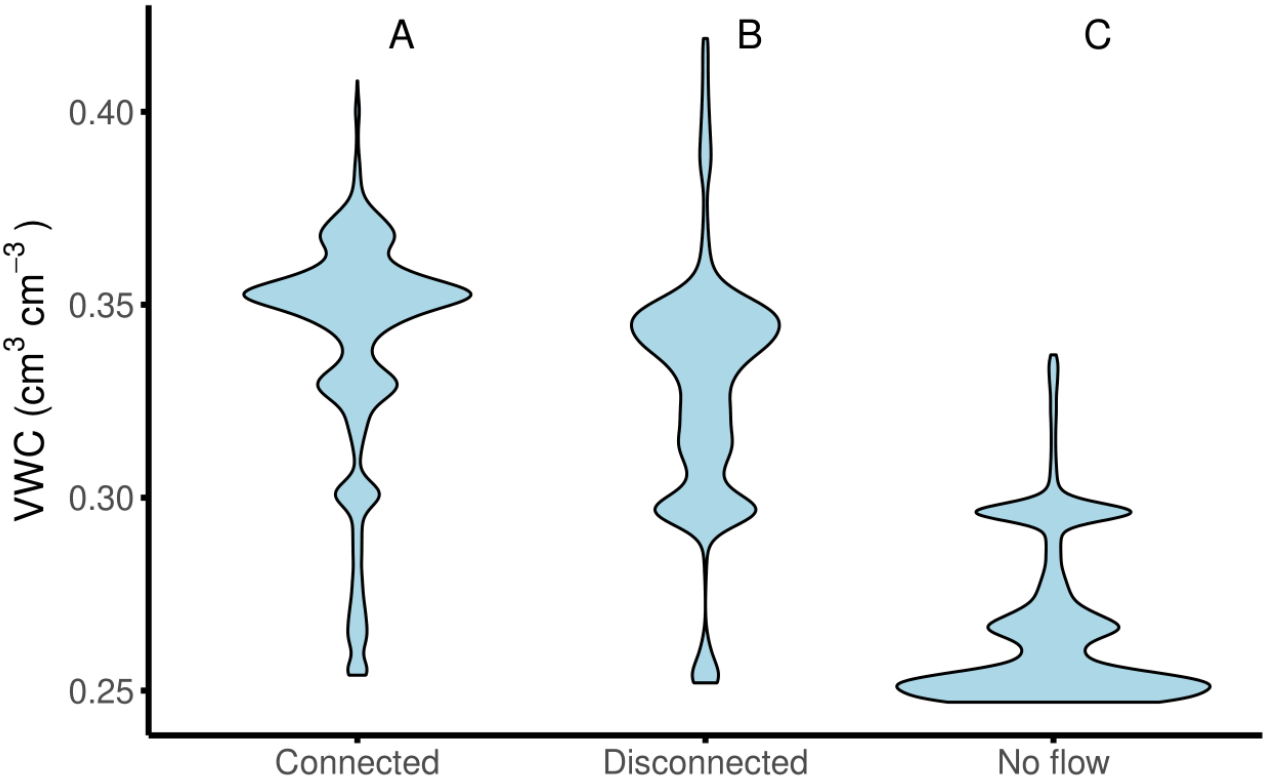

Fig. 3-13. Violin plot of streambank volumetric soil water content (VWC; $cm^3\ cm^{-3}$) at the downstream site (SR2) at 100 cm depth in three simplified connectivity classes. Statistical significance ($\alpha = 0.05$) of Tukey's HSD pairwise post-hoc testing of one-way ANOVA is indicated when two categories have no letters in common.

Fig. 3-14. Condition of the swamp area (17.7663° N, 64.7611° W) near the mouth of the stream channel network at Sugar Bay on 26 October, 2023, representing normal conditions (dry ground).

Fig. 3-15. Condition of the swamp area (17.7663° N, 64.7611° W) near the mouth of the stream channel network at Sugar Bay on 8 May, 2024, displaying evidence of sheet flow connecting the discharge observed at SR2 with discharge to Sugar Bay. No defined stream channel exists in this zone, and sheet flow through the swamp is the means of surface connection between Salt River watershed and Salt River Bay in sufficiently wet conditions.

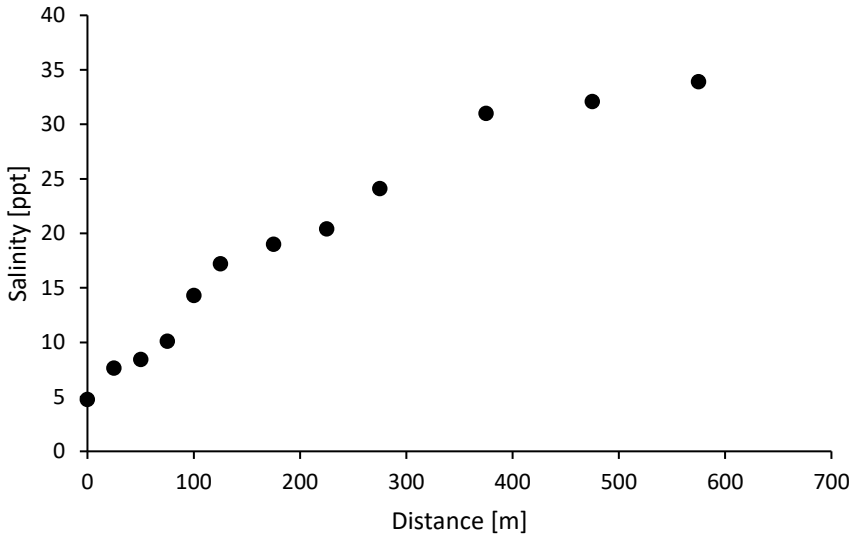

Fig. 3-16. Surface salinity (ppt) in Sugar Bay on 6 May, 2024 at 4:00 PM, measured as distance from the edge of the mangrove forest at the mouth of the stream network.

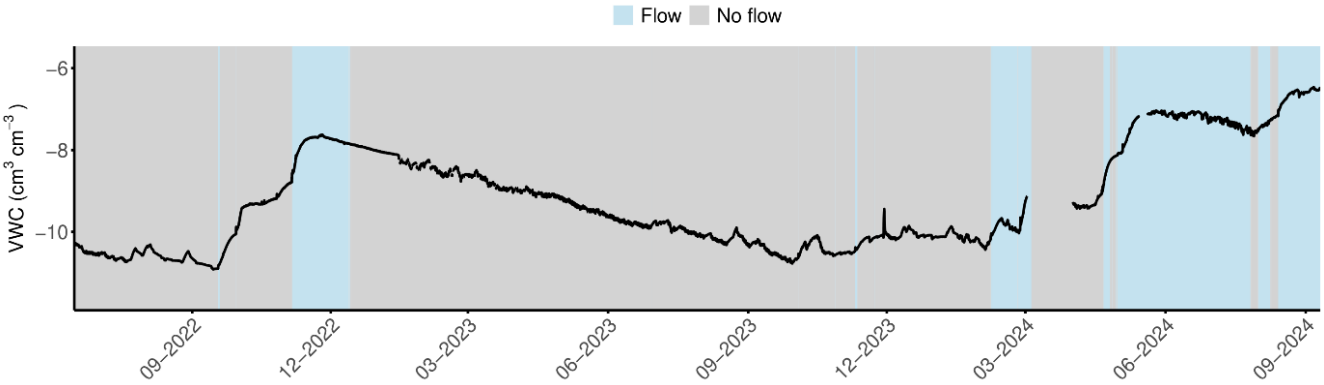

Fig. 3-17. Groundwater level below ground surface (m) at USGS monitoring well, Estate Adventure, St. Croix, 6.7 km from SR2 downstream site (17.7172° N, 64.8099° W) over conditions of streamflow or no streamflow at SR2.

Chapter 4
Application of the Water Erosion Prediction Project (WEPP) Model to the Virgin Islands

Abstract

Soil erosion and sedimentation is a major problem in many small tropical islands worldwide. Rates of erosion are often influenced by human land uses and management practices, but adequate data in small islands to allow data-driven decision-making aimed at sediment reduction is usually lacking. In the Virgin Islands, erosion and sedimentation are considered problems because of the loss of productive agricultural soil, siltation of small reservoirs, and deterioration of marine water quality following sediment plumes, which are thought to harm coral reefs. To gain a better understanding of the hydrologic function and sediment yield of Virgin Islands watersheds, we applied the Water Erosion Prediction Project (WEPP) model to the Virgin Islands for the first time, in Canaan Valley, St. Croix. Using field-collected hydrometeorological data and limited suspended sediment observations, we created five parameterization attempts in order to compare performance and fit with observed data. We found that the scenario automatically selected by a Bayesian optimization process performed the best, though no scenario was able to satisfactorily simulate the shape of the actual hydrograph. Sedimentation estimates produced by the optimized parameters in a thirty-year simulation, however, are plausible and in line with tropical forest erosion rates worldwide, showing the potential promise of WEPP in the Virgin Islands with further calibration.

Introduction

Many small tropical islands worldwide experience elevated erosion rates and problems with sedimentation due to steep topography, soil characteristics, and torrential rainstorms (Rad et al., 2013). At the same time, soil conservation and erosion control are often important on such islands for sustained agricultural production (Campbell and Broughton, 1965; Cox et al., 2006), maintenance of surface water reservoirs (Matos-Llavona et al., 2022), threatened marine ecosystems (Rogers and Ramos-Scharrón, 2022), and support of tourism economies (Lancellotti and Hensley, 2024). There is a need to better understand landscape-scale processes driving water erosion in order for small island governments, usually capacity-limited, to make targeted, data-driven management decisions that address this persistent issue (Suárez-Castro et al., 2021). For example, data-driven management can provide target areas for forest conservation to protect coral reef ecosystems (Klein et al., 2012), identify agricultural practices that both support island food sovereignty and protect coral reefs (which was done, e.g., with taro cultivation in Palau; Koshiba et al., 2013), or help design stormwater or stream channel interventions that prevent downstream sedimentation (Boardman et al., 2019).

The Virgin Islands, part of the Lesser Antilles in the northeastern Caribbean, has had documented problems with landscape erosion and marine sedimentation going back to the colonial period (e.g., under Danish rule on the island of St. Croix; Quin, 1907). Although the period of major agricultural exploitation of the islands ended in the middle of the 20th century (Jordan, 1972), erosion remains a major environmental concern (Ramos-Scharrón et al., 2023). Two key obstacles to addressing this acknowledged problem exist. First is the chronic lack of capital resources and general capacity in small island governments worldwide, including those with tourism-driven economies (McElroy and Hamma, 2010), and the various governments of the Virgin Islands are no exception (Granvorka and Strobl, 2013). Second, and also typical of

small islands, is a general lack of environmental data that would allow for targeted decision-making to address the problem with the greatest efficiency of investment (Lancellotti and Hensley, 2024; Lumbroso et al., 2011).

Process-based or physically-based hydrological models apply theoretical understanding and well-validated empirical relationships to simulate a hydrological process (Migliaccio and Srivastava, 2007). One of the most attractive features of such a model is that, once adequately calibrated for a particular area, managers can use it to simulate conditions in ungauged catchments where data collection is infeasible (Kastridis and Stathis, 2020). Though the parameterization process does require some initial data collection and input, the model calibration process is ultimately less resource-intensive than maintaining a large network of environmental monitoring services (which is extremely uncommon in the Caribbean; Lumbroso et al., 2011).

For erosion simulations, the Water Erosion Prediction Project (WEPP) may be a good choice for Virgin Islands environmental managers. The WEPP model, once calibrated, can predict runoff and soil erosion at multiple scales for long-term simulation or simulation of discrete storm events (Laflen et al., 1997). Though WEPP has not yet been applied to an area in the Caribbean, it is a promising choice for a process-based model to address erosion concerns. With hundreds of small, sometimes remote bays and steep, densely vegetated catchments, many watersheds in the Virgin Islands have remained persistently understudied for practical reasons (Lancellotti and Hensley, 2024). The WEPP model, if calibrated well in a few strategically chosen pilot watersheds, could eventually be used to helpfully predict erosion and runoff in such ungauged catchments (Dobre et al., 2022a; Dobre et al., 2022b).

One of the other significant strengths of process-based models is the ability to simulate possible or proposed future conditions (Dobre et al., 2022a; Srivastava et al., 2020), or to estimate past conditions (e.g., past land use change effect on reef sedimentation in St. Lucia; Bégin et al., 2014). Assisting with this, the WEPP model has dozens of parameters related to land cover and management that have been developed over decades to simulate the effect of land cover, plant cover, and management changes to runoff and erosion in hillslopes and watersheds. These are in addition to a variety of soil hydrological parameters that may be subject to land use effects (Lew et al., 2022). The Virgin Islands have been experiencing rapid land-cover changes with the rise of the tourism economy and, in the U.S. Virgin Islands, large in-migration of mainland Americans purchasing real estate and constructing homes, even as the agricultural land covers of the past have become rarer (Ramos-Scharrón et al., 2023; Roopnarine, 2020). Simulating additional or proposed land use changes, as well as various possible climate or storm scenarios, could be invaluable for land use and planning for the Virgin Islands in the future. Therefore, our objective in this study is to provide an initial calibration of the WEPP model to a Virgin Islands watershed, the Canaan Valley of St. Croix.

Methods

Site description

The Canaan Valley of St. Croix is a subcatchment of the larger Salt River Bay watershed (1.5 km^2; Fig. 4-1). Located at the eastern end of St. Croix's Northside Range, the headwaters of this stream network rise in the north on the slopes, and the stream course proceeds south out of Canaan Valley into the Central Valley of St. Croix, eventually turning northeast, leading to Salt River Bay. Canaan Valley is the headwaters subcatchment. Soils in the study area are dominated

by the Victory-Southgate soil complex, a Mollisol clay loam of volcanic origin found on steep slopes throughout the Virgin Islands (83.3% by area), and the Cramer-Victory soil complex, a Mollisol clay loam found on valley floors of mountain areas (USDA-NRCS, 2024). The groundwater in the study area is dominated by fractured rock hydrogeology (Miller et al., 1999). The stream course of the valley (called Canaan Gut or Salt River Gut; gut is the local term for a stream) is typically ephemeral, with limited baseflow during wet periods (Lancellotti and Hensley, 2025). A more complete description of the Salt River basin and Canaan Valley can be found in Chapter 3.

Data collection and processing

Field data collection

In the upland area of the subcatchment (17.7606° N, 64.8000° W), we installed a weather station (ATMOS 41, Meter Group, Pullman, WA, USA) to record precipitation, solar radiation, temperature, wind speed, wind direction, and barometric pressure at 15-minute timesteps. At the outlet of the valley (17.7533° N, 64.7926° W), we installed a stream gauge data logger (HOBO U-10, Onset, Bourne, MA, USA), recording at 10-minute intervals deployed in the thalweg of the stream course to capture the ephemeral flows of the stream. Finally, we deployed soil moisture sensors at a hillside location in Victory-Southgate soil (17.7594° N, 64.7996° W) and a streambank location in the valley floor in Cramer-Victory soil (17.7538° N, 64.7931° W) in pits with depths of 10, 30, 50, and 100 cm, recording volumetric water content at 15-minute intervals. To produce a streamflow hydrograph for the subcatchment, we developed a rating curve by comparing stage height with measured flows using a FlowTracker2 acoustic doppler velocimeter (Xylem, Inc., Washington, DC, USA). More information on sensor installation, sites, and data

collection is reported in Chapter 3. Stream gauges were active from 1 January, 2022 to December 31, 2024, and soil sensors became active on 22 May, 2022. The primary weather station used in this study became active on 13 September, 2022. Prior to that date in 2022, we used weather data from a nearby weather station of the same model, deployed in 2021 to represent the entire Salt River watershed. This weather station (17.7536° N, 64.7755° W) was 1.8 km east-southeast of the stream gauge, while the primary weather station was 1.1 km northwest of the gauge. Our study period encompassed the calendar years of 2022–24.

Periodically during flow events, grab samples were taken from the midpoint of the streamflow at the stream gauge. These samples were sent to the Illinois State Water Survey Sediment Analysis Laboratory, where they were processed for suspended sediment content (mg L^{-1}) using 1.5 µm filtration (to capture suspended sediments) and firing at 550 °C to remove the volatile suspended sediment fraction (based on Guy, 1969). During the high flow event of 8 May 2024, we collected grab samples at 30-minute intervals from the peak flow stage through the falling limb of the hydrograph to capture the decay characteristics sediment concentrations.

At the soil moisture sensor sites, we also sampled soil for bulk density (AMS, Inc., American Falls, ID, USA bulk density sampler) at the four depths of installation (10, 30, 50, and 100 cm) to calculate measured porosity assuming a 2.65 g cm^{-3} particle density, and measured particle size distributions of these samples using sieves and an automated hydrometer (PARIO, Meter Group, Pullman, WA, USA). Complete descriptions of these soil physical measurements are presented in Chapter 3.

Data processing

Raw time series data (weather, streamflow, and soil moisture) were subjected to a quality assurance/control process to allow for uninterrupted datasets. This resulted in a continuous time series (no gaps) of all weather and streamflow data, though in the case of soil moisture data, some gaps occurred that were too long for reliable gap-filling. Because WEPP runs on daily timesteps, we formatted observed data into daily summaries for comparison with the model output. As noted above, the soil moisture dataset did not begin until 22 May 2022. From the precipitation time series, we delineated rain events using a minimum inter-event time (MIT) of 6 hours and a threshold for event initiation of 0.1575 mm. We describe these processing approaches fully in the previous chapter.

We also performed a hydrograph separation to estimate baseflow, which was needed to delineate flow events in the streamflow record. To do this, we followed the technique described by Duncan (2019), which resulted in a baseflow recession constant of 0.87 (based on daily timesteps). Using this separated hydrograph, we delineated flow events in the hydrograph based on a combination of the "peaks-over-threshold" approach and the baseflow threshold approach (Wasko and Guo, 2022). We also fully describe the flow event delineation in Chapter 3.

Sediment yield rating curve

We also calculated total sediment yields based on the grab-sample suspended sediment concentrations and the full hydrograph. This allowed us to provide a point of comparison of estimated total sediment delivery based on observed data as opposed to the sediment load estimates made by WEPP. To do this, we used multiple linear regression to predict suspended sediment concentration based on flow (Q; $m^3\ s^{-1}$) and time (t; h) since peak flow. "Peak flow," in

this instance, was based on the peak flow of delineated flow events. These two variables were chosen because both appeared to be related to suspended sediment concentration, but they were not correlated with one another. We used this approach rather than a standard sediment rating curve based only on *Q* because of the need to account for the relatively clear waters observed during baseflow conditions. In our hydrograph, though Canaan Gut is ephemeral, periods of baseflow do occur well after flow events have passed in which very little sedimentation is observable. The results of this multiple regression are shown in Fig. 4-2. Although the small number of data points ($n = 9$) prevents the resulting sediment yields from being considered fully reliable (especially in extreme conditions), they provide a physically-based comparison to the modeling processes performed in WEPP.

Model description

The WEPPcloud interface

The Water Erosion Prediction Project (WEPP) is a model used to predict erosion by processed-based modeling of hydrology, erosion, and sediment transport (Laflen et al., 1997). This model has been in use for the past few decades and has been applied to cropland and rangeland, as well as forest. In our application of WEPP, we made use of the WEPPcloud online interface for initializing WEPP runs, which uses "*wepppy*" Python framework to execute WEPP (Lew et al., 2022). The simulations described in this study were initially set up via WEPPcloud before being downloaded and run iteratively using "*wepppy-win-bootstrap*," an open-source Python package (Lew, 2021).

As a processed-based model, WEPP's core functioning works on a hillslope basis. To model a watershed, a catchment is divided into a topological network of hillslopes, channel

segments, and (optionally) impoundments. In initializing a WEPPcloud run, the user first identifies an area of interest on a map, from which a channel network is built based on a digital elevation model (30 m resolution; Lew et al., 2022). The user then selects an outlet, which was chosen at the location of the Canaan Valley stream gauge, and WEPPcloud delineates hillslopes and channels using TOPAZ (Garbrecht and Martz, 1997). Within each delineated hillslope, WEPPcloud then queries the U.S. Geological Survey National Landcover Database (NLCD) and U.S. Soil Survey soil data (USDA-NRCS, 2024) to determine the dominant soil and land use/land cover of each hillslope and record the relevant parameters (Lew et al., 2022). Certain soil physical parameters of the surface layer of the soils are automatically altered based on the land cover type, in an attempt to account for the expected effects (e.g., Levi et al., 2010) of the land cover on those properties. Because NLCD data is not available for the Virgin Islands, U.S Forest Service Landscape Change Monitoring System (LCMS) data from 2023 was used, and land covers were translated to "quasi-NLCD" categories (Housman et al., 2024). In this data, 99.8% of our catchment was classed as "forest" land cover.

Input files and parameters

The data collected from these sources are used to write several of WEPP's input files: slope, soil, and management files. Each hillslope and channel segment is assigned its own input file in the model (Flanagan and Livingston, 1995). Beyond these spatial inputs, WEPP accepts climate information in the form of climate files. To reflect our observed weather, we constructed "breakpoint" climate files for upload to WEPPcloud. Breakpoint climate files reflect subdaily changes in precipitation (highly preferable for the occasionally intense rainstorms of the Virgin Islands), with each daily timestep recording up to 50 "breakpoints." These files were formatted

using a custom script in R (v4.2.3, R Core Team, Vienna, Austria, 2025). An option to use CLIGEN, a built-in stochastic climate generator based on the nearest available weather station for a given number of years of simulation, is also provided (Lew et al., 2022). For our study site, the nearest weather data used for CLIGEN is at Charlotte Amalie, the capital of the U.S. Virgin Islands on the island of St. Thomas (67 km north of Canaan Valley).

In addition to climate files, WEPP can optionally accept data on impoundments, passed as an impoundment file, where impoundments such as culverts are placed with defined stage heights, lengths, slopes, roughness, etc., at a particular location in the channel network. These are then incorporated in WEPP's calculations of both streamflow and sedimentation. With or without impoundments, a channel file is also passed to the model, which specifies Manning's roughness coefficient and channel erosiveness parameters (Flanagan and Livingston, 1995). WEPPcloud does not natively prepare impoundment files, and channel files are generated with default parameters. Finally, WEPPcloud also makes use of a groundwater input file, specifying groundwater flux coefficients of baseflow and deep seepage (a.k.a. aquifer loss; Lew et al., 2022). A summary with descriptions of the parameters altered from default values over the course of this study is presented in Table 4-1.

Hydrological model

The WEPP model begins from daily precipitation (or breakpoint data) in the climate file, then applies the incoming precipitation to the hillslope, where infiltration (percolation) is calculated at the surface soil horizon given for each hillslope (Fig. 4-3). From bulk density (*BD*) information and the existing soil water calculation, the model either allows surface runoff or infiltration; runoff can proceed as infiltration excess or saturation excess flow. Once infiltrated,

within each soil horizon, the ability of water to percolate to deeper horizons is given by equations described in Dun et al. (2009). In these equations, percolation depends on soil water content (θ), wilting point (θ_{wp}), field capacity (θ_{fc}), porosity, horizon thickness, and saturated hydraulic conductivity (K_{sat}), all of which are given as or calculated from parameters in WEPP soil files. Notably, WEPP does not route water to lower soil horizons unless θ_{fc} has been reached (Dun et al., 2009). Water percolating below the deepest soil horizon enters the groundwater reservoir, and the saturated hydraulic conductivity of this "restricting layer" is given as a separate parameter in all soil files (K_{sub}). In WEPPcloud, water from this groundwater reservoir is allowed to be lost and exit the model domain ("deep seep"), where the coefficient represents a fraction of water lost (or gained, when negative) per day. Groundwater may also be added to streamflow as baseflow, calculated as the daily product of the groundwater storage volume and the baseflow coefficient in the same manner as deep seepage (Lew et al., 2022). We also used the option (default in WEPPcloud) to compute seepage on an hourly rather than daily basis for improved results (especially on steep or short hillslopes; Lew et al., 2022).

Daily evapotranspiration (ET) is also estimated by WEPP as daily extraction from the soil water. When wind data is provided in the climate file, the Penman-Monteith method (Allen et al., 1998) is used to calculate potential ET. Parameters primarily from the management files, including rooting depth and leaf area index (LAI) for each land cover type provide the calculation of simulated ET. A further parameter for a crop coefficient (K_c) is used by WEPPcloud for each land cover type to further modify ET. In addition to fluxes exiting the hillslope as runoff, seepage, and ET, WEPP permits lateral flow calculations to enter the channel network when running a modified routine created by Dun et al. (2009), which we used in our simulations. Once water is routed to the channel network, it is still subjected to calculations of

ET and percolation (channel segments each have soil and climate information as well), until it reaches the outlet.

Erosion model

Soil erosion and sediment deposition is simulated in WEPP both at hillslopes and in channel segments. Important parameters governing the modelling of soil detachment are groundcover parameters in the management files, as well as critical shear stress and rill/interill erodibility parameters in the soil files. The channel bed critical shear stress is also an important parameter in determining the ultimate sediment load (Dobre et al., 2022b). Impoundments have the effect of permitting sediment deposition and reducing yields at the outlet, and many of the impoundment parameters (impoundment shape, slope, length, roughness, stage height, etc.) are used especially to govern this aspect of catchment-wide sediment yields. The default parameters from WEPPcloud for the percent groundcover, erodibilities, and critical shear stress, were obtained from field observations in various forest soils (Dobre et al., 2022b; Lew et al., 2022), and were not altered in our parameterizations. This was especially because our primary objective was to simulate the hydrological fluxes accurately, to provide a basis for comparison with observed sedimentation and provide opportunities for further erosion parameterization in the future.

Parameterization

Evaluation

We developed a series of scenarios, representing values of a suite of relevant hydrological parameters, to compare their performance in simulating the observed behavior of

the Canaan Valley watershed. Using the 'hydroGOF' package in R (Zambrano-Bigiarini, 2024), we calculated the Kling-Gupta Efficiency (KGE), Nash-Sutcliffe Efficiency (NSE), and percent bias (PBIAS) for each of these scenarios and for all attempted model runs after altering parameters. These scores provide feedback on the fit of the entire simulated streamflow hydrograph compared to the observed. However, baseflow, lateral flow, and runoff may all comprise varying proportions of this hydrograph. As a result, we also evaluated the total water balance of the watershed over the entire simulation period to assess its departure from observed values. The ratio of baseflow to quickflow and the overall runoff coefficient (of total streamflow) was especially of interest for this. Additionally, although we did not directly parameterize any explicitly erosion-related inputs (and notwithstanding the likely limitations of the observed sediment rating curve), we also evaluated the monthly fit of observed sediment yields with simulated sediment yields as a general guide. Finally, we compared the observed vs. simulated soil water storage. To make our field data, measured as volumetric water content, comparable to the WEPP simulation, given as soil water storage in millimeters, we used the hillside VWC station's data, and multiplied each represented soil layer by its thickness to obtain a soil water storage term for the entire 1000 mm profile.

A number of parameters were manually examined for their sensitivity, and those that had no, or a negligible effect on hydrograph fitting were not including in the following parameterizations. These included: rock fragments (%), bare soil albedo, canopy cover coefficient, flat residue cover (m^2 kg^{-1}), mature plant stem diameter (m), maximum canopy height (m), optimal plant growth temperature (°C), plant-specific drought tolerance, in-row plant spacing (m), maximum rooting depth (m), root-shoot ratio (m m^{-1}) maximum root mass (kg m^{-2}), senescence period (d), and maximum temperature for plant growth (°C).

"Vanilla," "high percolation," and "field calculated" parameter scenarios

Once the WEPPcloud run was initialized on the web interface, it was run and downloaded to a local environment for further manipulation in R. For evaluation, a series of five "scenarios" were created based on a set of assumptions or methods to evaluate the performance of each. The first scenario, termed "*vanilla*," made use of all the default values given from the initialized WEPPcloud run. A summary of the parameters selected in each scenario is shown in Table 4-1.

Based on the percolation equations given by Dun et al. (2009), we then manually selected universal (i.e., across all soils and depths) parameters to promote ultra-high percolation. The most sensitive parameters for percolation, according to the formulas, are θ_{fc}, *BD*, K_{sat}, and K_{sub}. However, we also lowered θ_{wp} and initial soil saturation (Table 4-1). We refer to this as the "*high percolation*" scenario.

Because some field-measured soil physical properties were available for the soils in our study area, we also calculated reasonable estimates for a number of parameters to run as a scenario. Based on the particle size measurements (described in Chapter 3), we applied a correction constant of +16.1% to sand and –16.1% to clay fractions across the soil files. We then used these particle size distributions to generate *BD* estimates according to the pedotransfer functions of Tomasella and Hodnett (1998). The K_{sat} values for all soils were next calculated from the Ottoni et al. (2019) pedotransfer function which takes percent silt, clay, and *BD* as inputs. Based on the average resulting porosity across the soils, and the starting values of soil moisture when monitoring began, we estimated a value of 0.3 initial saturation of porosity at simulation start. The baseflow coefficient, which can be considered the inverse of Duncan's

constant *k* (Duncan, 2019), was set at 0.13, derived from the *k* value of 0.87 set during the baseflow separation process (q.v. above). Finally, we altered the maximum LAI to 4, down from 10, as a more reasonable representation of the tropical dry forests of this catchment. We termed this simulation scenario the "*field calculated*" scenario.

Bayesian optimized and synthesized scenarios

We also took an objective optimization approach to set the values of a variety of parameters in order to provide a simulation scenario with reasonable parameter fits without human manual judgment. For this, we used the 'ParBayesianOptimization' package in R (Wilson, 2022) to perform Bayesian optimization of 11 parameters: deep seepage, baseflow coefficient, initial groundwater reservoir storage, K_c, maximum LAI, soil water lateral anisotropy (the preference for vertical or lateral flow), θ_{fc}, initial saturation, *BD*, K_{sat}, and K_{sub}. In the case of soil parameters, which may vary by depth or soil type, we allowed the optimization routine to modify these by a log-transformed coefficient (of the original set of parameters represented by the "*field calculated*" scenario). The other values were modified directly. The Bayesian optimization routine receives possible ranges of parameter input values. These are summarized in Table 4-2. The optimization process was given 55 initial runs to explore the parameter space using Latin hypercube sampling and a further 220 iterations to optimize the objective function. In this case, the objective function was written to optimize the KGE, selected as the most balanced single score for fitting to observed streamflow data. After receiving the optimized set of input parameters, we made a few manual reasonable adjustments to create the "*Bayesian optimized*" scenario: initial groundwater storage was set to zero (drought conditions prevailed at

the start of 2022; Menne et al., 2012), initial saturation was maintained at 0.3 (the same as "*field calculated*"), and deep seepage and baseflow coefficient were reduced from 0.27 to 0.1.

From the starting point of the "*Bayesian optimized*" simulation, we made a series of manual alterations in an effort to better reflect realistic parameters, particularly for soil hydrological variables, to produce a scenario we termed "*synthesized*" from all previous scenarios. Major changes to "*Bayesian optimized*" included increasing *BD* from the ultra-low values selected by the computer, increasing K_{sat} by an order of magnitude (the computer selected ultra-low values around 3.5 mm h^{-1}), increasing anisotropy by a factor of 100 (i.e., permitting more lateral flow), changing K_{sub} to 3.6 mm h^{-1} (from 3.6×10^6), and maximum LAI from 10 to 3.

Impoundments

Several bridges and low-water crossings exist across Canaan Gut, many of which use culverts to direct flow under the road. Because of this, we located three possible impoundments along the steam course to model WEPP with impoundment inputs (Fig. 4-4). In each case, we selected the "culvert" impoundment type (WEPP also allows for rectangular, concrete culverts more resembling the bridge in Fig. 4-4c). For parameters, we selected a stream gauge height of zero at simulation start, culvert length of 5 m (the width of the roadway), and a 1 m inlet and outlet stage height. We ran all five scenarios above with these impoundments to examine them for potential effects. Additionally, we field-scouted these impoundment locations to survey the actual conditions of these culverts and bridges in January 2025 (Fig. 4-4).

Thirty-year simulation

Using the parameters from "*Bayesian optimized*," we also created a 30-year simulation based on a stochastically generated CLIGEN climate file. Because interannual variability in weather conditions can be high in the Virgin Islands, we used the 30-year simulation to provide context for what may be the estimated streamflow and soil losses of Canaan Valley over a longer timeframe. However, the CLIGEN weather station, located in Charlotte Amalie, is subject to certain variation over what is likely to be the prevailing long-term climate in Canaan Valley. On the western slopes of the valley, St. Croix's second-highest peak, Blue Mountain (337 m), likely acts as an orogenic source of precipitation, whereas the Charlotte Amalie station, on the southern shore of St. Thomas, may see less rainfall and faster evaporation. But overall, the Charlotte Amalie CLIGEN runs can be considered a useful approximation of the prevailing climatic conditions of the Virgin Islands over long periods of time.

Results and Discussion

Performance of hydrological simulations

In the default "*vanilla*" scenario, the most notable behavior of the hydrograph was the dominance of rapid runoff peaks and immediate recession of the hydrograph back to zero or near-zero flow (Fig. 4-5). This may be a reasonable assumption to a certain extent, given the high degree of rainfall variability and the large size of certain discrete storms (viz., Tropical Storm [TS] Fiona with 164 mm of rain on 17–18 September 2022, visible as a spike of runoff in all five scenarios). However, it does not align well with observed data. Though observations do display a rapid increase of streamflow related to storm activity, they do not peak as high as the "*vanilla*" model run and display a much slower flow recession, including baseflow (Fig. 4-5).

The likely cause of this behavior was the inability of incoming precipitation to percolate below the soil profile, resulting in surface runoff (Table 4-3). In the water balance, simulated quickflow accounted for 84.2% of all streamflow (the sum of quickflow, baseflow, and lateral flow; Table 4-3), as compared to 28.2% in the observed dataset. We found that increasing K_{sat} and K_{sub} alone was not enough to promote percolation and only changed the dominant process to saturation excess overland flow as opposed to Hortonian flows.

This behavior is explained by the way WEPP calculates percolation (Dun et al., 2009), where water is not routed to the layer below unless θ exceeds θ_{fc}, and where the quantity percolated to the next layer is reduced proportionally to the saturated porosity of the destination layer. This means that percolation is governed mainly by *BD* and θ_{fc}, leading to the "*high percolation*" scenario, where we set these to extremely low values universally across all soils and horizons. The near-complete extinction of surface runoff is visible in this scenario (only 1.5% of streamflow; Table 4-3), though notably, the peak flow during TS Fiona still exceeded actual observations (Fig. 4-5). The effect on soil water storage is also noticeable, with soil becoming more responsive to rainfall (Fig. 4-6), though the "*high percolation*" scenario did not perform better than "*vanilla*" in goodness-of-fit metrics for soil water storage (Table 4-4).

Because percolation is so high in this scenario, the majority of incoming water that eventually becomes streamflow is first abstracted to the groundwater reservoir and then released over time as baseflow according to the baseflow coefficient (loss of 0.04 of the total reservoir volume per day). The overall goodness-of-fit of "*high percolation*" simulated streamflow is notably improved over "*vanilla*" streamflow (Table 4-4), but this improvement is entirely driven by improvement in simulating baseflow rather than quickflow. In other words, although the periods of baseflow in the observed hydrograph have a satisfactory relationship to "*high*

percolation" simulated baseflow, the process of runoff generation, still critical to the overall stream hydrology in Canaan Valley (and to soil erosion), is completely neglected.

The soil parameters used in this scenario may not be realistic because at 0.8 g cm^{-3}, the universal *BD* of this scenario represents 69.8% porosity, much higher than anything observed during field data collection. However, the soils of the catchment are generally stony (as high as 44.8% rocks by weight; see Chapter 3), which does have an acknowledged, positive effect on porosity (Nasri et al., 2015), owing to the skeletal structure that can be formed by the rock matrix to resist compaction. For the soil water retention curve, and thus θ_{fc} and θ_{wp}, it is often assumed that stonier soils effectively lower both these parameters, with the idea that the volumetric space occupied by the stones displaces any volumetric water. However, it has also been found that at higher levels of stoniness (i.e., > 40% rocks by mass), this predictive relationship breaks down (Naseri et al., 2019), as the physical structure of very stony soil can permit the formation of large voids and low bulk densities of the soil matrix around the stones (Coppola et al., 2013). To some extent then, it is possible that values for BD and θ_{fc} may vary more than might be expected for some areas of the Canaan Valley catchment.

In the "*field calculated*" scenario, we made several calculations based on observed soil physical properties to provide a scenario based as closely as possible on measured values—notwithstanding the limitations of such measurements in stony soils. In this scenario, the quickflow proportion of total streamflow conformed much more closely to observed data, at 28.8% (compared to the observed 28.2%; Table 4-3), but the overall proportion of precipitation routed to streamflow was a consistent underestimate (–20.6 % PBIAS; Table 4-4), though this was also true of the "*vanilla*" and "*high percolation*" scenarios. With percolation no longer permitted to such a degree as in "*high percolation*," we do observe the flashy "peaking" behavior

of runoff in this scenario, seen already in the "*vanilla*" run. However, the goodness-of-fit scores for total streamflow, quickflow, and baseflow, are all improvements over those of "*vanilla*" (Table 4-4).

The "*Bayesian optimized*" parameters apparently also favored high percolation, with low *BD*, θ_{fc}, and anisotropy favoring downward water flux, but K_{sat} was an order of magnitude lower than what was calculated from the pedotransfer function for "*field calculated*," and K_{sub} was several orders of magnitude greater than the default (Table 4-1). This scenario was notable in a number of ways. First, the goodness-of-fit scores among several simulated water fluxes were better in this scenario than any of the others, most especially in baseflow and soil water storage (Table 4-3; Fig. 4-6). The sharp peaking behavior was still present, but the higher percolation parameters meant the absolute peaks were closer to observed peaks than in the "*field calculated*" model run (Fig. 4-5). Also, peaks occurred more often (apparently due to low K_{sat}) than in the "*field calculated*" scenario. This could be considered an improvement over the previous scenario, though, because percolation under "*field calculated*" parameters was apparently high enough that observed peaks from rain storms often did not result in any simulated response in the hydrograph. In the "*Bayesian optimized*" case, these peaks do occur with the correct timing, though they remain too extreme and too "flashy."

The proportion of quickflow of the total streamflow (29.5%) correctly mirrors the observed proportion, but ET in this simulation is unrealistically low, at 40.9% (Table 4-3). This is almost entirely explained by the high deep seepage coefficient (0.1) that routed the water to aquifer loss instead, which accounted for 22.9% of the water balance. There is no existing data in any detail on either the total ET or deep seepage in water budgets of the Virgin Islands (Lancellotti and Hensley, 2024), but aquifer loss could theoretically be relevant in this system.

Fractured rock storage could transit between catchments and valleys in joints or faults, and a deep water table would have only occasional direct interaction with shallow groundwater and surface water. It is not known to what degree groundwater laterally moves between valley catchments in this region, but records of well depths on the weathered mantle-bedrock aquifers of the Virgin Islands do exist and often indicate water depths below ground surface of 6–30 m (Green and Cherry, 1994; Renken et al., 2002). Robinson (1972) Jordan (1975), meanwhile, provide estimates of 88–96% for the typical annual share of ET in the water balance of St. Croix, which they describe as "rough" estimates. Because of the unusually wet conditions of 2024, this is most likely an overestimate for our study period but is probably reasonable in normal conditions. The most sensitive parameters to ET in our scenarios, K_c and maximum LAI, were both part of the Bayesian optimization routine: the K_c was set relatively low (0.5), but the maximum LAI selected was 10, at the upper bound. Like K_{sub}, the deep seepage parameter is important for WEPP to model catchments with complex hydrogeology successfully (Dobre et al., 2022b), but is not usually known and must be fit to observed data (Lew et al., 2022).

Following the Bayesian optimization, the "*synthesized*" scenario was created to make alterations to the optimized choices to better fit realistic values for the process-based model. We did this mainly by increasing *BD* and K_{sat}, and reducing K_{sub}. This scenario produced the best KGE for total streamflow *Q*, at 0.34, and PBIAS, at –9.7 indicating an approximately correct total proportion of water routed to streamflow (Table 4-4). However, like all other scenarios, the "*synthesized*" run failed to produce a positive KGE or NSE for quickflow, which would indicate that the model outperforms the global mean as a predictor. The changed parameters primarily had the effect of increasing baseflow, such that the baseflow PBIAS, only –0.5 in the "*Bayesian optimized*" scenario, was 19.7 in the "*synthesized*" attempt.

All but one ("*vanilla*") scenario had a positive KGE for baseflow, compared to none for quickflow (Table 4-4). The baseflow component of the hydrograph was always simulated to slowly rise and then recede as water percolates through the soil into the reservoir and is extracted as baseflow before the reservoir runs out again (Fig. 4-5). The shape of the receding limb is relatively straightforward to fit by manipulating the baseflow coefficient, helping explain the simulations' ability to provide better fits for baseflow. But the delay in rising baseflow, after the sharp decline of the quickflow earlier, is a consistent problem with the simulated hydrograph. This contrasts with the behavior of the observed hydrograph data, in which sharp rises from stormflow do occur but do not sharply decline as quickly as the simulations, instead allowing baseflow and quickflow to slowly merge together as the hydrograph eventually becomes entirely baseflow and recedes back to a dry stream (Fig. 4-5). The "observed" baseflow is admittedly dependent on the estimation techniques of hydrograph separation (i.e., baseflow was not directly measured in the observed data), but the ability of baseflow to recharge during high flow events was our primary motivation for using Duncan's (2019) technique. The distinguishing feature of this technique is its allowance for baseflow to increase during peaks of the hydrograph, rather than simple linear graphic separation techniques (e.g., Blume et al., 2007), which is a better match with the actual hydrograph than the delayed baseflow response seen in the WEPP simulations. For the purposes of erosion predictions, it is not necessarily crucial to distinguish between baseflow and quickflow during peaks of the hydrograph (as high flows will result in major channel erosion in any case), but the rapid return to baseline of all water routed as runoff in our simulations represents a problem in the hydrological realism of these simulations.

Impoundments

The shape of the observed hydrograph, with fast peaks but a slow recession from the peak, cannot be modeled only by manipulating baseflow since the baseflow recession constant causes a delay in the rising baseflow. Instead, it would need to also involve a delayed release of quickflow from the precipitation event, either through lateral flow pathways or on the surface. In our simulations, we were unsuccessful in producing any meaningful quantities of lateral flow, and WEPP routes surface runoff immediately to the channel, producing the rapid peak and return to zero behavior that prevents a good fit with quickflow. For this reason, we also investigated the effect of impoundments in WEPP on all five of these scenarios.

Impoundments in the stream channel can be any one of several types available in WEPP; we chose to use culverts as the most common and straightforward among these. A number of bridges and low-water crossings over Canaan Gut exist within our study area, suggesting the possibility that, in dry conditions, a storage capacity of these impoundments may first need to be met before flow is released downstream. As discussed above, we identified three possible impoundments in the channel network (Fig. 4-4a) and included them in the input files to WEPP. We set the inlet and outlet stage of these culverts at 1 m to provide an impoundment capacity. The actual effect of the impoundments, however, was to impound effectively all baseflow and produce even more extreme peak flows than without, in all scenarios (for example, see Fig. 4-7).

The likely explanation for this is that the impoundment, once filled, releases all stored water from before the event, though it is not clear why WEPP does not retain appreciable quantities of water stored behind the impoundment. Runs tested with unrealistically high inlet stages (e.g., 100 m) did show a slight overall reduction in total streamflow, but not the complete extinction of streamflow as might be expected. In general, even the 1 m impoundment height tested is not realistic to field conditions. All impoundments visited in the field did not appear to

have a higher inlet stage than the streambed (Fig 4-4b; Fig. 4-4c), with unimpeded flow apparently possible. Certainly, impoundments are available in WEPP as much for reasons of erosion simulation (e.g. sediment deposition or channel bed scouring) as for hydrological reasons, but because of the poor performance of the impoundment simulations and the lack of any important features of water impoundment at the actual road crossings, we ultimately did not run the five scenarios described above with any impoundments.

It is possible that the lack of a delayed release from surface runoff would be alleviated with a finer resolution of hillslopes (in some versions of WEPP, hillslopes can be divided into overland flow elements or OFEs), though once water is routed to surface runoff, it is not clear what, other than slope length, delays the entry of water to the stream channel. The lack of lateral flow in our simulations could be a contributing factor to the poor fit with the hydrograph. If lateral flows to the stream from a given rain event take several days and are released over time, this could help "soften" the sharp runoff peaks and allow baseflow to "catch up" to the falling limb of the hydrograph to produce the correct shape in line with observed data. Although anisotropy, introduced to WEPP by Dun et al. (2009) in a new soil input file format, was designed to better model lateral flows in steep catchments, we observed no major changes to the hydrograph or water balance when manually exploring the effect of anisotropy, even at extreme values (e.g., 10,000). Interaction effects may nevertheless exist that were not captured in these parameter runs and could be constrained better in future efforts.

Performance of erosion simulations

The best-performing hydrological simulation was the "*Bayesian optimized*" parameter scenario, judged by goodness-of-fit scores (Table 4-4). However, for simulated sediment yields,

no parameter scenario produced KGE and NSE scores above zero. This lack of convergence is likely due more to the difficulties in modeling the correct quickflow behavior, than in the erosion parameters themselves, which we did not alter from default values. In a typical example, the "*field calculated*" scenario saw an overestimate of sedimentation in the first year (due to the overestimate of runoff from TS Fiona that was common to all simulations), but an underestimate in the following years because of a lack of major runoff spikes in that scenario (Fig. 4-5). The method for estimating observed sedimentation, based on the sediment rating curve, also carries great uncertainty extrapolated outside the measurement range. For these reasons, to provide a more forgiving performance check of erosion simulations, we aggregated observed and simulated sedimentation into monthly data (Fig. 4-8).

Goodness-of-fit scores for monthly sedimentation simulation improve over daily scores, but most simulations still fail to produce KGE or NSE scores > 0 (Fig. 4-8). The "*Bayesian optimized*" simulation received the best of these, with KGE = 0.16, though PBIAS for all simulations was > ±48, demonstrating the difficulties with correctly simulating quickflow (neither baseflow nor lateral flow contribute to sedimentation except in the channel bed). When considered annually, the "*Bayesian optimized*" scenario performed well in 2023 (40.7 t observed, 38.4 t simulated) and 2024 (38.7 t observed, 48.4 t simulated), but overestimated for 2022 in common with the other simulations (4.8 t observed, 38.2 t simulated).

The year before simulation began, 2021, was a historically dry year. Among rain gauges reporting to the Global Historical Climatology Network (Menne et al., 2012) within a 2.5 km radius of the centroid of Canaan Valley, a mean of 677 mm of precipitation was recorded that year. In 2022 and 2023, conditions returned closer to the historical average, with 845 mm and 790 mm recorded, respectively. This was followed by the historic rainy conditions of 2024

(1449 mm), which was especially notable for the lack of a real dry season in the first half of the calendar year, breaking from the normal climatic pattern. In this context, because of the consistent difficulty of our simulations to correctly model the outcome of TS Fiona, which effectively broke an extended drought phase, we speculate that the antecedent precipitation of the previous year may partly predict the ability of the simulations to adequately model runoff and sedimentation. The extended period of sustained baseflow, visible in the observed hydrograph at the end of 2024, is certainly an outcome of the unprecedented period of high precipitation for the preceding months, but it remains to be seen how well these WEPP simulations may model conditions in 2025 following such a rainy year.

Thirty-year simulation results

The precipitation generated by CLIGEN for the 30-year simulation reflects the pronounced interannual variability of rainfall in the Virgin Islands, and is realistic (Fig. 4-9; Menne et al., 2012). The global runoff coefficient in this simulation 0.141, also reasonable for the catchment (Jordan, 1975, and see Chapter 3). A nonlinear relationship between precipitation and sediment yield appears to exist, which is consistent with the concept of a runoff threshold beyond which additional rainfall causes increasingly kinetic runoff flows (Melville et al., 2022; Mohamadi and Kavian, 2015; q.v. Chapter 3).

With reasonable caveats, it is possible to calculate an annual soil loss rate using this simulated data. The total sediment yield of the 30-year simulation was 746 t, equating to 0.165 t ha^{-1} yr^{-1} of soil loss in Canaan Valley. This soil loss rate would put the catchment in line with other forested catchments worldwide (0.02–0.12 t ha^{-1} is given as a range in a systematic review of reported tropical forest erosion rates; Labrière et al., 2015), including in the Caribbean (0.12–

0.52 t ha^{-1} reported in forest catchments of eastern Puerto Rico, Gellis et al., 2006; 0.5 t ha^{-1} reported for a secondary forest in the Jamaican Blue Mountains, McDonald et al., 2002; 0.74 t ha^{-1} yr^{-1} reported in St. Lucia; Cox et al., 2006), and so are at least plausible. Assuming porosity of 0.5 in deposited sediments, it is also possible to make rough predictions of sedimentation rates in various anthropogenic features in the Salt River Bay watershed. For example, 500 m downstream of our gauge, as Canaan Gut becomes Salt River (moving towards its outlet at Salt River Bay), the stream course has been diverted around a significant residential area to prevent flooding (USACE, 1987). This structure, according to U.S. Army Corps of Engineers documents and our field measurements, has a channel bed width of 23 m and a linear extent of 1.8 km, or 4.14 ha. We discussed in the previous chapter that the connected surface flow between Canaan Valley and the watershed discharge at Salt River Bay is frequently disrupted, with disconnection probably being increased after the construction of this flood control structure. It is reasonable to assume therefore (Boardman et al., 2019) that large portions of sediment flux from Canaan Valley are settled out in this wide artificial channel (the channel bed is built of stone gabions). Assuming, for example, that all discharged flow was impounded by this structure (an overestimate), the sedimentation rate implied by the estimated annual sediment yield from Canaan Valley is 0.43 mm yr^{-1}. Other tributaries of the main stream channel also enter this control structure, however. Still, this extremely slow siltation rate and significant depth of the structure (6 m) permit the reasonable prediction that the structure would take some 7.5 ka to fill to 50% capacity with sediments. Natural sedimentation in Salt River Bay, feeding an important mangrove lagoon and U.S. National Park and Ecological Preserve (where altered sedimentation rates are a matter of concern to park managers; K. Ewen, pers. comm.), may thus be affected by this structure for millennia, barring other kinds of alterations. It is also important to point out that

significant quantities of stored sediments, captured by stone gabions in this structure, may flush out during extreme events, which would not necessarily be captured by a standard sediment rating curve, and could be especially problematic for downstream ecosystems.

This kind of flood control structure, however, is not common throughout the Virgin Islands. But small anthropogenic ponds, usually originally built as livestock ponds in the middle of the 20th century, are found throughout St. Croix in particular, and across the Virgin Islands (USDA-NRCS, 1973). A typical example is the Estate Windsor pond located 1.5 km east of our stream gauge on a tributary of the Salt River watershed (17.7562 °N, 64.7787 °W; Fig. 4-10) with a catchment area of 110 ha. This pond, with a surface area of approximately 0.17 ha, is a typical size for a Virgin Islands freshwater pond (Jordan, 1975), and can be assumed to have been constructed with an average depth of 2 m, which was typical during the period of pond construction that lasted ca. 1940–1970 (B. Lawaetz, pers. comm.). The pond, which already displays visible signs of siltation (vegetation growing in shallow water in much of the pond area; Fig. 4-10), is vulnerable to further degradation without maintenance. At the soil loss rates estimated for Canaan Valley, this pond, whose upstream subcatchment is adjacent to Canaan Valley and has similar slope, soil, and land cover, would have a sedimentation rate of 11.3 mm yr^{-1}, or approximately 88 years before being filled to 50% capacity (the pond was most likely built 65–75 years ago).

The estimated soil loss rate produced by this simulation is of course subject to a number of caveats, even though the final annualized loss rate is in line with expectations from forests around the world (Labrière et al., 2015). The work of Ramos-Scharrón in particular showed high rates of erosion and sedimentation on the island of St. John to be caused by networks of paved and unpaved roadways (Ramos-Scharrón and MacDonald, 2005), especially in steep terrain. A

review of this work, which includes work elsewhere in the northeastern Caribbean, reported soil loss rates of 0.3–3.7 t ha^{-1} yr^{-1}, said to be 3 to 40 times the background rate without roads (Ramos-Scharrón et al., 2023). Similar road networks, as well as a number of hillside homesites, are present in Canaan Valley, and the smaller scale effects of these, though they could be important in reality, would not be captured by these WEPP simulations that operate on the hillslope scale.

Additionally, the Virgin Islands are subject to extreme weather in the form of major hurricanes; recent important examples are Hurricanes Maria and Irma (2017), Lenny (1999), Marilyn (1995), and Hugo (1989). Although the CLIGEN climate generated does account for some degree of the natural variability of rainfall in the Virgin Islands that stems from these cyclonic systems, the dataset from Charlotte Amalie, collected over 40 years, would include only a few major storms. Furthermore, stations typically malfunction or cease to be maintained in the aftermath of the most serious hurricanes. The precipitation record of the weather station used by CLIGEN, at Charlotte Amalie Harbor (airport) has missing data for 5 months due to Hurricane Hugo, 6 months missing due to Hurricane Marilyn, and 3 months missing due to Hurricanes Irma and Maria (Menne et al., 2012). Even in simulations longer than 30 years, the rarity and data difficulties of these major rain events means CLIGEN may be unable to adequately capture this aspect of the Virgin Islands climate. Research in the region indicates that a major proportion of total long-term erosion and sedimentation can occur during such events. Soil losses in such events may exceed 30 t ha^{-1} (Rad et al., 2013); a reservoir in Puerto Rico witnessed a nearly tenfold increase compared to the background rate of sedimentation based on sediment cores (Matos-Llavona et al., 2022). These examples highlight the possible long-term importance of such extreme events in the overall water and sediment budget of the Virgin Islands.

Conclusions

To address these caveats and provide more reliable predictions of erosion and sedimentation in Virgin Islands watersheds, we suggest several areas of work. First of all, improved climate data, which includes at least the simulation of the extreme precipitation of hurricanes, would allow for better modeling of these events, even if actual monitoring instruments are destroyed or not maintained because of the natural hazards. Even a WEPP model well-calibrated in normal Virgin Islands climate conditions may struggle to accurately predict hydrological and erosion behaviors, which may necessitate special calibrations for such scenarios to be blended with the ordinary WEPP model. This would also bring the benefit of using WEPP's "single storm" functionality, which allows a user to model the runoff and erosion of a single event. Improved climate data would also permit more confident predictions relating to the expected effects of climate change on runoff and erosion in Virgin Islands watersheds. Additional weather stations or study of the spatial variability of precipitation patterns at the sub-island scale in the Virgin Islands would also help improve predictions instead of relying on a spatially invariable climate input.

Besides climate inputs, the major point to address to improve WEPP's performance in this region is to constrain the runoff hydrograph more correctly, preventing the rapid peak-and-decline behavior seen in all five of our scenarios. This could possibly be addressed by the use of additional OFEs to delay runoff surface flows and improve modeling of surface depression storage, and improve spatial resolution more generally. Another important angle of inquiry would be the lack of lateral flow seen in our simulations. Parameterizations that allow for significant lateral flow would not only reflect the likely reality of subsurface flow pathways in

Canaan Valley but could also assist with the slow rise of baseflow to meet the falling limb of the hydrograph. Year-by-year calibration approaches (for example, allowing deep seepage or baseflow coefficients to vary) may assist in correctly modeling possible year-over-year effects and interactions with the hydrogeology, though practically speaking, recalibrating parameters for every year could also cause overfitting. Also, improved groundwater data or hydrogeological information would assist in providing realism to many of the inferred parameters of K_{sub} and deep seepage.

Impoundments may likely be important in many Virgin Islands watersheds (for example, the Estate Windsor pond mentioned above effectively acts as an impoundment in the channel of that subcatchment). But in Canaan Valley, we found that impoundments are not an important component of hydrologic and erosion modeling, because adding them exacerbated problems in the hydrograph instead of improving the fit. Most importantly, we found no known examples of raised impoundments in the stream channel that would stop or delay flows downstream (Fig. 4-4).

More data points to describe a good sediment rating curve is the most important factor that would help improve estimates of erosion and sedimentation. As seen above, it is theoretically possible to obtain reasonable estimates of erosion if observed erosion rates are available for comparison by calibrating for this output, even if certain aspects of the hydrograph are not well simulated. When a sediment rating is better constrained and represents a wider range of flow conditions and antecedent situations, it would be more warranted to investigate erosion parameters (which we neglected in this study).

Our study provided a preliminary effort to calibrate WEPP in a Caribbean watershed, and highlighted the above areas of importance to continue to improve WEPP's simulation

capabilities in this region. Even the output of the current simulations, though flawed, provides believable estimates of erosion in a forested catchment. With useable estimates of sedimentation rates, managers in the region will be able to make important planning decisions, for example, siltation rates of ponds and reservoirs, agricultural soil loss, water conservation, road construction, property development, zoning, and sedimentation impacts to marine ecosystems. These various utilities highlight the importance of continued work to improve the capabilities of the WEPP model in watersheds of the Virgin Islands and the wider Caribbean.

Tables and Figures

Table 4-1. Parameter selections for WEPP hydrological and erosion simulations under five scenarios: "*vanilla*" (default parameters), "*high percolation*," (intentionally promoting high percolation), "*field calculated*" (based on observed soil physical properties), "*Bayesian optimized*" (the result of a Bayesian optimization parameter selection process), and "*synthesized*" (manual adjustments to the Bayesian optimization). Parameters are displayed in a range of minimum to maximum values (when different across several soil depths) for each parameter in the given feature (i.e., soil type or land use type): bulk density (BD), saturated hydraulic conductivity (K_{sat}), soil water flux lateral anisotropy (aniso.), field capacity (θ_{fc}), wilting point (θ_{wp}), sand fraction, clay fraction, crop coefficient (K_c), initial saturation of porosity at simulation start (initial sat.), saturated hydraulic conductivity of the "bedrock" restricting layer ($\underline{K_{sub}}$), groundwater reservoir storage at simulation start (groundwater), baseflow coefficient, deep seepage coefficient, and maximum leaf area index (max. LAI).

Parameter	Unit	Feature	"*Vanilla*"	"*High percolation*"	"*Field calculated*"	"*Bayesian optimized*"	"*Synthesized*"
BD	g cm^{-3}	Cramer-Victory	1.18–1.52	0.8	1.13–1.34	0.56–0.67	0.9–1.07
BD	g cm^{-3}	Victory-Southgate	1.52–1.6	0.8	1.23–1.49	0.62–0.74	0.98–1.19
BD	g cm^{-3}	Southgate rock	1.52–1.58	0.8	1.22–1.35	0.61–0.68	0.98–1.08
BD	g cm^{-3}	Channel	1.5	0.8	1.5	0.75	1.2
BD	g cm^{-3}	Developed	1.6	0.8	1.6	0.8	1.28
K_{sat}	mm h^{-1}	Cramer-Victory	9.72–54	50	32.98–38.05	3.3–3.81	32.98–38.05
K_{sat}	mm h^{-1}	Victory-Southgate	9.72–180	50	32.24–39.03	3.22–3.9	32.24–39.03
K_{sat}	mm h^{-1}	Southgate rock	9.72–151.2	50	30.13–35.9	3.01–3.59	30.13–35.9
K_{sat}	mm h^{-1}	Channel	0.5	50	35.99	3.6	35.99
K_{sat}	mm h^{-1}	Developed	10.5	50	10.5	1.05	10.5
Aniso.	–	Cramer-Victory	1–10	1–10	1–10	0.01–0.1	1–10
Aniso.	–	Victory-Southgate	1–10	1–10	1–10	0.01–0.1	1–10
Aniso.	–	Southgate rock	10	10	10	0.1	10
Aniso.	–	Channel	1	1	1	0.01	1
Aniso.	–	Developed	1	1	1	0.01	1
θ_{fc}	cm^3 cm^{-3}	Cramer-Victory	0.19–0.44	0.2	0.19–0.44	0.14–0.33	0.14–0.33
θ_{fc}	cm^3 cm^{-3}	Victory-Southgate	0.19–0.36	0.2	0.19–0.36	0.14–0.26	0.14–0.26
θ_{fc}	cm^3 cm^{-3}	Southgate rock	0.19–0.25	0.2	0.19–0.25	0.14–0.19	0.14–0.19
θ_{fc}	cm^3 cm^{-3}	Channel	0.24	0.2	0.24	0.18	0.18
θ_{fc}	cm^3 cm^{-3}	Developed	0.28	0.2	0.28	0.21	0.21
θ_{wp}	cm^3 cm^{-3}	Cramer-Victory	0.09–0.24	0.1	0.09–0.24	0.09–0.24	0.09–0.24
θ_{wp}	cm^3 cm^{-3}	Victory-Southgate	0.09–0.17	0.1	0.09–0.17	0.09–0.17	0.09–0.17
θ_{wp}	cm^3 cm^{-3}	Southgate rock	0.09–0.14	0.1	0.09–0.14	0.09–0.14	0.09–0.14
θ_{wp}	cm^3 cm^{-3}	Channel	0.11	0.1	0.11	0.11	0.11
θ_{wp}	cm^3 cm^{-3}	Developed	0.16	0.1	0.16	0.16	0.16
Sand	%	Cramer-Victory	22.1–66.8	22.1–66.8	47.56–66.1	22.1–66.8	22.1–66.8
Sand	%	Victory-Southgate	43–66.8	43–66.8	55.69–84.4	43–66.8	43–66.8
Sand	%	Southgate rock	39.2–66.8	39.2–66.8	53.52–57.34	39.2–66.8	39.2–66.8
Sand	%	Channel	66.8	66.8	66.8	66.8	66.8
Sand	%	Developed	25	25	25	25	25
Clay	%	Cramer-Victory	7–50	7–50	12.2–19.1	7–50	7–50
Clay	%	Victory-Southgate	7–18.5	7–18.5	3.9–7.28	7–18.5	7–18.5
Clay	%	Southgate rock	7–23.5	7–23.5	5.73–16.34	7–23.5	7–23.5
Clay	%	Channel	7	7	7	7	7
Clay	%	Developed	30	30	30	30	30
K_c	–	Forest land	0.95	0.95	0.95	0.5	0.5
K_c	–	Forest land	0.95	0.95	0.95	0.5	0.5
K_c	–	Developed land	0.95	0.95	0.95	0.5	0.5
Initial sat.	–	Universal	0.75	0.1	0.3	0.3	0.3
K_{sub}	mm h^{-1}	Universal	0	50	35.99	3599	3.6
Groundwater	mm	Universal	0	0	0	0	0
Baseflow	d^{-1}	Universal	0.04	0.04	0.13	0.1	0.1
Deep seep	d^{-1}	Universal	0	0	0	0.1	0.1
Max. LAI	–	Universal	14	14	4	10	3

Table 4-2. Upper and lower bounds for "*Bayesian optimized*" parameter selection routine. Values given with natural logarithms were used to modify the "*field calculated*" scenario's parameters, owing to several soils across the simulation domain. Logarithmic values were back-transformed within the objective function that was optimized. Parameters listed are: deep seepage out of the groundwater reservoir, baseflow coefficient, groundwater reservoir storage, crop coefficient (K_c), maximum leaf area index (LAI), soil water lateral anisotropy (aniso.), initial saturation of soil at simulation start (initial sat.), bulk density (*BD*), and saturated hydraulic conductivity of soil (K_{sat}) and the restricting "bedrock" layer (K_{sub}).

Parameter	**Unit**	**Lower bound**	**Upper bound**
Deep seep	d^{-1}	–0.9	0.9
Baseflow	d^{-1}	0	0.5
Groundwater	mm	0	500
K_c	–	0.5	2.5
Max. LAI	–	3	10
Aniso.	–	ln 0.01	ln 50
θ_{fc}	$cm^3\ cm^{-3}$	ln 0.1	ln 3
Initial sat.	–	ln 0.1	ln 5
BD	$g\ cm^3$	ln 0.5	ln 2
K_{sat}	$mm\ h^{-1}$	ln 0.1	ln 10
K_{sub}	$mm\ h^{-1}$	ln 0.5	ln 100000

Table 4-3. Water balance % of total rainfall.

	"Vanilla"	***"High percolation"***	***"Field calculated"***	***"Bayesian optimized"***	***"Synthesized"***
ET	71.73	67.99	69.41	40.91	40.25
Baseflow	1.43	25.57	18.43	22.88	27.54
Quickflow	20.37	0.39	7.07	9.59	1.45
Lateral flow	2.42	0.07	0.37	0.00	0.14
Aquifer loss	0.00	0.64	0.00	22.88	27.54
Soil storage change	2.94	3.59	3.59	2.61	1.80
Groundwater storage change	0.05	0.58	0.00	0.02	0.19
Sum	96.52	98.77	98.5	98.9	98.77

Table 4-4. Score metrics for five WEPP parameter "scenarios": Kling-Gupta Efficiency (KGE), Nash-Sutcliffe Efficiency (NSE), and percent bias (PBIAS) from daily data across five simulated and observed variables: all streamflow (*Q*; mm), baseflow (mm), quickflow (mm), soil water storage (mm), and sediment load (t). Positive KGEs and NSEs, and PBIAS <10 (absolute value) in bold.

Variable	Metric	"*Vanilla*"	"*High percolation*"	"*Field calculated*"	"*Bayesian optimized*"	"*Synthesized*"
	KGE	–0.67	**0.25**	**0.08**	**0.22**	**0.34**
Q	NSE	–5.05	**0.11**	–1.50	–0.85	–0.10
	PBIAS	–32.1	–19.2	–20.6	**1.1**	**–9.7**
	KGE	–0.58	**0.40**	**0.39**	**0.32**	**0.35**
Baseflow	NSE	–0.19	**0.11**	–0.02	**0.24**	–0.02
	PBIAS	–93.8	11.1	–19.9	**–0.5**	19.7
	KGE	–3.70	–0.41	–1.26	–0.76	–0.21
Quickflow	NSE	–26.57	–0.18	–8.05	–5.44	–1.30
	PBIAS	123.5	–95.7	–22.4	**5.3**	–84.1
	KGE	**0.65**	**0.51**	**0.65**	**0.82**	**0.39**
Soil water	NSE	–1.41	–4.32	–2.28	**0.32**	–2.81
	PBIAS	–26.9	–42.5	–33.2	–12.3	–34.3
	KGE	–0.02	–0.68	–0.21	–0.24	–0.61
Sediment	NSE	–1.07	–0.03	–0.31	–2.59	–0.02
	PBIAS	–50.9	–98.8	–74.2	48.5	–96.5

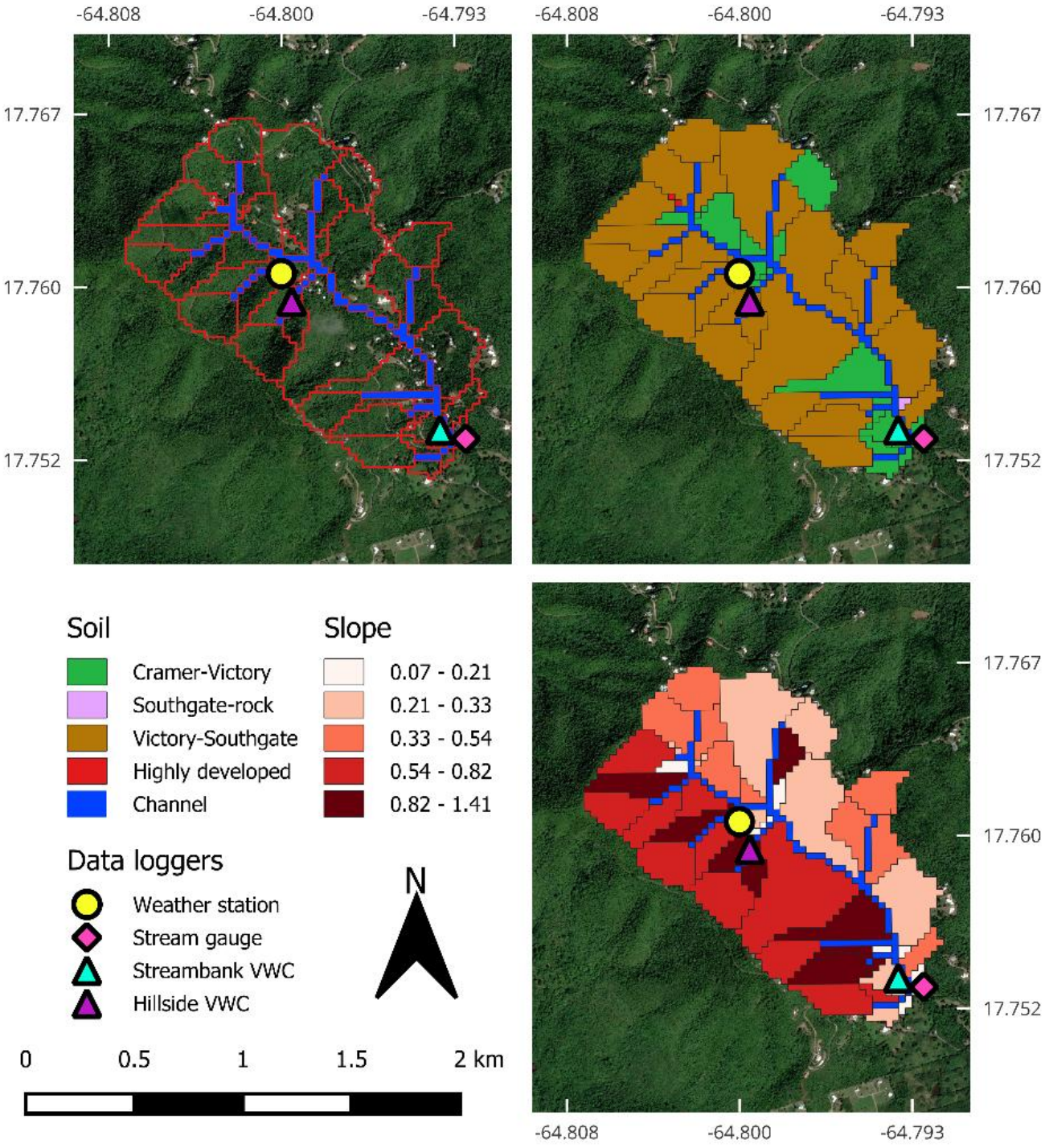

Fig. 4-1. From top left to bottom right: Canaan Valley study area delineated into hillslopes and channels for WEPP simulations with data logger locations; hillslopes according to dominant soil type; and hillslopes according to slope.

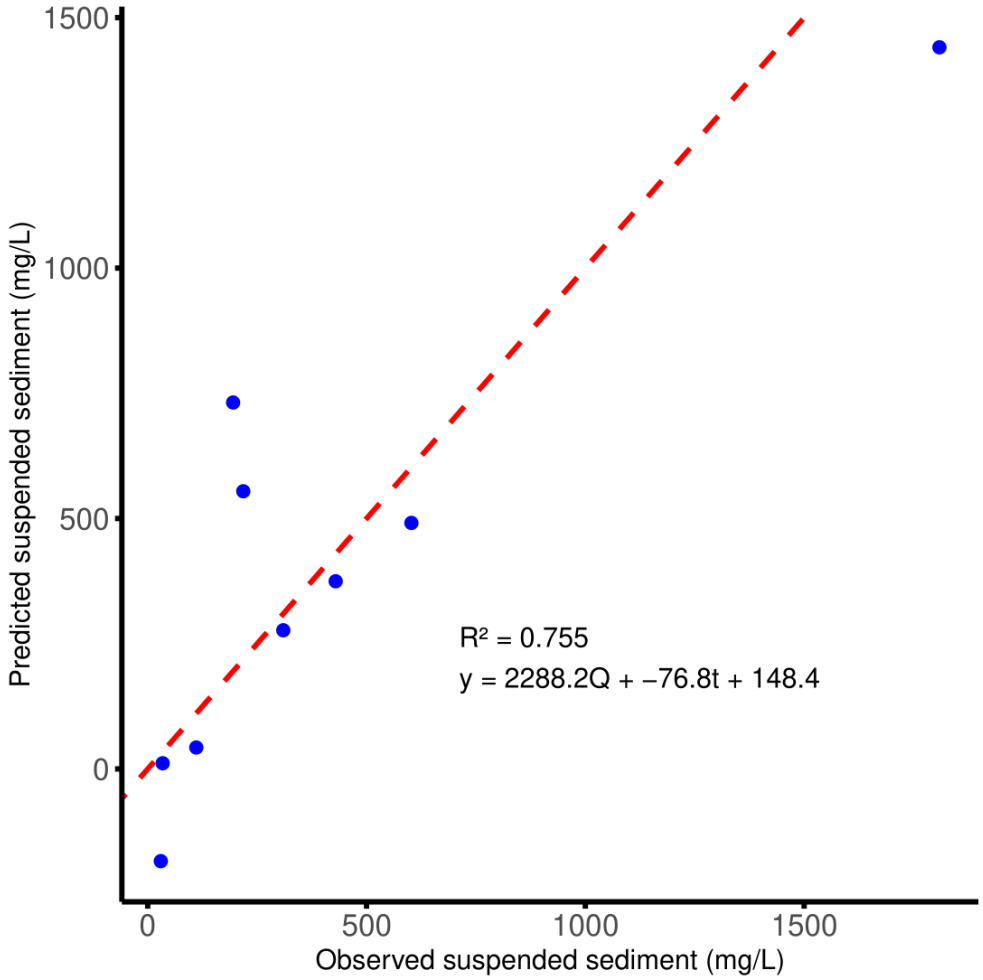

Fig. 4-2. Performance of sediment rating curve, relating streamflow Q (m^3 s^{-1}) and time since peak flow t (h) to predict suspended sediments (mg L^{-1}) in a multiple regression; the red dashed line represents a 1:1 relationship.

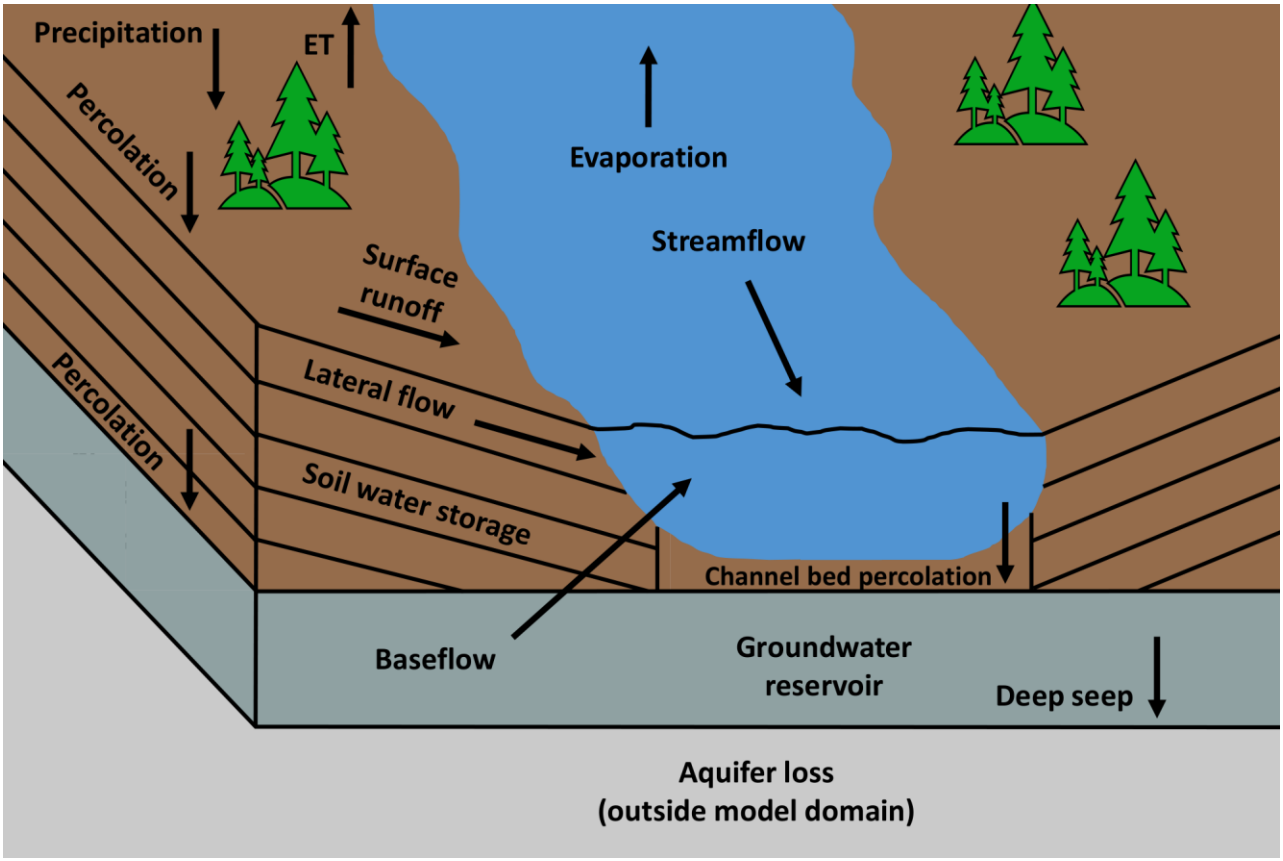

Fig. 4-3. Conceptual diagram of WEPP hydrological processing, encompassing incoming precipitation, abstraction of surface runoff and streamflow, percolation, evapotranspiration (ET; including from surface water), percolation through soil horizons and into groundwater reservoir, baseflow from reservoir into streamflow, lateral flow through soil horizons to streamflow, percolation through channel bed soil, and deep seepage of water out of the model domain from the groundwater reservoir.

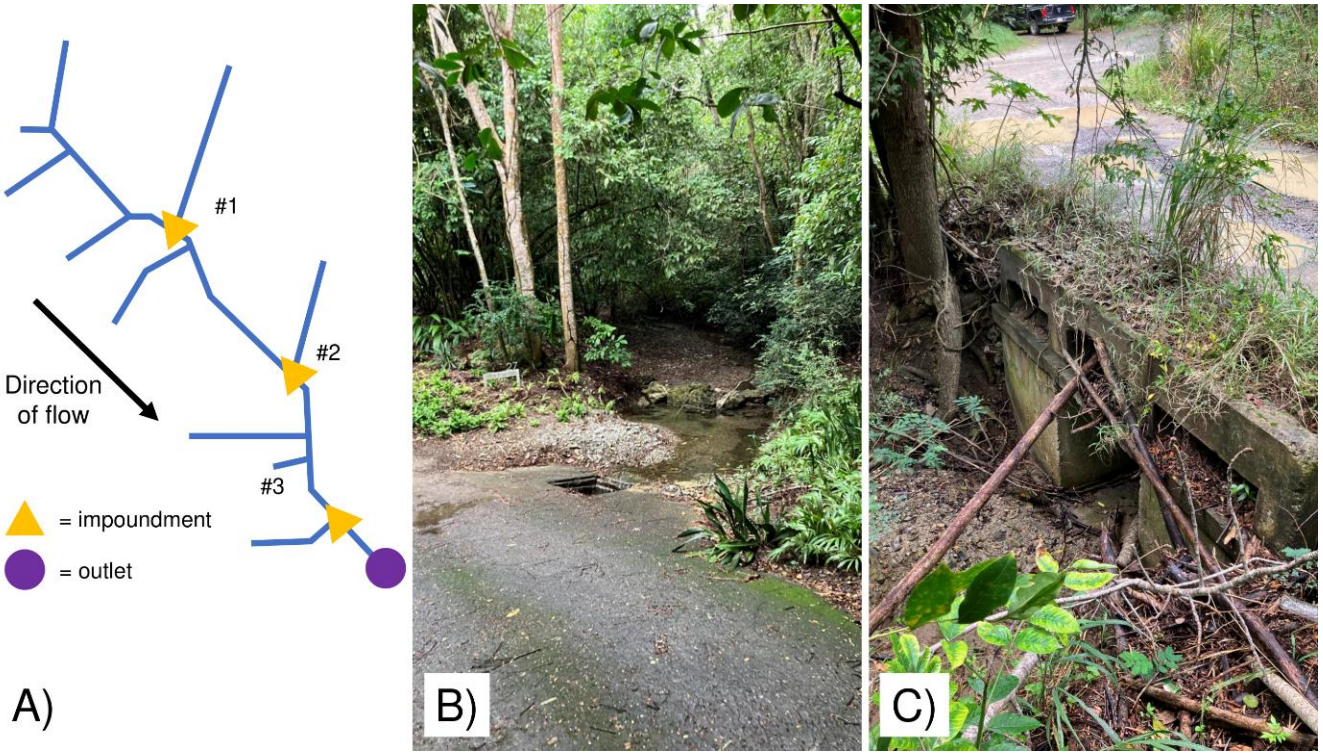

Fig. 4-4. A) Conceptual diagram of locations of three impoundments in the Canaan Valley catchment. Individual channel segments (19 total) were determined by WEPP; impoundments are located at confluences nearest their actual location; B) inlet of impoundment #2 at a low water crossing of the stream, with gravity fed structure and no rise from the level of the streambed visible; C) inlet of impoundment #3 nearest the catchment outlet, a bridge over a rectangular concrete culvert structure, without any rise from the level of the streambed.

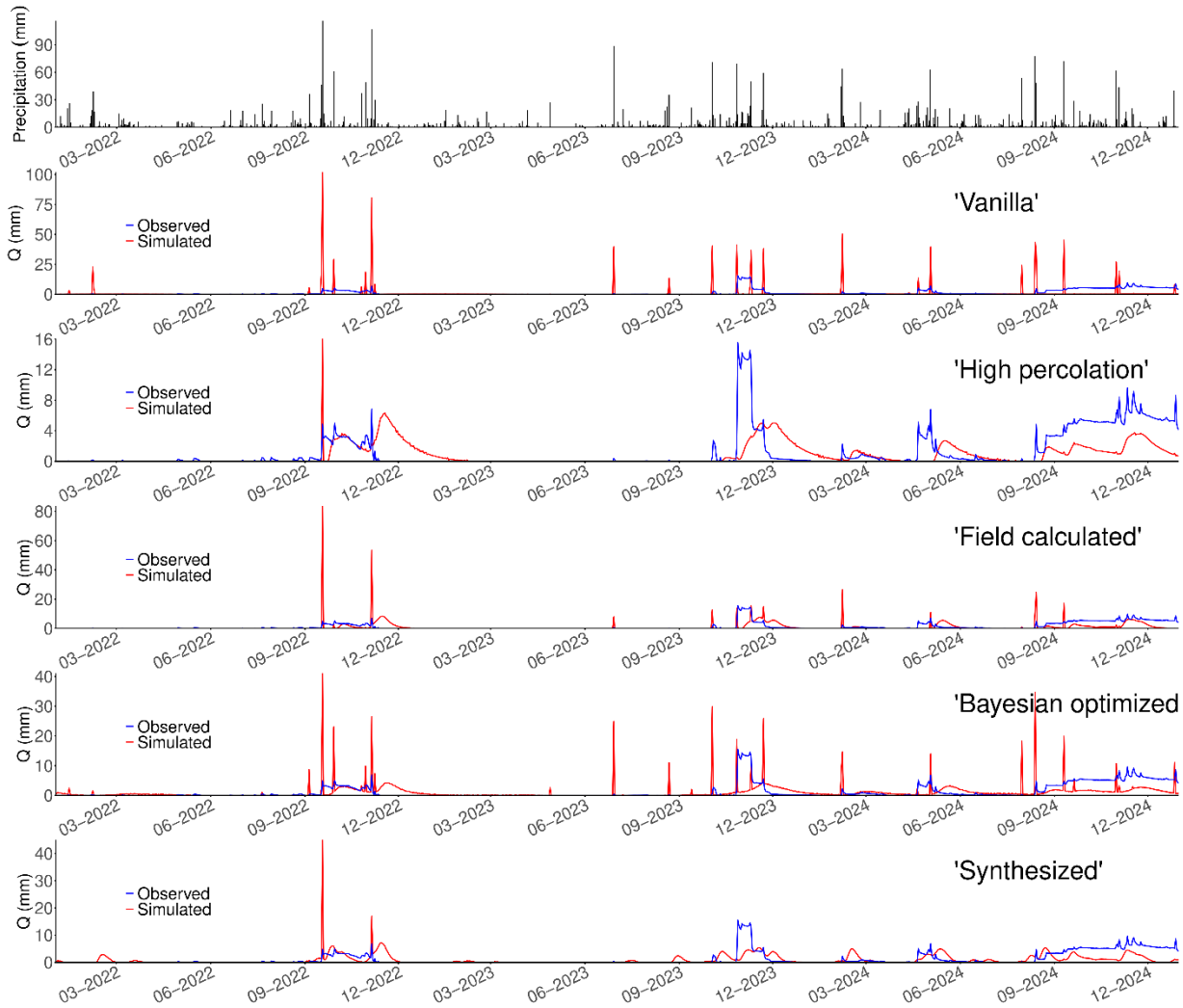

Fig. 4-5. Observed and simulated hydrographs (with precipitation input) of five WEPP parameter "scenarios;" n.b., y-axes not standardized.

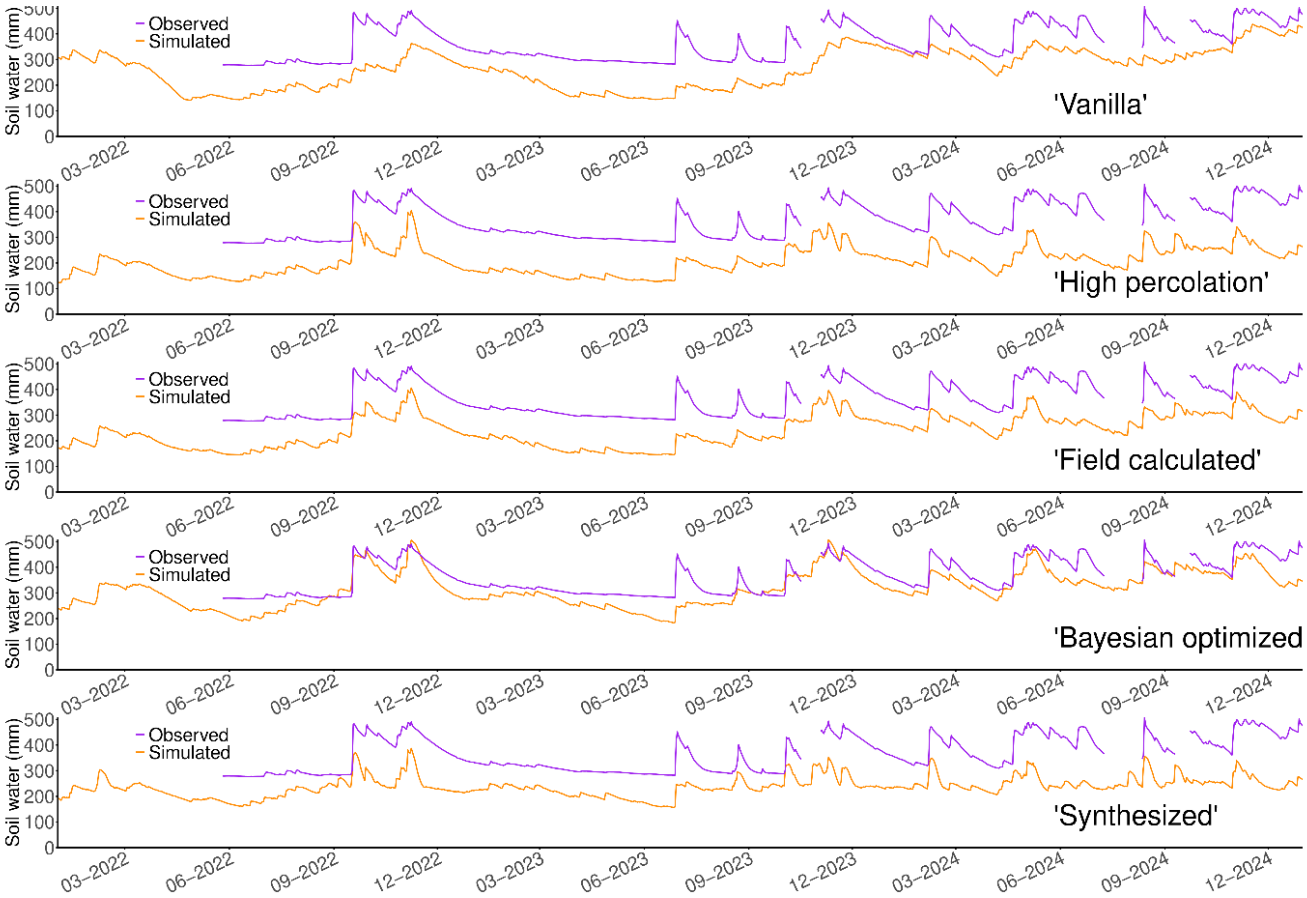

Fig. 4-6. Observed and simulated soil volumetric water storage (mm) of five WEPP parameter "scenarios."

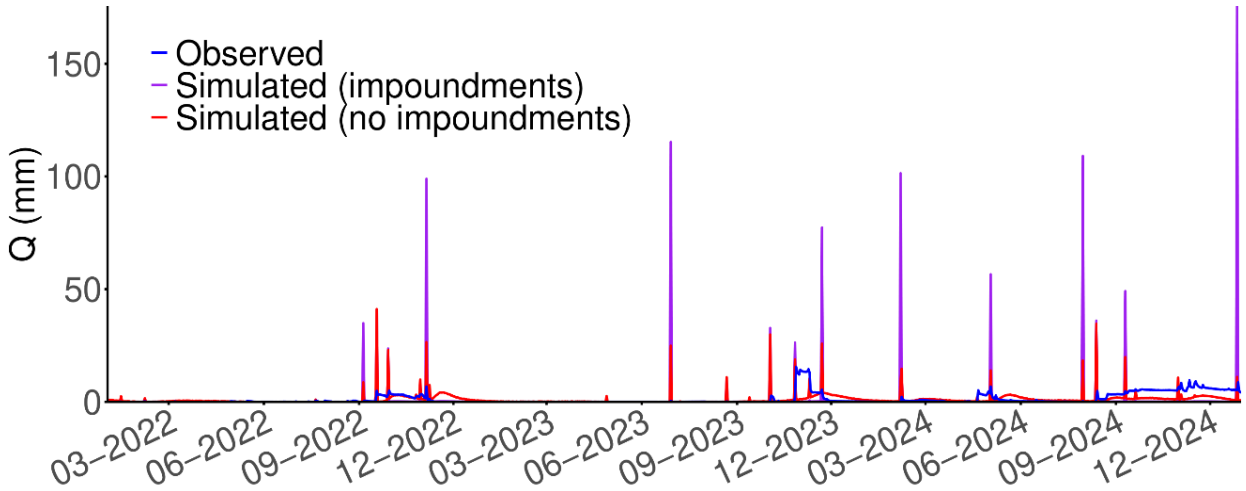

Fig. 4-7. Observed streamflow (*Q*) in Canaan Valley versus WEPP simulated streamflow ("*Bayesian optimized*" scenario) with and without impoundments added to the stream channel.

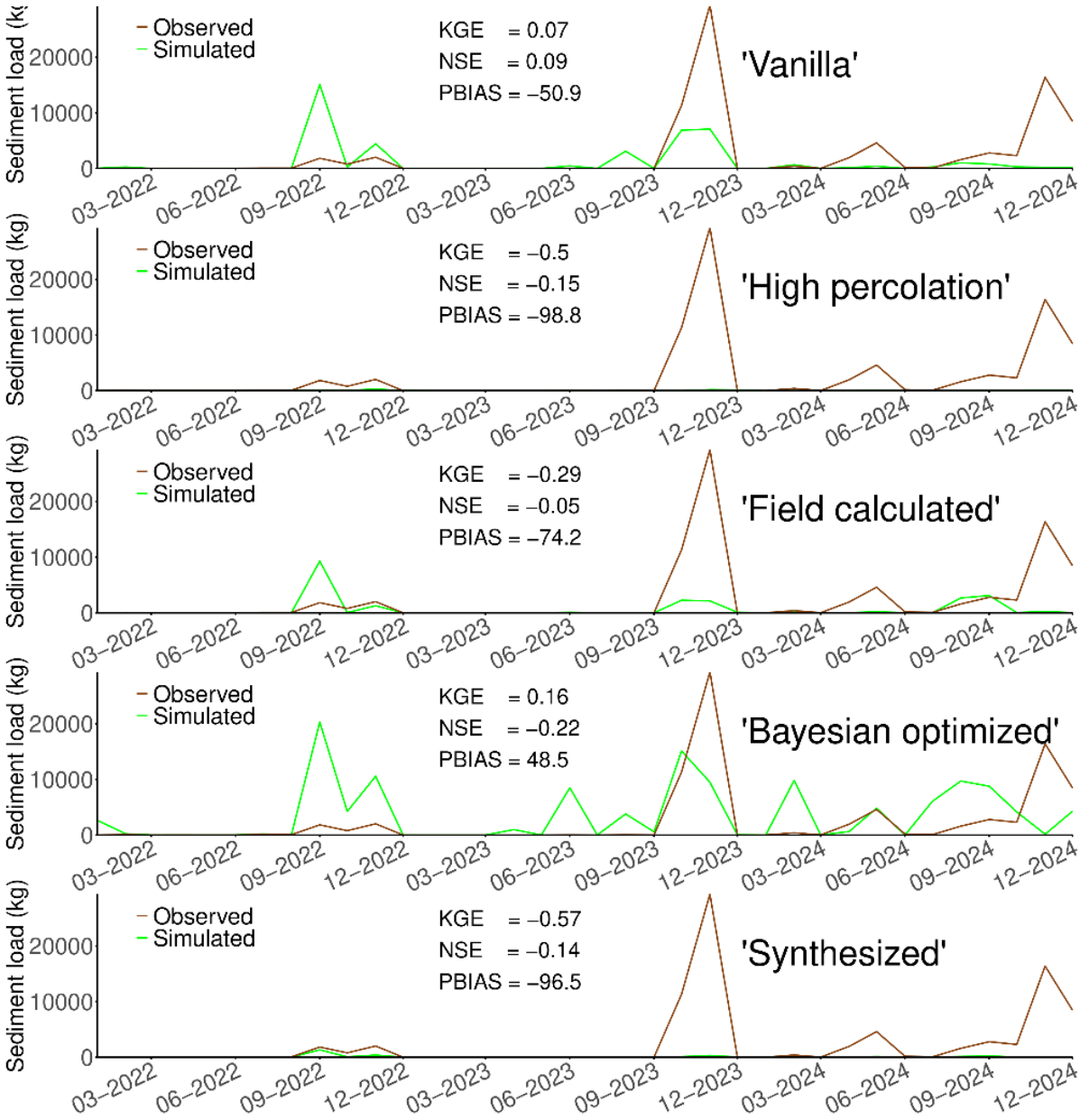

Fig. 4-8. Monthly sediment load (observed and simulated; kg) in five WEPP parameter "scenarios," with goodness-of-fit scores (Kling-Gupta Efficiency, KGE; Nash-Sutcliffe Efficiency, NSE; percent bias, PBIAS) for each.

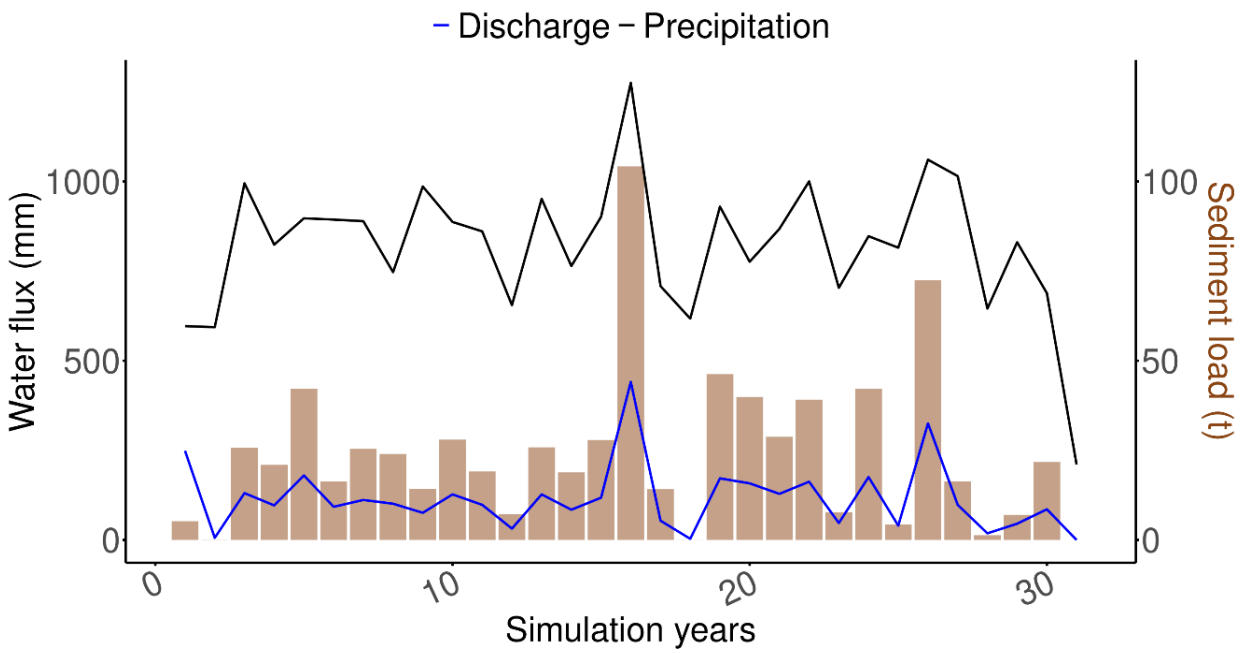

Fig. 4-9. Simulated sediment load (t) and water fluxes of precipitation (mm) and stream discharge (mm) of the Canaan Valley, St. Croix, in a 30-year simulated CLIGEN climate from the Charlotte Amalie, St. Thomas weather station.

Fig. 4-10. Estate Windsor pond in February 2025. Photo taken after extremely wet conditions of 2024, but standing vegetation along pond banks demonstrates ongoing sedimentation of the pond bed.

Chapter 5
Conclusion

The water resources of the Virgin Islands, as anywhere on Earth, are mediated to a large degree by the soil hydrology of the landscape and in the vadose zone. Land and water resources have an elevated importance on small islands, even compared to other places, because of the necessary limitations that the island environment places on both. It was this critical situation especially that motivated the research presented in the previous chapters, since soil hydrological science is so well suited to providing practical and fundamental answers to urgent questions for the community and leadership of the Virgin Islands.

Rapid changes continue in the land use of the islands, and history gives us concerning indications that water resources may be on a long-term decline. In this situation, it is extremely important for the future habitability of the islands that a better mechanistic understanding be gained of the status and functions of the soil-water system of the islands. Lack of concerted action to adequately protect both land and water resources have unfortunately characterized the recent history of the Virgin Islands. Many complicating factors have contributed: political boundaries across the archipelago, economic constraints, and problems of scale and capacity, but for our purposes here, the most important has been the lack of information available. If the recurring obstacles of resources, will, and opportunity are overcome to implement management decisions for the benefit of the Virgin Islands, lack of information should not be the final barrier to informed, beneficial action.

The three studies presented in this document have gathered additional information that can be used by managers and future researchers to make information a much less significant barrier to action. In the first (Chapter 2), we focused on soil water in agricultural production,

because a frequently expressed desire for greater food sovereignty must not at the same time cause even further pressure on land and water resources. The use of mulch under plantain production, though a promising concept for improved harvest and water savings, was not proven to be successful within a single season in our study, though it was cut short by outside circumstances. Usefully though, the study resulted in a much better soil hydrological characterization of a major agricultural soil in the Virgin Islands. That data can be used in a number of future experiments or tools that assist in the overall goal of conserving water resources while expanding local agriculture. In addition, the methods and approaches developed for that study show promise as a blueprint for continuing work that will provide even more descriptions of water movement in Virgin Islands agroecosystems.

In the second study (Chapter 3), we described runoff generation and watershed connectivity in Salt River, St. Croix, an important watershed of the Virgin Islands in its own right. But with critical marine habitats in the bay, mixed land use, and a mixture of volcanic and carbonate hydrogeology, it also served as an ideal case study to learn lessons applicable to other Virgin Islands watersheds. We found, in line with the original reports on Virgin Islands hydrology from the 1960s and 70s, that runoff is driven by soil saturation, and in the mountains (which share much in common with the majority of Virgin Islands land area), runoff is generated more easily than in sedimentary lowlands. One of the most important outcomes of this study was to confirm that significant quantities of upland runoff can be rerouted to alluvial coastal plains and captured rather than discharged to the sea. This helps us better understand the disrupted connectivity that is often seen in Virgin Islands guts. Much more work remains to be done to apply this concept in a variety of cases, including when various anthropogenic impoundments exist or in the smaller and shorter stream channels of the alluvial plains found outside St. Croix.

Still, and like other chapters, the methods and approaches we developed from hydrological science to apply to our watersheds will be useful in doing similar work in other targeted watersheds of the Virgin Islands in the future. With such data in place, it is now much more plausible to imagine a data-driven, realistic water budget for the entire island or even a working hydrological model. These would be critical milestones on the path toward a sustainable program of land and water management in any part of the Virgin Islands.

In the final study (Chapter 4), we applied the WEPP model to the upstream subcatchment of Salt River (Canaan Valley). Because erosion is such a commonly cited problem across the islands, so closely tied to runoff generation and soil hydrology, we hoped to use the framework provided by WEPP to gain an increased understanding of sedimentation processes in Virgin Islands catchments. Canaan Valley was a useful pilot for the study, with soil, slope, land use, and hydrogeology similar to many areas all across the Virgin Islands. Although we were unable to satisfactorily constrain the hydrological modeling of runoff performed by the model, the calibration process did reveal some important areas for investigation.

Sediment grab sampling, relatively simple to accomplish given enough time, is a useful area of effort for researchers and public workers going forward. These, combined with our improving understanding of streamflow, will, on their own, give us a more confident grasp of the flux of sediment and loss of soil in Virgin Islands watersheds — especially when they can be timed with important flow events. In addition, continued attempts at parameterizing lateral flow are a priority to mimic observed flow conditions accurately. The likely importance of subsurface stormflow and pre-event water in hydrographs, which our work in the previous chapter indicated, means that an accurate process-based modeling of that aspect of flow will be a major step forward in producing a finalized WEPP model ready for use by managers. Further, and finally,

the already obvious importance of both precipitation monitoring and groundwater monitoring was highlighted by our efforts. Both efforts, although not trivial in cost, would benefit from even the most incremental of improvements anywhere in the Virgin Islands, and would have useful applications well outside of calibrating hydrological erosion models. The potential application of WEPP to simulate storms or land use changes remains immensely attractive, and our study laid an important foundation for the continued effort to produce usable models for the islands.

Scientific progress is often incremental. On the periphery of well-resourced or powerful regions of the world, where research is highly developed and has seen extensive useful applications, progress may often come in the form of performing tasks or beginning initiatives that would be seen as relatively basic in other regions. Results are not always immediately applied, or further study is often required to produce an actionable result. Many of these circumstances characterize in the broadest sense the challenge of conducting environmental science in the Virgin Islands. But even when this is the case, it is striking that new progress, when it is made, is often based heavily on the fundamental work carried out in the past; our extensive reference to the work of Jordan and Ramos-Scharrón in this dissertation are testaments to this. The results and methods we present in this study represent important developments in soil and water science in the Virgin Islands and the Caribbean region. We hope that further work will be shortly carried out to advance these areas of research. Even if this does not take place, though, we are confident that this work will be useful to future researchers on the problems of soil, water, and land in the Virgin Islands. Such questions will always be relevant to inhabited islands across the world. Future work, whether of our own or of others, will always be necessary to provide the people of the Virgin Islands with the habitable, beautiful environment they so richly deserve. This concludes the current study, but we now look forward to the work to come.

References

Abdullateef, L., Tijani, M.N., Nuru, N.A., John, S., Mustapha. A., 2021. Assessment of groundwater recharge potential in a typical geological transition zone in Bauchi, NE-Nigeria using remote sensing/GIS and MCDA approaches. *Heliyon* 7(4): e06762. https://doi.org/10.1016/j.heliyon.2021.e06762.

Acharya, S., McLaughlin, D., Kaplan, D., Cohen, M.J., 2020. A proposed method for estimating interception from near-surface soil moisture response. *Hydrol. Earth Syst. Sci.* 24:1859–1870. https://doi.org/10.5194/hess-24-1859-2020.

Agricultural Plan Task Force, 2021. Virgin Islands Agricultural Plan. https://doa.vi.gov/wp-content/uploads/2022/05/Virgin-Islands-Agricultural-Plan_2021-VI-Ag-Plan-Task-Force.pdf (accessed 23 February 2025).

Ahmad, N., 2015. Soil water management systems for a drier Caribbean. *Caribbean Agricultural Research and Development Institute Review* 16:34–53. https://www.cardi.org/wp-content/uploads/downloads/2016/01/CARDI-Review-Issue-16-December-2015.pdf#page=35 (accessed 23 February 2025).

Al-Amri, N.S., Abdurahman, S.G., Elfeki, A.M., 2023. Modeling aquifer responses from flash flood events through ephemeral stream beds: Case studies from Saudi Arabia. *Water* 15:2735. https://doi.org/10.3390/w15152735.

Allen, R.G., Pereira, L.S., Raes, D., Smith, M., 1998. Crop evapotranspiration: Guidelines for computing crop requirements. Irrigation and Drainage Paper No. 56, United Nations Food and Agriculture Organization, Rome, Italy.

Amadio, M., 2014. Water security issue in the Caribbean Windward Islands. *Rev. Environ. Energy Econ*. https://papers.ssrn.com/sol3/papers.cfm?abstract_id=2462148 (accessed 23 February 2025).

Andrews, J.S., Sanders, Z.P., Cabrera, M.L., Hill, N.S., Radcliffe, D.E., 2020. Simulated nitrate leaching in annually cover cropped and perennial living mulch corn production systems. *J. Soil Water Conserv.* 75(1):91–102. https://doi.org/10.2489/jswc.75.1.91.

Atkinson, E.E., Marín-Spiotta, E., 2014. Land use legacy effects on structure and composition of subtropical dry forests in St. Croix, U.S. Virgin Islands. *For. Ecol. Manag.* 335:270–280. https://doi.org/10.1016/j.foreco.2014.09.033.

Bai, X., Shao, M., Jia, X., Zhao, C., 2022. Prediction of the van Genuchten model soil hydraulic parameters for the 5-m soil profile in China's Loess Plateau. *Catena* 210:105889. https://doi.org/10.1016/j.catena.2021.105889.

Banihabib, M.E., Vaziri, B., Javadi, S., 2018. A model for the assessment of the effect of mulching on aquifer recharging by rainfalls in an arid region. *J. Hydrol.* 567:102–113. https://doi.org/10.1016/j.jhydrol.2018.10.009.

Bathelemy, R., Brigode, P., Boisson, D., Tric, E., 2022. Rainfall in the Greater and Lesser Antilles: Performance of five gridded datasets on a daily timescale. *J. Hydrol.: Reg. Stud.* 43:101203. https://doi.org/10.1016/j.ejrh.2022.101203.

Beck, H.E., Zimmerman, N.E., McVicar, T.R., Vergopolan, N., Berg, A., Wood, E.F., 2018. Present and future Köppen-Geiger climate classication maps at 1-km resolution. *Sci. Data* 5:180214. https://doi.org/10.1038/sdata.2018.214.

Beckford, C.L., Campbell, D.R., 2013. *Domestic Food Production and Food Security in the Caribbean*. Palgrave Macmillan, New York, USA. https://doi.org/10.1057/9781137296993.

Bégin, C., Brooks, G., Larson, R.A., Dragićević, S., Ramos-Scharrón, C.E., Côté, I.M., 2014. Increased sediment loads over coral reefs in Saint Lucia in relation to land use change in contributing watersheds. *Ocean Coast. Manag.* 95:35–45. http://dx.doi.org/10.1016/j.ocecoaman.2014.03.018.

Beven, K., 2000. Uniqueness of place and process representations in hydrological modelling. Hydrol. *Earth Syst. Sci.* 4(2):203–213. https://doi.org/10.5194/hess-4-203-2000.

Beven, K., 2021. The era of infiltration. *Hydrol. Earth Sys. Sci.* 25:851–866. https://doi.org/10.5194/hess-25-851-2021

Black, A., Peskett, L., MacDonald, A., Young, A., Spray, C., Ball, T., Thomas, H., Werritty, A., 2021. Natural flood management lag time and catchment scale: Results from an empirical nested catchment study. *J. Flood Risk Manag.* 2021:14e12717. https://doi.org/10.1111/jfr3.12717.

Blume, T., Zehe, E., Bronstert, A., 2007. Rainfall-runoff response, event-based runoff coefficients and hydrograph separation. *Hydrol. Sci.* 52(5):843–862. https://doi.org/10.1623/hysj.52.5.843

Boardman, J., Vandaele, K., Evans, R., Foster, I.D.L., 2019. Off-site impacts of soil erosion and runoff: Why connectivity is more important than erosion rates. *Soil Use Manag.* 35(2):245–256. https://doi.org/10.1111/sum.12496.

Borgdorff, A.J., 2020. Measuring and modeling potable water demand in the United States Virgin Islands. Master's thesis, Naval Postgraduate School. https://apps.dtic.mil/sti/pdfs/AD1114654.pdf (accessed 23 February 2025)

Bowden, J.H., Terando, A.J., Misra, V., Wootten, A., Bhardwaj, A., Boyles, R., Gould, W., Collazo, J.A., Spero, T.L., 2021. *Int. J. Climatol.* 41(2):1305–1327. https://doi.org/10.1002/joc.6810.

Boyer, W.B., 2010. *America's Virgin Islands: A History of Human Rights and Wrongs, Second Edition*. Carolina Academic Press, Durham, USA.

Brandt, M.E., Ennis, R.S., Meiling, S.S., Townsend, J., Cobleigh, K., Glahn, A., Quetel, J., Brandtneris, V., Henderson, L.M., Smith, T., 2021. The emergence and initial impact of Stony Coral Tissue Loss Disease (SCTLD) in the United States Virgin Islands. *Front. Mar. Sci.* 8:715329. https://doi.org/10.3389/fmars.2021.715329.

Bremer, L.L., DeMaagd, N., Wada, C.A., Burnett, K.M., 2021. Priority watershed management areas for groundwater recharge and drinking water protection: A case study for Hawai'i Island. *J. Environ. Manag.* 286:111622. https://doi.org/10.1016/j.jenvman.2020.111622.

Brooks, G.R., Devine, B., Larson, R.A., Rood, B.P., 2007. Sedimentary development of Coral Bay, St. John, USVI: A shift from natural to anthropogenic influences. Caribb. J. Sci. 43(2):226–243. http://dx.doi.org/10.18475/cjos.v43i2.a8.

Brooks, G.R., Larson, R.A., Devine, B., Schwing., P.T., 2015. Annual to millennial record of sediment delivery to U.S. Virgin Island coastal environments. *Holocene* 25(6):1015–26. https://doi.org/10.1177/0959683615575357.

Burgess, C.P., Taylor, M.A., Stephenson, T., Mandal, A., 2015. Frequency analysis, infilling and trends for extreme precipitation for Jamaica (1895–2100). *J. of Hydrol.: Reg. Stud.* 3:424–443. http://dx.doi.org/10.1016/j.ejrh.2014.10.004

Buscemi, P.E., 2003. Integrating water resources management: Analysis of the St. Thomas, U.S. Virgin Islands, water market. Master's thesis, Massachusetts Institute of Technology. https://dspace.mit.edu/handle/1721.1/29324.

Cadmus Group, 2011. Watershed characterization and planning for pathogen source reduction in the U.S. Virgin Islands. Technical Report for U.S. Environmental Protection Agency (EPA). https://www.ncei.noaa.gov/data/oceans/coris/library/NOAA/CRCP/other/other_crcp_publication

s/Watershed_USVI/steer_exisiting_studies/usvi_phase3_report_092311_508.pdf (accessed 23 February 2025).

Campbell, L.G., Broughton, R.S., 1965. Problems of soil and water conservation in the Eastern Caribbean islands. *Canadian Ag. Eng.* 1965. https://library.csbe-scgab.ca/docs/journal/7/7_1_40_ocr.pdf (accessed 23 February 2025).

Canoy, M.J., Beets, J., Martin, F.D., Weichert, B., 1983. Effects of freshwater runoff on nearshore tropical marine fisheries. Caribbean Research Institute, College of the Virgin Islands Technical Report 16. https://www.uvi.edu/files/documents/Lost_and_Found/Effects_of_Freshwater_Runoff_on_Nearshore.pdf (accessed 23 February 2025).

Carr, M.K.V., 2009. The water relations and irrigation requirements of banana (*Musa* spp.). Expl. Agric. 45, 333–371. https://doi.org/10.1017/S001447970900787X.

Cederstrom, D.J., 1950. Geology and ground-water resources of St. Croix, Virgin Islands. U.S. Geological Survey Water Supply Paper 1067. https://doi.org/10.3133/wsp1067.

Cerdan, O., Le Bissonnais, Y, Govers, G., Lecomte, V., van Oost, K., Couturier, A., King, C., Dubreuil, N., 2004. Scale effect on runoff from experimental plots to catchments in agricultural areas in Normandy. *J. Hydrol.* 299:4–14. https://doi.org/10.1016/j.jhydrol.2004.02.017

Chanca, D.A., 1494. La carta que escribió a la cuidad de Seville, febrero a marzo 1494. In: *Colección de los viages y descrubimientos, que hicieron por mar los Españoles desde fines del Siglo XV*, Vol. 1, Naverrete, M.F. (ed.) pp. 206–07. Imprenta Real (1825), Madrid, Spain.

Crisman, T.L., Winters, Z.S., 2023. Caribbean small island developing states must incorporate water quality and quantity in adaptive management of the water-energy-food nexus. *Front. Environ. Sci.* 11 :1212552. https://doi.org/10.3389/fenvs.2023.1212552.

Collins, A.L., Walling, D.E., Sichingabula, H.M., Leeks, G.J.L., 2001. Suspended sediment source fingerprinting in a small tropical catchment and some management implications. *Appl. Geog.* 21:387–412. https://doi.org/10.1016/S0143-6228(01)00013-3.

Cook, H.F., Valdes, G.S.B., Lee, H.C., 2006. Mulch effects on rainfall interception, soil physical characteristics and temperature under *Zea mays* L. *Soil Tillage Res.* 91:227–235. https://doi.org/10.1016/j.still.2005.12.007.

Coppola, A., Dragonetti, G., Comegna, A., Lamaddalena, N., Caushi, B., Haikal, M.A., Basile, A., 2013. Measuring and modeling water content in stony soils. *Soil Till. Res.* 128:9–22. http://dx.doi.org/10.1016/j.still.2012.10.006

Cosgrove, W.J., Loucks, D.P., 2015. Water management: Current and future challenges and research directions. *Water Resour. Res.* 51:4823–4839. https://doi.org/10.1002/2014WR016869.

Cox, C.A., Sarangi, A., Madramootoo, C.A., 2006. Effect of land management on runoff and soil losses from two small watersheds in St. Lucia. *Land Degrad. Dev.* 17:55–72. https://doi.org/10.1002/ldr.694.

Culbertson, S., Nuñez-Neto, B., Acosta, J.D., Cook, C.R., Lauland, A., Leuschner, K.J., Natarak, S., et al., 2020. Recovery in the U.S. Virgin Islands: Progress, challenges, and options for the future. Homeland Security Operational Analysis Center, Rand Corporation. Report Number RR-A282-1. https://vtechworks.lib.vt.edu/bitstream/handle/10919/107677/RAND_RRA282-1.pdf?sequence=2&isAllowed=y (accessed 23 February 2025).

Daley, B.F., 2010. Neotropical dry forests of the Caribbean: Secondary forest dynamics and restoration in St. Croix, U.S. Virgin Islands. Doctoral dissertation, University of Florida. https://www.proquest.com/openview/e79e35a270462381343f753e95500fed/1?pq-origsite=gscholar&cbl=18750 (accessed 23 February 2025).

Damman, A.E., Nellis, D.W., 1992. *A Natural History Atlas to the Cays of the U.S. Virgin Islands*. Pineapple Press, Sarasota, USA.

Davison, A., Howard, G., Stevens, M., Callan, P., Fewtrell, L., Deere, D., Bartram, J., 2005. Water safety plans: Managing drinking-water quality from catchment to consumer. World Health Organization 05.06. https://www.who.int/publications/i/item/WHO-SDE-WSH-05.06 (accessed 23 February 2025).

DeGuzman, K., Knappenberger, T., Brantley, E., Olshansky, Y., 2023. Estimating runoff probability from precipitation data: A binomial regression analysis. *Hydrol. Process.* 37:e15029. https://doi.org/10.1002/hyp.15029

Department of Planning and Natural Resources (DPNR), 2004. The Virgin Islands Comprehensive Land and Water Use Plan: Development Plan. Report for the USVI. https://www.planusvi.com/s/VIDevelopment_Plan_2004.pdf (accessed 23 Feburary 2025).

Department of Planning and Natural Resources (DPNR), 2024. Planning our future: The Comprehensive Land and Water Use Plan. https://www.planusvi.com/final-draft-plan (accessed 23 February 2025).

Dita, M.A., Garming, H., Van den Bergh, I., Staver, C., Lescot, T., 2013. Banana in Latin American and the Caribbean: Current state, challenges, and perspectives. *Acta Hort.* 986:365–380. https://doi.org/10.17660/ActaHortic.2013.986.39.

Dobre, M., Long, J.W., Maxwell, C., Elliott, W.J., Lew, R., Scheller, R.M., 2022a. Water quality and forest restoration in the Lake Tahoe basin: Impacts of future management options. *Ecol. Soc.* 27(2):6. https://doi.org/10.5751/ES-13133-270206.

Dobre, M., Srivastava, A., Lew, R., Deval, C., Brooks, E.S., Elliot, W.J., and Robichaud, P.R., 2022b. WEPPcloud: An online watershed-scale hydrological modeling tool. Part II. Model performance

assessment and applications to forest management and wildfires. *J. Hydrol.* 610:127776. https://doi.org/10.1016/j.jhydrol.2022.127776.

Dookhan, I., 1994. *A History of the Virgin Islands of the United States*. Canoe Press, Kingston, Jamaica.

Dores, D., Glenn, C.R., Torri, G., Whittier, R.B., Popp, B.N., 2020. Implications for groundwater recharge from stable isotopic composition of precipitation in Hawai'i during the 2017-2018 La Niña. *Hydrol. Process.* 34(24):4675–4696. https://doi.org/10.1002/hyp.13907.

Dun, S., Wu, J.Q., Elliot, W.J., Robichaud, P.R., Flanagan, D.C., Frankenberger, J.R., Brown, R.E., Xu, A.C., 2009. Adapting the Water Erosion Prediction Project (WEPP) model for forest applications. *J. Hydrol.* 366(1–4):46–54. https://doi.org/10.1016/j.jhydrol.2008.12.019.

Duncan, H.P., 2019., Baseflow separation: A practical approach. *J. Hydrol.* 575:308–313. https://doi.org/10.1016/j.jhydrol.2019.05.040

Dunkerly, D.L., 2008. Intra-storm evaporation as a component of canopy interception loss in dryland shrubs: Observations from Fowlers Gap, Australia. *Hydrol. Process.* 22:1985–1995. https://doi.org/10.1002/hyp.6783.

Dunkerly, D.L., 2015. Intra-event intermittency of rainfall: An analysis of the metric of rain and no-rain periods. *Hydrol. Process.* 29:3294–3305. https://doi.org/10.1002/hyp.10454.

Dunkerly, D.L., 2022. Regional rainfall regimes affect the sensitivity of the Huff quartile classification to the method of event delineation. *Water* 14(7):1047. https://doi.org/10.3390/w14071047.

Dunne, T., 1978. Field studies of hillslope flow processes. In: *Hillslope Hydrology*, Kirkby, M.J. (ed.), pp. 227–293. John Wiley, New York, USA.

Eggers, H.F.A., 1879. *The Flora of St. Croix and the Virgin Islands*. Smithsonian Institution, Washington, USA.

Falkland, T., 1999. Water resources issues of small island developing states. *Nat. Resour. Forum* 23:245–260. https://doi.org/10.1111/j.1477-8947.1999.tb00913.x.

Farrick, K.K., Branfireun, B.A., 2014a. Infiltration and soil water dynamics in a tropical dry forest: It may be dry but definitely not arid. *Hydrol. Process.* 28:4377–4387. https://doi.org/10.1002/hyp.10177.

Farrick, K.K., Branfireun, B.A., 2014b. Soil water storage rainfall and runoff relationships in a tropical dry forest catchment. *Water Resour. Res.* 50:9236–9250. http://dx.doi.org/10.1002/2014WR016045.

Farrick, K.K., Branfireun, B.A., 2015. Flowpaths, source water contributions and water residence times in a Mexican tropical dry forest catchment. *J. Hydrol.* 529:854–865. http://dx.doi.org/10.1016/j.jhydrol.2015.08.059.

Feddes, R.A., Kowalik, P. J., Zaradny, H., 1978. *Simulation of Field Water Use and Crop Yield*. John Wiley & Sons, New York, USA.

Fér, M. Nikodem, A., Trejbalová, S., Klement, A., Pavlů, L., Kodešová, R., 2022. How various mulch materials can affect the soil hydro-physical properties. *J. Hydrol. Hydromech.* 70(3):269–275. https://doi.org/10.2478/johh-2022-0016.

Ferrarezi, R.S., Geiger, T.C., Greenidge, J., Dennery, S., Weiss, S.A., Vieira, G.H.S., 2020. Microirrigation equipment for okra cultivation in the U.S. Virgin Islands. *HortSci.* 55(7):1045–1052. https://doi.org/10.21273/HORTSCI15021-20.

Flanagan, D.C., Livingston, S.J., 1995. WEPP user summary. National Soil Erosion Research Laboratory, Agricultural Research Service, U.S. Department of Agriculture, NSERL Report 11.

Fogain, R., Gowen, R.S., 2005. Root morphology and development of banana and plantain root systems in relation to nematode population. *Fruits* 60 :297–302. https://doi.org/10.1051/fruits:2005035.

Francois, D.C., Thompson, T.P., Ajayi., O., 1983. Managing water supply operations in the Caribbean. *Nat. Resour. Forum* 7(4):351–62. https://doi.org/10.1111/j.1477-8947.1983.tb00279.x.

Friedman, J., Tibshirani, R., Hastie, T., 2010. Regularization paths for generalized linear models via coordinate descent. *J. Stat. Softw*. 33(1):1–22. https://doi.org/10.18637/jss.v033.i01.

Garbrecht, J., Martz, L.W., 1997. TOPAZ: An automated digital landscape analysis tool for topographic evaluation, drainage identification, watershed segmentation and subcatchment parameterization. U.S. Department of Agriculture, Agricultural Research Service Publication GRL 97-2.

Gardner, L., Henry, S., Thomas, T., 2008. Watercourses as landscapes in the U.S. Virgin Islands: A pilot study. Virgin Islands Water Resources Research Institute Report. https://www.uvi.edu/files/documents/Research_and_Public_Service/WRRI/changes_riverine.pdf (accessed 23 February 2025).

Garnier, S., Ross, N., Rudis, R., Carmago., A.P., Sciani, M., Scherer, C., 2024. viridis(Lite): Colorblind-friendly color maps for R. Viridis package version 0.6.5.

Gellis, A.C., Webb, R.M.T., McIntyre, S.C., Wolfe, W.J., 2006. Land-use effects on erosion, sediment yields, and reservoir sedimentation: A case study in the Lago Loíza basin, Puerto Rico. *Phys. Geog.* 27(1):39–69.

Gheuens, J., Nagabhatla, N., Perera, E.D.P., 2019. Disaster-risk, water security challenges and strategies in Small Island Developing States (SIDS). *Water* 11(4):637. https://doi.org/10.3390/w11040637.

Giani, G., Tarasova, L., Woods, R.A., Rico-Ramirez, M.A., 2022. An objective time-series-analysis method for rainfall-runoff event identification. *Water Resour. Res.* 58:e2021WR031283. https://doi.org/10.1029/2021WR031283.

Giannini, A., Kushnir, Y., Cane, M.A., 2001. Seasonality in the impact of ENSO and the North Atlantic High on Caribbean rainfall. *Phys. Chem. Earth B.* 26(2):143–147. https://doi.org/10.1016/S1464-1909(00)00231-8.

Gill, I.P., Hubbard, D.K., 1986. Groundwater geochemistry of the St. Croix carbonate aquifer system. Caribbean Research Institute, College of the Virgin Islands Technical Report 27. https://uvi.edu/files/documents/Research_and_Public_Service/WRRI/Groundwater_Geochemistry.pdf (accessed 23 February 2025).

Gill, I.P., Hubbard, D.K., McLaughlin, P.P., Moore, C.H., 1997. Geology and hydrogeology of St. Croix, Virgin Islands. In: *Geology and Hydrogeology of Carbonate Islands*, Vacher, H.L., Quinn, T.M. (eds.), pp. 359–379. Elsevier, Amsterdam, Netherlands.

Gomi, T., Sidle, R.C., Miyata, S., Kosugi, K., Onda, Y., 2008. Dynamic runoff connectivity of overland flow on steep forested hillslopes: Scale effects and runoff transfer. *Water Resour. Res.* 44:W08411. https://doi.org/10.1029/2007WR005894.

Gould, W.A., Fain, S.J., Pares, I.K., McGinley, K., Perry, A., Steele, R.F., 2015. Caribbean Regional Climate Sub Hub assessment of climate change vulnerability and adaptation and mitigation strategies. U.S. Department of Agriculture Forest Service, International Institute of Tropical Forestry. https://www.climatehubs.usda.gov/sites/default/files/Caribbean%20Region%20Vulnerability%20Assessment%20Final.pdf (accessed 23 February 2025).

Graham, S.L., Srinivasan, M.S., Faulkner, N., Carrick, S., 2018. Soil hydraulic modeling outcomes with four parameterization methods: Comparing soil description and inverse estimation approaches. *Vadose Zone J.* 17:170002. https://doi.org/10.2136/vzj2017.01.0002.

Grant, D.M., Dawson, B.D., 1997. The Manning formula. In: *Isco Open Channel Flow Measurement Handbook, Fifth Edition*, pp. 129–144. Isco, Inc, Lincoln, USA.

Granvorka, C., Strobl, E., 2013. The impact of hurricane strikes on tourist arrivals in the Carribean. *Tour. Econ.* 19(6):1401–1409. https://doi.org/10.5367/te.2013.0238.

Gray, S.C., Gobbi, K.L., Narwold, T.V., 2008. Comparison of sedimentation in bays and reefs below developed versus undeveloped watersheds on St. John, US Virgin Islands. 11th International Coral Reef Symposium 1(20):351–356.

Gray, S., Waddell, J., Fairey, L., 2017. Year 2: Assessment of the impact of watershed restoration on marine sediment dynamics in the USVI. National Oceanic and Atmospheric Administration Final Project Progress Report. https://repository.library.noaa.gov/view/noaa/17109/noaa_17109_DS1.pdf (accessed 23 February 2025).

Green, B.K., Cherry, G.S., 1994. Water wells on St. Croix, U.S. Virgin Islands. U.S. Geological Survey Open-File Report 91-503. https://doi.org/10.3133/ofr91503.

Guan, Z., Tang, X., Yang, J.E., Ok, Y.S., Xu, Z., Nishimura, T., Reid, B.J., 2017. A review of source tracking techniques for fine sediment within a catchment. *Environ. Geochem. Health* 39:1221–1243. https://doi.org/10.1007/s10653-017-9959-9.

Gutiérrez-Jurado, K.Y., Partington, D., Batelaan, O., Cook, P., Shanafield, M., 2019. What triggers streamflow for intermittent rivers and ephemeral streams in low-gradient catchments in Mediterranean climates. *Water Resour. Res.* 55:9926–9946. https://doi.org/10.1029/2019WR025041.

Guy, H.P., 1969. Laboratory Theory and Methods for Sediment Analysis. *Techniques of Water Resources Investigations of the United States Geological Survey, Book 5*. U.S. Government Printing Office, Washington, USA.

Hall, J., Scholl, M., Gorokhovich, Y., Uriarte, M., 2022. Forest cover lessens the impact of drought on streamflow in Puerto Rico. *Hydrol. Process.* 36:e14551. https://doi.org/10.1002/hyp.14551.

Hemmings, B., Whitaker, F., Gottsmann, J., Hughes, A., 2015. Hydrogeology of Montserrat review and new insights. *J. Hydrol.: Reg. Stud.* 3:1–30. http://dx.doi.org/10.1016/j.ejrh.2014.08.008.

Herbst, M., Diekkrüger, B., Vanderborght, J., 2006. Numerical experiments on the sensitivity of runoff generation to the spatial variation of soil hydraulic properties. *J. Hydrol.* 326:43–58. https://doi.org/10.1016/j.jhydrol.2005.10.036.

Hernandez, M., Miller, S.N., Goodrich, D.C., Goff, B.F., Kepner, W.G., Edmonds, C.M., Jones, K.B., 2000. Modeling runoff response to land cover and rainfall spatial variability in semi-arid watersheds. Environmental Monitoring and Assessment 64:285–298. https://doi.org/10.1023/A:1006445811859.

Hewlett, J.D., Hibbert, A.R., 1967. Factors affects the response of small watersheds to precipitation in humid areas. In: *Forest Hydrology*, Sopper, W.E., Lull, H.W. (eds.), pp. 275–290. Pergamon Press, New York, USA.

Highfield, A.R., 2013. *Sainte Croix, 1650–1733: A Plantation Society in the French Antilles*. Antilles Press, Christiansted, Virgin Islands.

Hodnett, M.G., Tomasella, J., 2002. Marked differences between van Genuchten soil water-retention parameters for temperature and tropical soils: A new water-retention pedo-transfer functions developed for tropical soils. *Geoderma* 108:155–180. https://doi.org/10.1016/S0016-7061(02)00105-2.

Holwerda, F., Bruijnzeel, L.A., Scatena, F.N., Vugts, H.F., Meesters, A.G.C.A., 2012. Wet canopy evaporation from a Puerto Rican lower montane rain forest: The importance of realistically estimated aerodynamic conductance. *J. Hydrol.* 414–415:1–15. https://doi.org/10.1016/j.jhydrol.2011.07.033.

Hood, M.J., Clausen, J.C., Warner, G.S., 2007. Comparison of stormwater lag times for low impact and traditional residential development. *J. Am. Water Resour. Assoc.* 43(4):1036–1046. https://doi.org/10.1111/j.1752-1688.2007.00085.x.

Hopkins, D.P., 1987. The Danish cadastral survey of St. Croix, 1733–1734 (Virgin Islands). Doctoral dissertation, Louisiana State University. Historical Dissertations and Theses 4399. https://doi.org/10.31390/gradschool_disstheses.4399.

Hothorn, T., Bretz, F., Westfall, P., 2008. Simultaneous inference in general parametric models. *Biom. J.* 50(3):346–363. https://doi.org/10.1002/bimj.200810425.

Housman, I.W., Heyer, J.P., Hardwick, E.A., Leatherman, L., Beck, H., Lecker, J., Megown, K., Ross, J., 2024. Forest Service landscape Change Monitoring System methods. U.S. Department of Agriculture, Forest Service, version 2023.9, GTAC-10252-RPT4. https://data.fs.usda.gov/geodata/rastergateway/LCMS/LCMS_v2023-9_Methods.pdf (accessed 23 February 2025).

Hsieh, Y.P., Grant, K.T., Bugna, G.C., 2009. A field method for soil erosion measurements in agricultural and natural lands. *J. Soil. Water. Conserv.* 64(6):374–382.

Hubbard, D.K., 1986. Sedimentation as a control of reef development: St. Croix USVI. *Coral Reefs* 5:117–125. https://doi.org/10.1007/BF00298179.

Hughes, J., Petheram, C., Taylor, A., Raiber, M., Davies, P., Levick, S., 2022. Water balance of a small island experiencing climate change. *Water* 14:1771. https://doi.org/10.3390/w14111771.

Irizarry, H., Vicente-Chandler, J., Silva, S., 1981. Root distribution of plantains growing on five soil types. *J. Agric. Univ. P. R.* 65(1):29–34. https://doi.org/10.46429/jaupr.v65i1.7559.

Island Resources Foundation (IRF), 1993. Salt River Bay Area of Particular Concern and Area of Preservation and Restoration: Draft management plan. Prepared for Virgin Islands Department of Planning and Natural Resources, Coastal Zone Management.

Island Resources Foundation (IRF), 2000. Virgin Islands Flood Hazard Mitigation Plan. http://www.irf.org/wp-content/uploads/2015/10/VIFloodHazardMitigationPlan_VITEMA_2000.pdf (accessed 23 February 2025).

Island Resources Foundation (IRF), 2013. An environmental profile of the island of Anegada, British Virgin Islands. British Virgin Islands Environmental Profile Series 3. http://www.irf.org/wp-content/uploads/2015/10/AnegadaEnvironmentalProfile_2013.pdf (accessed 23 February 2025).

Izuka, S.K., Abbott, L.L., 2010. Streamflow, suspended-sediment, and soil-erosion data from Kaulana and Hakioawa watersheds, Kaho'olawe, Hawai'i, 2006 to 2010. U.S. Geological Survey Open-File Report 2010-1182. https://pubs.usgs.gov/of/2010/1182/of2010-1182.pdf.

James, A.L., Roulet, N.T., 2007. Investigating hydrologic connectivity and its association with threshold change in runoff response in a temperate forested watershed. *Hydrol. Process.* 21(25):3391–3408. https://doi.org/10.1002/hyp.6554.

Jasechko, S., Seybold, H., Perrone, D., Fan, Y., Kirchner, J.W., 2021. Widespread potential loss of streamflow into underlying aquifers across the USA. *Nature* 591(7850):391–395. https://doi.org/10.1038/s41586-021-03311-x.

Jiménez, O.F., Lhomme, J.P., 1994. Rainfall interception and radiation regime in a plantain canopy. *Fruits* 49(2):133–139. https://repositorio.catie.ac.cr/handle/11554/8329.

Johnston, B.R., 1987. The political ecology of development: Changing resource relations and the impacts of tourism in St. Thomas, United States Virgin Islands. Doctoral dissertation, University of Massachusetts Amherst.

Jones, I.C., Banner, J.L., 2003. Estimating recharge thresholds in tropical karst island aquifers : Barbados, Puerto Rico, and Guam. *J. Hydrol.* 278:131–143. https://doi.org/10.1016/S0022-1694(03)00138-0.

Jordan, D.G., 1966. Test well sites and preliminary evaluation of ground water potential in Tortola, British Virgin Islands. U.S. Geological Survey. Work done in cooperation with the Government of the Virgin Islands, Ralph M. Paiewonksy, Governor. https://doi.org/10.3133/70263595.

Jordan, D.G., 1972. Land-use effect on the water regimen of the U.S. Virgin Islands. U.S. Geological Survey Professional Paper 800-D, D211–D216. https://doi.org/10.3133/pp800D.

Jordan, D.G., 1975. A survey of the water resources of St. Croix, Virgin Islands. U.S. Geological Survey Open-File Report 73-137. https://doi.org/10.3133/ofr73137.

Jordan, D.G., Cosner, O.J., 1973. A survey of the water resources of St. Thomas, Virgin Islands. U.S. Geological Survey Open-File report 72-201. https://doi.org/10.3133/ofr72201.

Jordan, D.G., Gilbert, B.K., 1976. Water supply and waste disposal, Culebra, Puerto Rico. Water-Resources Investigations Report 76-3. https://doi.org/10.3133/wri763

Juliá, F.E., Snyder, V.A., Vázquez, M.A., 2021. Validation of soil survey estimates of saturated hydraulic conductivity in major soils of Puerto Rico. *Hydrol.* 8(94). https://doi.org/10.3390/hydrology8030094.

Jury, M.R., Bernard, D., 2021. Nocturnal rainfall east of the Antilles islands. *Atmosphere-Ocean* 59(4–5):201–213. https://doi.org/10.1080/07055900.2021.1995317.

Karlen, D.L., Peterson, G.A., Westfall, D.G., 2014. Soil and water conservation: Our history and future challenges. *Soil Sci Soc. Am. J.* 78:1493–1499. http://dx.doi.org/10.2136/sssaj2014.03.0110.

Kastridis, A., Stathis, D., 2020. Evaluation of hydrologic and hydraulic models applied in typical Mediterranean ungauged watersheds using post-flash-flood measurements. *Hydrol.* 7(12). https://doi.org/10.3390/hydrology7010012.

Kendall, M.S., Takata, L.T., Jensen, O., Hillis-Starr, Z., Monaco, M.E., 2005. An ecological characterization of Salt River Bay National Historical Park and Ecological Preserve, U.S. Virgin Islands. NOAA Technical Memorandum NOS NCCOS 14.

Kennedy, E.J., 1984. Discharge ratings at gaging stations. In: *Techniques of Water-Resources Investigations* 03-A10. United States Geological Survey. https://doi.org/10.3133/twri03A10

Khan, F., Mohammed, F., 2022. The value of hydrometry in reducing fluvial flooding footprints across the Caribbean: A case study in Dennery, Saint Lucia. Proc. *Water Eff. Conf.* 2022:12–29.

Klein, C.J., Jupiter, S.D., Selig, E.R., Watts, M.E., Halpern, B.S., Kamal, M., Roelfsema, C., Possingham, H.P., 2012. Forest conservation delivers highly variable coral reef conservation outcomes. *Ecol. Appl.* 22(4):1246–1256. https://doi.org/10.1890/11-1718.1.

Knappenberger, T., Jayakaran, A.D., Hinman, C.H., 2017. Monitoring porous asphalt stormwater infiltration and outflow. *J. Irrig. Drain. Eng.* 143(8). https://doi.org/10.1061/(ASCE)IR.1943-4774.0001197.

Knox, J.P., 1852. *A Historical Account of St. Thomas*. Scribner, New York, USA.

Koshiba, S., Besebes, M., Soaladaob, K., Isechal, A.L., Victor, S., Golbuu, Y., 2013. Palau's taro fields and mangroves protect the coral reefs by trapping eroded fine sediment. *Wetlands Ecol. Manag.* 21:157–164. https://doi.org/10.1007/s11273-013-9288-4.

Kundu, P.K., Siddani, R.K., 2011. Scale dependence of spatiotemporal intermittence of rain. *Water Resour. Res.* 47(8):W08522. https://doi.org/10.1029/2010WR010070.

Labrière, N., Locatelli, B., Laumonier, Y., Freycon, V., Bernoux, M., 2015. Soil erosion in the humid tropics: A systematic quantitative review. *Agric. Ecosyst. Environ.* 203:127–139. http://dx.doi.org/10.1016/j.agee.2015.01.027.

Laflen, J.M., Elliot, W.J., Flanagan, D.C., Meyer, C.R., Nearing, M.A., 1997. WEPP–Predicting water erosion using a process-based model. *J. Soil Water Conserv.* 52:96–102. https://www.jswconline.org/content/52/2/96.short (accessed 23 February 2025).

Lancellotti, B.V., Hensley, D.A., 2024. The state of knowledge of freshwater resources in the U.S. Virgin Islands: Data scarcity and implications. *J. Am. Water. Resour. Assoc.* 60:1270–1292. https://doi.org/10.1111/1752-1688.13241.

Lancellotti, B.V., Hensley, D.A., 2025. Controls on nitrogen export to an ephemeral stream network of St. Croix, U.S. Virgin Islands. *J. Environ. Qual.* https://doi.org/10.1002/jeq2.20667.

Lancellotti, B.V., Hensley, D.A., Stryker, R., 2023. Detection of heavy metals and VOCs in streambed sediment indicates anthropogenic impact on intermittent streams of the U.S. Virgin Islands. *Sci. Rep.* 13:17238. https://doi.org/10.1038/s41598-023-44455-2.

Larsen, M.C., Torres-Sanchez, A.J., 1990. Rainfall-soil moisture relations in landslide-prone areas of a tropical rain forest, Puerto Rico. *Proc. Int. Symp. Tropic. Hydrol.* 121–130.

Larson, R.A., Brooks, G.R., Devine, B., Schwing, P.T., Holmes, C.W., Jilbert, T., Reichart, G., 2015. Elemental signature of terrigenous sediment runoff as recorded in coastal salt ponds: U.S. Virgin Islands. *Appl. Geochem.* 63:573–585. https://doi.org/10.1016/j.apgeochem.2015.01.008.

Levi, M.R., Shaw, J.N., Wood, C.W., Hermann, S.M., Carter, E.A., Feng, Y., 2010. Land management effects on near-surface soil properties of Southeastern U.S. coastal plain kandiudults. *Soil Sci. Soc. Am. J.* 74:258–271. https://doi.org/10.2136/sssaj2009.0015.

Lew, R., 2021. wepppy-win-bootstrap. https://github.com/rogerlew/wepppy-win-bootstrap. https://doi.org/10.5281/zenodo.4902236.

Lew, R., Dobre, M., Srivastava, A., Brooks, E.S., Elliot, W.J., Robichaud, P.R., Flanagan, D.C., 2022. WEPPcloud: An online watershed-scale hydrological modeling tool. Part I. Model description. *J. Hydrol.* 608:127603. https://doi.org/10.1016/j.jhydrol.2022.127603.

Li, C., Gao, X., Li, S., Bundschuh, J., 2020. A review of the distribution, sources, genesis, and environmental concerns of salinity in groundwater. *Environ. Sci. Poll. Res.* 27:41157–41174. https://doi.org/10.1007/s11356-020-10354-6.

Li, Y., Wright, D.B., Bledsoe, B.P., 2022. Watershed controls and tropical cyclone-induces changes in river hydraulic geometry in Puerto Rico. *J. Hydrol.: Reg. Stud.* 44:101268. https://doi.org/10.1016/j.ejrh.2022.101268.

Lindner, J. R., Rodriguez, M. T., Strong, R., Jones, D., Layfield, D., 2016. New technologies, practices, and products adoption decisions. American Association for Agricultural Education national research agenda, 2016–2020, pp. 19–27.

Linh, N.T.M., MacDonald, L., Gomi, T., Dung B.X., 2024. Runoff and erosion from three unpaved road segments in northern Vietnam. *J. Hydrol.: Reg. Stud.* 51:101625. https://doi.org/10.1016/j.ejrh.2023.101625.

Lumbroso, D.M., Boyce, S., Bast, H., Walmsley, N., 2011. The challenges of developing rainfall intensity-duration-frequency curves and national flood hazard maps for the Caribbean. *J. Flood Risk. Manag.* 4(1):42–52. https://doi.org/10.1111/j.1753-318X.2010.01088.x.

Lyne, V., Hollick, M., 1979. Stochastic time-variable rainfall-runoff modeling. Institution of Engineers Australia National Conference, pp. 89–92.

Ma, G., Li, G., Mu, X., Hou, W., Ren, Y., Yang, M., 2022. Effect of raindrop splashes on topsoil structure and infiltration characteristics. *Catena* 212:106040. https://doi.org/10.1016/j.catena.2022.106040.

Maass, M., Ahedo-Hernández, R., Araiza, S., Verduzco, A., Martínez-Yrízar, A., Jaramillo, V.J., Parker, G., Pascual, F., García-Méndez, G., Sarukhán, J., 2018. Long-term (33 years) rainfall and runoff dynamics in a tropical dry forest ecosystem in western Mexico: Management implications under extreme hydrometeorological events. *For. Ecol. Manag.* 426:7–17. https://doi.org/10.1016/j.foreco.2017.09.040.

Madramootoo, C.A., Dodds, G.T., Norville, P., 1999. Sustainable hillside farming systems for the Eastern Caribbean. *West Indian J. Eng.* 21(1):1–9. https://sta.uwi.edu/eng/wije/vol2101_jul1998/documents/HillsideFarming.pdf (accessed 23 February 2025).

Marconi, L., Armengot, L., 2020. Complex agroforestry systems against biotic homogenization: The case of plants in the herbaceous stratum of cocoa production systems. *Agric. Ecosyst. Environ.* 287:106664. https://doi.org/10.1016/j.agee.2019.106664.

Martin-Kaye, P.H.A., 1954. *Water Supplies of the British Virgin Islands*. Lithographic Co. Ltd., Georgetown, Guyana.

Mather, J.D., 1971. Report on the water resources of Tortola and Beef Islands, British Virgin Islands. Institute of Geological Sciences, Hydrogeological Department Internal Report WD/71/8. https://resources.bgs.ac.uk/PublicationPDFs/19794742.pdf (accessed 23 February 2025).

Matos-Llavona, P.I., Woodruff, J.D., Yellen, B., Hughes, S.K., Bayouth García, D., 2022. Sedimentation patterns in reservoirs following Hurricane Maria: Sediment yield and basin connectivity. Abstract, Frontiers in Hydrology, San Juan, Puerto Rico. https://ui.adsabs.harvard.edu/abs/2022frhy.conf22748M/abstract (accessed 23 February 2025).

McDonald, M.A., Healey, J.R., Stevens, P.A., 2002. The effects of secondary forest clearance and subsequent land-use on erosion losses and soil properties in the Blue Mountains of Jamaica. *Agric. Ecosyst. Environ.* 92(1):1–19. https://doi.org/10.1016/s0167-8809(01)00286-9.

McDonnell, J.J., Spence, C., Karran, D.J., van Meerveld, H.J.(I.), Harman, C.J., 2021. Fill-and-spill : A process description of runoff generation at the scale of the beholder. *Water Resour. Res.* 57:e2020WR027514. https://doi.org/10.1029/2020WR027514.

McElroy, J.L., Hamma, P.E., 2010. SITEs revisited: Socioeconomic and demographic contours of small island tourist economies. *Asia Pac. Viewp.* 51(1):36–46. https://doi.org/10.1111/j.1467-8373.2010.01412.x.

McIntyre, B.D., Speijer, P.R., Riha, S.J., Kizito, F., 2000., Effects of mulching on biomass, nutrients, and soil water in banana inoculated with nematodes. *Agron. J.* 92:1081–1085. https://doi.org/10.2134/agronj2000.9261081x.

McNair, D.B., Yntema, L.D., Cramer-Burke. C., 2006. Use of waterbird abundance for saline wetland site prioritization on St. Croix, United States Virgin Islands. *Caribb. J. Sci.* 42(2):220.

Melville, T., Wuddivira, M., Sutherland, M., 2022. Geospatial modelling of rainfall erosivity in the humid subtropics using remotely sensed data. Earth Sci. Inform. 15:891–904. https://doi.org/10.1007/s12145-022-00773-z.

Menne, M.J., Imke, D., Korzeniewski, B., McNeill, S., Thomas, K., Yin, X., Anthony, S., Ray, R., Vose, R.S., Gleason, B.E., Houston, T.G., 2012. Global Historical Climatology Network - daily

(GHCN – Daily), Version 3. NOAA National Climatic Data Center. https://doi.org/10.7289/V5D21VHZ.

Migliaccio, K.W., Srivastava, P., 2007. Hydrologic components of watershed-scale models. *Trans. Am. Soc. Agric. Biol. Eng.* 50(5):1695–703. https://doi.org/10.13031/2013.23955.

Miller, J.A., Whitehead, R. L., Oki, D.S., Gingerich, S. B., Olcott, P.G., 1999. Ground water atlas of the United States: Segment 13, Alaska, Hawaii, Puerto Rico, and the U.S. Virgin Islands. United States Geological Survey 730-N:N1–N36. https://doi.org/10.3133/ha730N.

Miller, S.A., Webber, J.S., Jastram, J.D., Aguilar, M.F., 2023. Using high-frequency monitoring data to quantify city-wide suspended-sediment load and evaluate TMDL goals. *Environ. Monit. Assess.* 195:1372. https://doi.org/10.1007/s10661-023-11905-3.

Mirus, B.B., Loague, K., 2013. How runoff begins (and ends): Characterizing hydrologic response at the catchment scale. Water Resources Research 49:2987–3006. https://doi.org/10.1002/wrcr.20218.

Mohamadi, A.M., Kavian, A., 2015. Effects of rainfall patterns on runoff and soil erosion in field plots. *Int. Soil Water Conserv. Res.* 3(4):273–281. https://doi.org/10.1016/j.iswcr.2015.10.001.

Molina-Sanchis, I., Lázaro, R., Arnau-Rosalén, E., Calvo-Cases, A., 2016. Rainfall timing and runoff: The influence of the criterion for rain event separation. *J. Hydrol. Hydromech.* 64(3):226–236. https://doi.org/10.1515/johh-2016-0024.

Moraes, F.D.S., Mote, T.L., Rasmussen, T.C., 2023. The role of physical geography on Puerto Rico's water budget. *J. Hydrol. Reg. Stud.* 47:101382. https://doi.org/10.1016/j.ejrh.2023.101382.

Moraes, F.D.S., Mote, T.L., Seymour, L., 2022. Ocean-atmosphere variability and drought in the insular Caribbean. *Int. J. Climatol.* 2022:1–22. https://doi.org/10.1002/joc.7517.

Mounirou, L.A., Yonaba, R., Koïta, M., Paturel, J.-E., Mahé, G., Yacouba, H., Karambiri, H., 2021. Dimensionless runoff indices across scales in a semi-arid catchment. *J. Arid Environ.* 193:104590. https://doi.org/10.1016/j.jaridenv.2021.104590.

Mounirou, L.A., Zouré, C.O., Yonaba, R, Paturel, J.-E., Mahé, G., Niang, D., Yacouba, H., Karambiri, H., 2020. Multi-scale analysis of runoff from a statistical perspective in a small Sahelian catchment under semi-arid climate. *Arab. J. Geosci.* 13:154. https://doi.org/10.1007/s12517-020-5141-2.

Muñoz-Villers, L.E., McDonnell, J.J., 2013. Land use change effects on runoff generation in a humid tropical montane cloud forest region. *Hydrol. Earth Syst. Sci.* 17:3543–3560. https://doi.org/10.5194/hess-17-3543-2013.

Mycoo, M.A., Roopnarine, R.R., 2024. Water resource sustainability: Challenges, opportunities and research gaps in the English-speaking Caribbean Small Island Developing States. *PLOS Water* 3(1):e0000222. https://doi.org/10.1371/journal.pwat.0000222.

Nagle F., Hubbard, D.K., 1989. St. Croix geology since Whetten: An introduction. Proceedings of the 12th Caribbean Geological Conference, West Indies Laboratory, pp. 1–7. https://www.aoml.noaa.gov/general/lib/CREWS/Cleo/St.%20Croix/salt_river180.pdf (accessed 23 February 2025).

National Oceanic and Atmospheric Administration (NOAA), 2023. Applied Climate Information System. https://xmacis.rcc-acis.org (accessed 1 December 2023).

Naseri, M., Iden, S.C., Richter, N., Durner, W., 2019. Influence of stone content on soil hydraulic properties: Experimental investigation and test of existing model concepts. *Vadose Zone J.* 18:180163. https://doi.org/10.2136/vzj2018.08.0163.

Nasri, B., Fouché, O., Torri, D., 2015. Coupling published pedotransfer functions for the estimation of bulk density and saturated hydraulic conductivity in stony soils. *Catena* 131:99–108. http://dx.doi.org/10.1016/j.catena.2015.03.018.

Nemeth, D., Platenberg, R.J., 2007. Diversity of freshwater fish and crustaceans of St. Thomas watersheds and its relationship to water quality as affected by residential and commercial development. Virgin Islands Water Resources Research Institute. https://uvi.edu/files/documents/Research_and_Public_Service/WRRI/diversity_freshwater.pdf (accessed 23 February 2025).

Nemeth, R.S., Nowlis, J.S., 2001. Monitoring the effects of land development on the near-shore reef environment of St. Thomas, USVI. *Bull. Mar. Sci.* 69(2):759–75.

Ngetich, K.F., Diels, J., Shisanya, C.A., Mugwe, J.N., Mucheru-muna, M., Mugendi, D.N., 2014. Effects of selected soil and water conservation techniques on runoff, sediment yield and maize productivity under sub-humid and semi-arid conditions in Kenya. *Catena* 121:288–296. https://doi.org/10.1016/j.catena.2014.05.026.

Nicolini, E., Rogers, K., Rakowski, D., 2016. Baseline geochemical characterisation of a vulnerable tropical karstic aquifer: Lifou, New Caledonia. *J. Hydrol. Reg. Stud.* 5:114–130. https://doi.org/10.1016/j.ejrh.2015.11.014.

Nielsen, D.R., Wendroth, O., 2003. *Spatial and Temporal Statistics: Sampling Field Soils and Their Vegetation*. Catena-Verlag, Stuttgart, Germany.

Oldendorp, C.G.A., 1777. *History of the Mission of the Evangelical Brethren on the Caribbean Islands of St. Thomas, St. Croix, and St. John*. Bossard, J.J. (ed.), Highfield, A.R., Barac, V. (trans. 1987). Karoma Publishers, Ann Arbor, USA.

Oliver, L.M., Fisher, W.S., Fore, L., Smith, A., Bradley, P., 2018. Assessing land use, sedimentation, and water quality stressors as predictors of coral reef condition in St. Thomas, U.S. Virgin Islands. *Environ. Monit. Assess.* 190:213. https://doi.org/10.1007/s10661-018-6562-1.

Oliver, L.M., Lehrter, J.C., Fisher, W.S., 2011. Relating landscape development intensity to coral reef condition in the watersheds of St. Croix, U.S. Virgin Islands. Mar. Ecol. Prog. Ser. 427:293–302. https://doi.org/10.3354/meps09087.

Ottoni, M.V., Filho, T.B.O., Lopes-Assad, M.L.R.C., Filho, O.C.R., 2019. Pedotransfer functions for saturated hydraulic conductivity using a database with temperate and tropical climate soils. *J. Hydrol.* 575:1345–1358. https://doi.org/10.1016/j.jhydrol.2019.05.050.

Pait, A.S., Hartwell, S.I. Apeti, D.A., 2020. An assessment of chemical contaminants, toxicity, and benthic infauna in sediments from the Salt River Bay National Historical Park and Ecological Preserve, St. Croix, U.S. Virgin Islands. National Oceanic and Atmospheric Administration Technical Memorandum NOS NCCOS 290.

Pak, L.T., 2013. Modélisation hydrologique distribuée des écoulements surface-souterrain à l'échelle d'un bassin versant bananier en milieu tropical volcanique (Guadeloupe, France). Centre International D'Etudes Supérieures en Sciences Agronomiques. Doctoral dissertation (in French). https://agritrop.cirad.fr/577809/1/Pak_2013.pdf (accessed 23 February 2025).

Panek, J.W., Sorrells, M.R., 1996. Elevation correction factor for absolute pressure measurements. National Aeronautics and Space Administration Technical Memorandum 107420.

Pappas, C., Papalexiou, S.M., Koutsoyiannis, D., 2014. A quick gap filling of missing hydrometeorological data. *J. Geophys. Res. Atmos.* 119(15):9290–9300. https://doi.org/10.1002/2014JD021633.

Peart, M.R., Walling, D.E., 1988. Techniques for establishing suspended sediment sources in two drainage basins in Devon, UK: A comparative assessment. In: *Sediment Budgets*, Bordas, M.P, Walling, D.E. (eds.), pp. 269–279. Wallingford: IAHS (Publication No. 174).

Peña-Angulo, D., Estrany, J., García-Comendador, J., Fortesa, J., Tomàs-Burguera, M., Company, J., Alorda, B., Nadal-Romero, E., 2021. Influence of weather types on the hydrosedimentary response in three small catchments on the Island of Mallorca, Spain. *Envron. Res.* 192:110324. https://doi.org/10.1016/j.envres.2020.110324.

Penna, D., Tromp-van Meerveld, H.J., Gobbi, A., Borga, M., Fontana, G.D., 2011. The influence of soil moisture on threshold runoff generation processes in an alpine headwater catchment. *Hydrol. Earth Syst. Sci.* 15:689–702. https://doi.org/10.5194/hess-15-689-2011.

Phillips, J., Barclay, J., Cole, P., Johnson, M., Miller, V., Robertson, R., 2024. Impacts and prospective hazard analysis of rainfall-triggered lahars on St. Vincent 2021–22. In: Roberston, R.E.A., Joseph, E.P., Barclay, J., Sparks, R.S.J. (eds.), *The 2020–21 eruption of La Soufrière volcano, St. Vincent. Geological Society, Special Publications* 539:245–266. https://doi.org/10.1144/sp539-2022-313,

Piggott, A.R., Moin, S., Southam, C., 2009. A revised approach to the UKIH method for the calculation of baseflow. *Hydrol. Sci. J.* 50(5):911–920. https://doi.org/10.1623/hysj.2005.50.5.911.

Pinheiro, J., Bates, D., R Core Team., 2022. nlme: Linear and Nonlinear Mixed Effects Models. R package version 3.1-160. https://CRAN.R-project.org/package=nlme.

Pratomo, R.A., Jetten, V., Alkema, D., 2016. A comparison of flash flood response at two different watersheds in Grenada, Caribbean Islands. *IOP Conf. Series: Earth Environ. Sci*. 29:012004. https://doi.org/10.1088/1755-1315/29/1/012004.

Puertas, F., Arévalo, E., Zúñiga, L., Alegre, J., Loli, O., Soplin, H., Baligar, V., 2008. Establecimiento de cultivos de cobertura y extracción total de nutrients en un suelo de trópico húmedo en la amazonia peruana. *Ecol. Apl.* 7:23–28. https://doi.org/10.21704/rea.v7i1-2.356.

Quin, J.T., 1907. *The Building of an Island: Being a Sketch of the Geological Structure of the Danish West Indian Island of St. Croix, or Santa Cruz*. Chauncey Holt, New York, USA.

R Core Team, 2025. R: A language and environment for statistical computing. R Foundation for Statistical Computing, Vienna, Austria. https://www.R-project.org/.

Rad, S., Rivé, K., Vittecoq, B., Cerdan, O., Allègre, C.J., 2013. Chemical weathering and erosion rates in the Lesser Antilles: An overview in Guadeloupe, Martinique and Dominica. *J. S. Am. Earth. Sci.* 45:331–344. https://doi.org/10.1016/j.jsames.2013.03.004.

Ramos-Scharrón, C.E., Alicea, E.E., Sánchez, Y.F., LaFevor, M.C., McLaughlin, P., MacDonald, L.H., Reale-Munroe, K., Thomaz, E.L., Ríos, R.V., 2023. Three decades of road and trail runoff and erosion work in the northeastern Caribbean: A research program perspective. *J. ASABE* 66(1):35–45. https://doi.org/10.13031/ja.15078.

Ramos-Scharrón, C.E., LaFevor, M.C., 2016. The role of unpaved roads as active source areas of precipitation excess in small watersheds drained by ephemeral streams in the northeastern Caribbean. *J. Hydrol.* 533:168–179. https://doi.org/10.1016/j.jhydrol.2015.11.051.

Ramos-Scharrón, C.E., LaFevor, M.C., 2018. Effects of forest roads on runoff initiation in low-order ephemeral streams. *Water Resour. Res.* 54(11):8613–8631. https://doi.org/10.1029/2018WR023442

Ramos-Scharrón, C.E., MacDonald, L.H., 2005. Measurement and prediction of sediment production from unpaved roads, St. John, U.S. Virgin Islands. *Earth Surf. Process. Landf.* 30:1283–1304. https://doi.org/10.1002/esp.1201.

Rawls, W.J., Brakensiek, D.L., 1989. Estimation of soil water retention and hydraulic properties. In: *Unsaturated Flow in Hydrologic Modeling: Theory and Practice*, Morel-Seytoux, H.J. (ed.), pp. 275–300. Kluwer Academic Publishers, New York, USA.

Reges, H.W., Doesken, N., Turner, J., Newman, N., Bergantino, A., Schwalbe, Z., 2016. COCORAHS: The evolution and accomplishments of a volunteer rain gauge network. *Bull. Am. Meteor. Soc.* 97:1831–1846. https://doi.org/10.1175/BAMS-D-14-00213.1.

Renken, R.A., Ward, W.C., Gill, I.P., Gómez-Gómez, F., Rodríguez-Martínez. J., 2002. Geology and hydrogeology of the Caribbean islands aquifer system of the Commonwealth of Puerto Rico and the U.S. Virgin Islands. U.S. Geological Survey Professional Paper 1419. https://doi.org/10.3133/pp1419.

Rennis, D.S., Finney, C.M., Devine, B.E., 2006. Evaluating the sediment retention function of salt pond systems in the U.S. Virgin Islands. Virgin Islands Water Resources Research Institute. Report. https://www.uvi.edu/files/documents/Research_and_Public_Service/WRRI/evaluating_sediment.pdf (accessed 23 February 2025).

Righter, E., 2002. *The Tutu Archaeological Village Site: A Multidisciplinary Case Study in Human Adaptation*, Vol. 2. London: Psychology Press, London, United Kingdom.

Robins, N.S., 2013. A review of small island hydrogeology: Progress (and setbacks) during the recent past. *Q. J. Eng. Geol. Hydrogeol.* 46:157–165. https://doi.org/10.1144/qjegh2012-063.

Robins, N.S., Lawrence, A.R., 2000. Some hydrogeological problems peculiar to various types of small islands. *Water Environ. J.* 14(5):341–346. https://doi.org/10.1111/j.1747-6593.2000.tb00271.x.

Robinson, T.M., 1972. Ground water in central St. Croix, U.S. Virgin Islands. U.S. Geological Survey Open-File Report, 72-137. https://doi.org/10.3133/ofr72319.

Rogers, C.S., Ramos-Scharrón, C.E., 2022. Assessing effects of sediment delivery to coral reefs: A Caribbean watershed perspective. *Front. Mar. Sci*. 8:773968. https://doi.org/10.3389/fmars.2021.773968.

Roopnarine, L., 2020. White American-Continental migration to the United States Virgin Isalnds: Development or dominance? *Res.: Interdiscip. J.* 30(1):1–19.

Ross, C.A., Ali, G.A., Spence, C., Courchesne, F., 2021. Evaluating the ubiquity of thresholds in rainfall-runoff response across contrasting environments. *Water Resour. Res.* 57:e2020WR027498. https://doi.org/10.1029/2020WR027498.

Saffarpour, S., Wester, A.W., Adams, R., McDonnell, J.J., 2016. Multiple runoff processes and multiple thresholds control agricultural runoff generation. *Hydrol. Earth Syst. Sci*. 20:4525–4545. https://doi.org/10.5194/hess-20-4525-2016.

Santosh, D.T., Tiwari, K.N., 2019. Estimation of water requirement of banana crop under drip irrigation with and without plastic mulch using dual crop coefficient approach. *IOP Conf. Ser.: Earth Environ. Sci.* 344:012024. https://doi.org/10.1088/1755-1315/344/1/012024.

Scalley, T.H., 2012. Freshwater resources in the insular Caribbean: An environmental perspective. *Caribb. Stud.* 40(2):63–93. https://doi.org/10.1353/crb.2012.0030.

Schellekens, J., 2000. The interception and runoff generating processes in the Bisley Catchment, Luquillo Experimental Forest, Puerto Rico. *Phys. Chem. Earth (B)* 25(7–8):659–664. https://doi.org/10.1016/s1464-1909(00)00081-2.

Scott, G.J., 2020. A review of root, tuber, and banana crops in developing countries: Past, present and future. *Int. J. Food Sci. Tech.* 56:1093–1114. https://doi.org/10.1111/ijfs.14778.

Seaman, G.A., 1980. *Ay-Ay: An Island Almanac*. MacMillan Caribbean, London, United Kingdom.

Serrano-Notivoli, R., Martínez-Salvador, A., García-Lorenzo, R., Espín-Sánchez, D., Conesa-García, C., 2022. Rainfall-runoff relationships at event scale in western Mediterranean ephemeral streams. *Hydrol. Earth Syst. Sci.* 26(5):1243–1260. https://doi.org/10.5194/hess-26-1243-2022.

Shepherd, F.P., Dill, R.F., 1977. Currents in submarine canyon heads off north St. Croix, U.S. Virgin Islands. *Mar. Geol.* 24:M39–M45.

Simpson, A., Turner, I, Brantley, E., Helms, B., 2014. Bank erosion hazard index as an indicator of near-bank aquatic habitat and community structure in a southeastern Piedmont stream. *Ecol. Indic.* 43:19–28. https://doi.org/10.1016/j.ecolind.2014.02.002.

Šimůnek, J., van Genuchten, M.Th., Šejnam, M., 2005. The HYDRUS-1D software package for simulating the one-dimensional movement of water, heat, and multiple solutes in variably-saturated media. Version 3.0. HYDRUS Softw. Ser. 1. Dep. of Environ. Sci., Univ. of California, Riverside.

Singh, N.K., Emanuel, R.E., McGlynn, B.L., Miniat, C.F., 2021. Soil moisture responses to rainfall: Implications for runoff generation. *Water Resour. Res.* 57:e2020WR028827. https://doi.org/10.1029/2020WR028827.

Smith, T.B., Brandt, M.E., Calnan, J.M., Nemeth, R.S., Blondeau, J., Kadison, E., Taylor, M., Rothenberger, P., 2013. Convergent mortality responses of Caribbean coral species to seawater warming. *Ecosphere* 4(7):87. http://dx.doi.org/10.1890/ES13-00107.1.

Soden, D.L., 1990. Preferred alternative uses of water resources: Views of environmental activists in the U.S. Virgin *Islands. Proc. Int. Symp. Trop. Hydrol.*, San Juan, Puerto Rico, pp. 11–19.

Speed, R., 1989. Tectonic evolution of St. Croix: Implications for tectonics of the northeastern Caribbean. In: *Terrestrial and Marine Geology of St. Croix, U.S. Virgin Islands*, Hubbard, D.K. (ed.), Special Publication 8:9–22. West Indies Laboratory, St. Croix, Virgin Islands.

Srivastava, A., Brooks, E.S., Dobre, M., Elliot, W.J., Wu, J.Q., Flanagan, D.C., Gravelle, J.A., Link, T.E., 2020. Modeling forest management effects on water and sediment yield from nested, paired watersheds in the interior Pacific Northwest, USA using WEPP. *Sci. Tot. Environ.* 701:134877. https://doi.org/10.1016/j.scitotenv.2019.134877.

Stapel, S.R., 2023. Rainfall-runoff modelling to assess flood hazard on Sint Eustatius, Caribbean Netherlands. Master's thesis, Universiteit Utrecht. https://studenttheses.uu.nl/handle/20.500.12932/45778 (accessed 23 February 2025).

Stryker, R., 2023. The effectiveness of local and exotic vegetative buffers at reducing runoff generation and sediment production in the United States Virgin Islands. Master's thesis, University of the Virgin Islands.

Suárez-Castro, A.F., Beyer, H.L., Kuempel, C.D., Linke, S., Borrelli, P., Hoegh-Guldberg, O., 2021. Global forest restoration opportunities to foster coral reef conservation. *Glob. Change Biol.* 27(20):5238–5252. https://doi.org/10.1111/gcb.15811.

Sultan, D., Tsunekawa, A., Tsubo, M., Haregeweyn, N., Adgo, E., Meshesha, D.T., Fenta, A.A., Ebabu, K., Berihun, M.L., Setargie, T.A., 2022. Evaluation of lag time and time of concentration estimation methods in small tropical watersheds in Ethiopia. *J. Hydrol.: Reg. Stud.* 40:101025. https://doi.org/10.1016/j.ejrh.2022.101025.

Tao, Z., Li, M., Si, B., Pratt, D., 2021. Rainfall intensity affects runoff responses in a semi-arid catchment. *Hydrol. Process.* 35(4):e14100. https://doi.org/10.1002/hyp.14100.

Tarasova, L., Basso, S., Zink, M., Merz, R., 2018. Exploring controls on rainfall-runoff events: 1. Time series-based event separation and temporal dynamics of event runoff response in Germany. *Water Resour. Res.* 54:7711–7732. https://doi.org/10.1029/2018WR022587.

Thornton, M.M., Shrestha, R., Wei, Y., Thornton, P.E., Kao, S-C., 2022. Daymet: Daily surface weather data on a 1-km grid for North America, Version 4 R1. ORNL DAAC, Oak Ridge, Tennessee, USA. https://doi.org/10.3334/ORNLDAAC/2129.

Tomasella, J., Hodnett, M.G., 1998. Estimating soil water retention characteristics from limited data in Brazilian Amazonia. *Soil Sci.* 163(3):190–202. https://journals.lww.com/soilsci/abstract/1998/03000/estimating__soil_water_retention_characteristics.3.aspx (accessed 23 February 2025).

Tomasella, J., Hodnett, M.G., 2004. Pedotransfer function for tropical soils. *Dev. Soil Sci.* 30. https://doi.org/10.1016/S0166-2481(04)30021-8.

Tombs, J.M.C., Barton, K.J., 1979. Geophysical surveys over alluvial deposits in Tortola, British Virgin Islands, for the Hydraulics Research Station. Institute of Geological Sciences Applied Geophysics Unit Report No. 75. https://resources.bgs.ac.uk/PublicationPDFs/19801148.pdf (accessed 23 February 2025).

Torres-Gonzalez, S., 1989. Reconnaissance of the ground-water resources of Vieques Island, Puerto Rico. Water-Resources Investigations Report 86-4100. https://doi.org/10.3133/wri864100.

Torres-Gonzalez, S., Rodriguez-del-Rio, F., 1990. Potentiometric surface of the Kingshill Aquifer and hydrologic conditions. U.S. Geological Survey Water-Resources Investigations Report 89-4085. https://doi.org/10.3133/wri894085.

Turner, D.W., Fortescue, J.A., Thomas, D.S., 2007. Environmental physiology of the bananas (*Musa* spp.). *Braz. J. Plant Physiol.* 19(4):463–484. https://doi.org/10.1590/S1677-04202007000400013.

Tuure, J., Räsänen, M., Hautala, M., Pellikka, P., Mäkelä, P.S.A., Alakukku, L., 2021. Plant residue mulch increases measured and modelled soil moisture content in the effective root zone of maize in semi-arid Kenya. *Soil Tillage Res.* 209:104945. https://doi.org/10.1016/j.still.2021.104945.

Tymchak, M.P., Torres, R., 2007. Effects of variable rainfall intensity on the unsaturated zone response of a forested sandy hillslope. *Water Resour. Res.* 43(6):e2005WR004584. https://doi.org/10.1029/2005wr004584.

Tyson, G.F., 2020. Unpublished land use and population records from Danish National Archives (Rigsarkivet) and U.S. National Archives, 1742–1924. Communication with author.

U.S. Army Corps of Engineers (USACE), 1987. Estate Mon Bijou, St. Croix, Virgin Islands: Final detailed project report and environmental assessment. U.S. Army Corps of Engineers Jacksonville District.

U.S. Army Corps of Engineers (USACE), 1992. Creque Dam, St. Croix, U.S. Virgin Islands: Technical report, dam safety analysis, and reservoir yield evaluation. U.S. Army Corps of Engineers Jacksonville District.

U.S. Census Bureau, 2020. Population of the United States Virgin Islands: 2010 and 2020. https://www2.census.gov/programs-surveys/decennial/2020/data/island-areas/us-virgin-islands/population-and-housing-unit-counts/us-virgin-islands-phc-table01.pdf (accessed 23 February 2025).

U.S. Department of Agriculture, National Agricultural Statistics Service (USDA-NASS), 2018. Census of agriculture: Virgin Islands of the United States (2018) territory and island data. https://www.nass.usda.gov/Publications/AgCensus/2017/Full_Report/Outlying_Areas/usvi.pdf (accessed 23 February 2025).

U.S. Department of Agriculture, Natural Resources Conservation Service (USDA-NRCS), 1973. Fresh water ponds: Virgin Islands of the United States. Research Conservation and Development Project, USDA Soil Conservation Service, Hyattsville, MD.

U.S. Department of Agriculture, Natural Resources Conservation Service (USDA-NRCS), 2022. Geospatial Data Gateway. https://datagateway.nrcs.usda.gov/. (accessed 15 March 2022).

U.S. Department of Agriculture, Natural Resources Conservation Service (USDA-NRCS), 2024. Web Soil Survey. https://websoilsurvey.sc.egov.usda.gov/App/HomePage.htm (accessed 15 January 2024).

U.S. Geological Survey (USGS), 1984. National Water Summary 1984: Hydrologic events, selected water-quality trends and ground-water resources. U.S. Geological Survey Water Supply Paper 2275. https://doi.org/10.3133/wsp2275.

U.S. Geological Survey (USGS), 2024. USGS water data for the Nation: U.S. Geological Survey National Water Information System database. https://doi.org/10.5066/F7P55KJN.

van Dam, J.C., Huygen, J., Wesseling, G.J., Feddes, R.A., Kabat, P, van Walsum, P.E.V., Groenendijk, P, van Diepen, C.A., 1997. Theory of SWAP version 2.0 Simulation of water flow, solute transport and plant growth in the Soil-Water-Atmosphere-Plant environment. Wageningen Agricultural University Technical Document 45.

van der Velde, M., Green, S.R., Vanclooster, M., Clothier, B.E., 2007. Sustainable development in small island developing states: Agricultural intensification, economic development, and freshwater resources management on the coral atoll of Tongatapu. *Ecol. Econ.* 61(2–3):456–468. http://dx.doi.org/10.1016/j.ecolecon.2006.03.017.

van Genuchten, M.T., 1980. A closed-form equation for predicting the hydraulic conductivity of unsaturated soils. *Soil Sci. Soc. Am. J.* 44(5):892–898. https://doi.org/10.2136/sssaj1980.03615995004400050002x.

Varadarajan, S., Fábrega, J., Leung, B., 2022. Precipitation interpolation, autocorrelation, and predicting spatiotemporal variation in runoff in data sparse regions: Application to Panama. *J. Hydrol.: Reg. Stud.* 44:101252. https://doi.org/10.1016/j.ejrh.2022.101252.

Vereecken, H., Amelung, W., Bauke, S.L., Bogena, H., Brüggemann, N., Montzka, C., Vanderborght, J., Bechtold, M., Blöschl, G., Carminati, A., Javaux, M., Konings, A.G., Kusche, J., Neweiler, I., Or, D., Steele-Dunne, S., Verhoef, A., Young, M., Zhang, Y., 2022. Soil hydrology in the Earth system. *Nat. Rev. Earth Environ.* 3:573–587. https://doi.org/10.1038/s43017-022-00324-6.

Wang, S., Fu, Z., Chen, H., Nie, Y., Xu, Q., 2020. Mechanisms of surface and subsurface runoff generation in subtropical soil-epikarst systems: Implications f rainfall simulation expierments on karst slope. *J. Hydrol.* 580:124370. https://doi.org/10.1016/j.jhydrol.2019.124370.

Wang, S., Yan, Y., Fu, Z., Chen, H., 2022. Rainfall-runoff characteristics and their threshold behaviors on a karst hillslope in a peak-cluster depression region. *J. Hydrol.* 6–5:127370. https://doi.org/10.1016/j.jhydrol.2021.127370.

Wang, Y., Shao, M., Han, X., Liu, Z., 2014. Spatial variability of soil parameters of the van Genuchten model at a regional scale. *Clean Soil Air Water* 42:1–8. https://doi.org/10.1002/clen.201300903.

Ward, P.E., Jordan, D.G., 1963. Water resources of the Virgin Islands: A preliminary appraisal, 1963. U.S. Geological Survey Open-File Report 64-158. https://doi.org/10.3133/ofr64158.

Wasko, C., Guo, D., 2022. Understanding event runoff coefficient variability across Australia using the hydrEvents R package. *Hydrol. Process.* 36:e14563. https://doi.org/10.1002/hyp.14563.

Wells, J., 2006. Derivation of the word ghaut. Email communication as transcribed by Glaser, T., archived at JISC Mail. https://www.jiscmail.ac.uk/cgi-bin/wa-jisc.exe?A2=CARIBBEAN-STUDIES;a7dfa2af.06 (accessed 23 February 2025).

White, I., Falkland, A., Crennan, L., Jones, P., Metutera, T., Etuati, B., Metai, E., 1999. Issues, traditions and conflicts in groundwater use and management. International Hydrological Programme. UNESCO IHP-V, Technical Documents in Hydrology 26.

Wickham, H., 2016. Ggplot2: Elegant graphics for data analysis. Springer-Verlag, New York. https://ggplot2.tidyverse.org.

Wickham, H., François, R., Henry, L., Müller, K., Vaughan, D., 2023a. Dplyr: A grammar of data manipulation. R package version 1.1.4. https://CRAN.R-project.org/package=dplyr.

Wickham, H., Pedersen, T., Seidel., D., 2023b. Scales: Scale functions for visualization. R package version 1.3.0. https://CRAN.R-project.org/package=scales.

Wilson S., 2022. ParBayesianOptimization: Parallel Bayesian optimization of hyperparameters. R package version 1.2.6. https://CRAN.R-project.org/package=ParBayesianOptimization.

Yonaba, R., Biaou, A.C., Koïta, M., Tazen, F., Mounirou, L.A., Zouré, C.O., Queloz, P., Karambiri, H., Yacouba, H., 2021. A dynamic land use/land cover input helps in picturing the Sahelian paradox: Assessing variability and attribution of changes in surface runoff in Sahelian watershed. *Sci. Tot. Environ.* 757:143792. https://doi.org/10.1016/j.scitotenv.2020.143792.

Zambrano-Bigiarini, M., 2024. hydroGOF: Goodness-of-fit functions for comparison of simulated and observed hydrological time series. R package version 0.6–0.1. https://cran.r-project.org/package=hydroGOF.

Zeileis, A., Grothendieck, G., 2005. Zoo: S3 infrastructure for regular and irregular time series. *J. Stat. Softw.* 14(6):1–27. https://doi.org/10.18637/jss.v014.i06.

Zengui, S., Li, Z., Ruiqing, Z., Jichang, H., Huanyuan, W., Jiakun, Y., 2023. Spatial variability of soil water content at the crop row scale with and without straw mulch inside a corn field in semi-humid Northeastern China. *Arid Land Res. Manag.* 37(4):473–493. https://doi.org/10.1080/15324982.2023.2190047.

Zhang, W., Zhu, X., Chen, C., Zeng, H., Jiang, X., Wu, J., Zou, X., Yang, B., Liu, W., 2021. Large broad-leaved canopy of banana (*Musa nana* Lour.) induces dramatically high spatial-temporal variability of throughfall. *Hydrol. Res.* 56(6):1223. https://doi.org/10.2166/nh.2021.023.